ISTANBUL TECHNICAL UNIVERSITY ★ GRADUATE SCHOOL OF SCIENCE ENGINEERING AND TECHNOLOGY

CELLULAR CHARACTERIZATION OF IMMUNE CELLS IN NON-SMALL CELL LUNG CANCER AND MESOTHELIOMA

M.Sc. THESIS

Gönül SEYHAN

Department of Molecular Biology- Genetics and Biotechnology

Molecular Biology- Genetics and Biotechnology Programme

Thesis Advisor: Assoc. Prof. Ayça SAYI YAZGAN

JUNE 2017

ISTANBUL TECHNICAL UNIVERSITY ★ GRADUATE SCHOOL OF SCIENCE ENGINEERING AND TECHNOLOGY

CELLULAR CHARACTERIZATION OF IMMUNE CELLS IN NON-SMALL CELL LUNG CANCER AND MESOTHELIOMA

M.Sc. THESIS

Gönül SEYHAN
(521141109)

Department of Molecular Biology-Genetics and Biotechnology

Molecular Biology-Genetics and Biotechnology Programme

Thesis Advisor: Assoc. Prof. Ayça SAYI YAZGAN

JUNE 2017

ISTANBUL TEKNİK ÜNİVERSİTESİ ★ FEN BİLİMLERİ ENSTİTÜSÜ

KÜÇÜK HÜCRELİ DIŞI AKCİĞER KANSERİ VE MEZOTELYOMADA İMMÜN HÜCRELERİN HÜCRESEL KARAKTERİZASYONU

YÜKSEK LİSANS TEZİ

Gönül SEYHAN
(521141109)

Moleküler Biyoloji-Genetik ve Biyoteknoloji Anabilim Dalı

Moleküler Biyoloji-Genetik ve Biyoteknoloji Programı

Tez Danışmanı: Doç. Dr. Ayça Sayı Yazgan

HAZİRAN 2017

Gönül Seyhan, a M.Sc. student of ITU Graduate School of Science Engineering and Technology student ID 521141109, successfully defended the thesis entitled "CELLULAR CHARACTERIZATION OF IMMUNE CELLS IN NON-SMALL CELL LUNG CANCER AND MESOTHELIOMA", which she prepared after fulfilling the requirements specified in the associated legislations, before the jury whose signatures are below.

Thesis Advisor :	**Assoc. Prof. Ayça SAYI YAZGAN** Istanbul Technical University	.....
Jury Members :	**Assoc. Prof. Dr. Ceren ÇIRACI** Istanbul Technical University	.....
	Prof. Dr. Akif Turna Istanbul University	.....

Date of Submission : 5 May 2017
Date of Defense : 7 June 2017

To my family and friends,

FOREWORD

I would like to thank my advisor Assoc. Prof. Ayça SAYI YAZGAN for giving me the opportunity to carry out my thesis, for her guidance, patience and help. It was a great honour to become a member of her Immunology lab. I would also like to thank Prof. Akif TURNA for his precious time, patience, help and for providing the samples for my thesis. I also thank to Assoc. Prof. Ceren ÇIRACI for her precious time to evaluate my thesis.

I owe special thanks to Doğuş ALTUNÖZ, also a member of ASY lab, for his help, support and friendship. I consider myself lucky to study with him during both my undergraduate and graduate studies.

I would also like to thank to former and other current members of ASY LAB: Sawsan SAID, Mantasha TABASSUM, Güliz Tuba BARUT, Aslı KORKMAZ, Rana FUÇUCUOĞLU, Zeynep ESENCAN, Noel NABA, Tevriz Dilan DEMİR and Elif Merve AYDIN for their support and friendship.

Finally, I wanted to show my incomparable gratitude to my mother Dilek SEYHAN, my father Mehmet SEYHAN, my sister Gizem Nur SEYHAN and my brother Furkan SEYHAN for supporting me of anytime I need.

June 2017 Gönül SEYHAN

TABLE OF CONTENTS

Page

ABBREVIATIONS

µg : Microgram
µm : Micrometer
µM : Micromolar
APC : Antigen Presenting Cell
BAFF : B-Cell Activating Factor
BAFF-R : B-Cell Activating Factor Receptor
BCA : Bicinchoninic Acid
BCR : B-Cell Receptor
Br1 : B Regulatory 1
Breg : Regulatory B cell
BSA : Bovine Serum Albumin
CD : Cluster of Differentiation
CD40L : CD40 Ligand
CFSE : 5(6)-Carboxyfluorescein diacetate N-succinimidyl ester
Ctrl : Control
DC : Dendritic Cell
DLBCL : Diffuse Large B Cell Lymphoma
DMSO : Dimethyl Sulfoxide
EAE : Experimental Autoimmune Encaphalomyelitis
EDTA : Ethylenediaminetetraacetic Acid
FBS : Fetal Bovine Serum
FITC : Fluorescein Isothiocyanate
Foxp3 : Forkhead Box P3
g : Gram
h : Hour
HBSS : Hank's Balanced Salt Solution
HCC : Hepatocellular Carcinoma
IFNγ : Interferon Gamma
IL-4 : Interleukin-4
IL-6 : Interleukin-6
IL-8 : Interleukin-8
IL-10 : Interleukin-10
IL-17 : Interleukin-17
LAG-3 : Lymphocyte-Activation Protein 3
LC : Lung Cancer
LPS : Lipopolysaccharide
LSM : Lymphocyte Seperation Medium
M : Molar
MDSC : Myeloid-Derived Suppressor Cell
MHC-I : Major Histocompatibility Complex Class I
MHC-II : Major Histocompatibility Complex Class II
min : Minute
ml : Mililiter
mM : Milimolar

mm : Milimeter
MT : Mesothelioma
MyD88 : Myeloid Differentiation Primary Response Gene 88
ng : Nanogram
NK : Natural Killer Cell
NKT : Natural Killer T cell
Nrp1 : Neuropilin 1
NSCLC : Non Small Cell Lung Cancer
PBMC : Peripheral mononuclear blood cell
PBS : Phosphate Buffered Saline
PD-1 : Programmed Cell Death Protein 1
PD-L1 : Programmed Death-Ligand 1
PD-L2 : Programmed Death-Ligand 2
PE : Phycoerythrin
PHA : Phytohaemagglutinin
PMA : Phorbol-12-Myristate-13-Acetate
rpm : Revolutions Per Minute
RPMI : Roswell Park Memorial Institute
SCLC : Small Cell Lung Cancer
T2-MZP : Transitional 2 Marginal-Zone Precursor
TAM : Tumor-Associated Macrophages
TCR : T-cell receptor
TGF-β : Transforming Growth Factor-Beta
Th1 : T Helper 1
Th2 : T Helper 2
Th3 : T Helper 3
Th17 : T Helper 17
TIL : Tumor infiltrating leukocyte
TIL-B : Tumor infiltrating B Cell
TLR : Toll-Like Receptor
TLS : Tertiary Lymphoid Structure
TNF-α : Tumor Necrosis Factor-Alpha
Tr-1 : T Regulatory-1
Treg : Regulatory T cell

LIST OF TABLES

Page

LIST OF FIGURES

Page

CELLULAR CHARACTERIZATION OF IMMUNE CELLS IN NON-SMALL CELL LUNG CANCER AND MESOTHELIOMA

SUMMARY

Lung cancer is the leading cause of cancer deaths worldwide for both women and men. Mesothelioma, form of cancer concerning membrane surrounding the lungs, is under-examined especially in terms of immune cells. Tumor microenvironment mainly affects immunological responses via either suppressing effector cells or converting them to the regulatory cell types. Secretion of immune suppressor cytokines by regulatory cell types contributes to suppression of immune responses within cancer microenvironment. Regulatory cell types including regulatory T and B cells contribute to the inhibitory responses with their ability to secrete anti-inflammatory cytokines such as Interleukin-10 (IL-10).

This study aims to characterize immune cells in non-small cell lung cancer and mesothelioma according to cell surface molecules and cytokine profiles of the cells. Cellular characterization of effector and regulatory immune cells in blood and tumor tissue samples of non-small cell lung cancer and mesothelioma patients is aimed to be performed. Our second aim was to investigate the effects of NSCLC microenvironment on healthy T and B cells. Overall, this study especially aims to identify types of peripheral and tumor infiltrating regulatory B cells that are not identified before in lung cancer and mesothelioma. Most of the studies in the literature regarding regulatory B cells are restricted to the studies of peripheral blood, which reflects only a systemic immune responses for NSCLC. For that reason, investigating regulatory B cells within its microenviroment is necessary. To investigate the relationship among $CD4^+$ T cells, $CD19^+$ B cells and their subsets, T cell specific (CD4 and CD8), regulatory B cell specific (CD19, CD24 ve CD38), and PD-1 and PD-L1 cell surface molecules were examined along with anti-inflammatory (IL-10) and pro-inflammatory (IFNγ and IL-17) cytokine profiles.

In this study, we performed flow cytometry analysis of peripheral blood and tumor tissue samples collected from patients with NSCLC and mesothelioma from Istanbul University, Cerrahpaşa Medical School, Thoracic Surgery Department. Peripheral Mononuclear Blood Cells (PBMC) were isolated from both healthy and patient samples. Tumor infiltrating lymphocytes were obtained from tumor tissues that were resected during surgery. PBMC and TILs were stimulated with CpG ODN K3 (0,7 μg/ml) for 24 hours and PMA/ionomycin before staining of IL-10 and regulatory B cell surface markers. Immune cell characterization was performed by flow cytometry using anti-CD4, anti-CD8, anti-CD19, anti-CD24, anti-CD38, anti-PD1, anti-IL10, anti-IFNγ and anti-IL-17 antibodies. To study the effects of NSCLC microenvironment, $CD4^+$ T cells and B cells were purified from healthy PBMCs by magnetic cell sorting with a column free commercial reagent kit (Stemcell). Then, B and T cells were cultured in either tumor or normal tissue conditioned medium which were obtained by culturing cells of tumor and normal tissue for 2 days. After that,

IL10, IFNγ and PD-L1 expression were analyzed. Proliferation assay was also performed for T cells.

7 healty controls (3 females and 4 males, median age was 36 years; range, 25 to 52 years), 16 non-small lung cancer (3 females and 13 males, median age was 59 years; range, 42 to 69) and 3 mesothelioma (3 males, median age was 66 years; range 55 to 78) patients were analyzed. IL-10 expression of $CD4^+$ and $CD19^+$ (0.82-24.1%; 0.85-17.3%) cells were increased in bloods and also in TILs (0-23.7%; 0-20%) of patients with NSCLC compared with healthy individuals. $CD4^+$ $IL10^+$ (0-35.7%) cell frequencies were significantly increased in blood samples of mesothelioma patients. In addition, $CD19^+IL10^+$ cells were significantly increased in their tumors. IL-10 expression by $CD19^+CD24^+CD38^+$ B cells (0-75%) from lung cancer patients' blood were greater than $CD19^+CD24^+CD38^+$ B cells of healthy controls. PD-1 and IL-10 double positive B cells were significantly increased in PBMCs of LC patients (0,68-5,45%) in comparison to healthy individuals (0-0,94%).

We observed increased IL-10 expression by both $CD4^+$ T cells (0.82-24.1%) and $CD19^+$ B cells (0.85-17.3%) for blood samples of the patients with lung cancer. Moreover, there was a high incidence of IL-10 expression in their tumor infiltrating $CD4^+$ T cells (0-23,7%) and $CD19^+$ B cells (0-20%). In addition, tumor infiltrating $CD19^+IL\text{-}10^+$ B cells (1,15-10%) were significantly increased in mesothelioma patients. Our results were also showed that $IFN\gamma^+$ cytotoxic T cells were significantly decreased in TIL of lung cancer patients to the healthy control level compared with their blood samples (20,3-94,9% to 3,03-53,2%). In addition, IFNγ producing $CD4^+$ T cell frequencies were significantly decreased in bloods of LC patients (10,4-38,3% to 1,82-21,4%). In turn, increased $CD4^+IL\text{-}10^+$ T cell frequencies suggests that $CD4^+$ T cell response shift to the anti-inflammatory responses for both systemic and local responses. Moreover, our *in vitro* studies showed that IFNγ expression by $CD4^+$ T cells decreased (15,2 to 10,7%) in tumor microenvironment compared to normal one. Also, IL-10 production was significantly elevated in healthy control B cells when they were cultured with supernatant of primary NSCLC tumor cells.

Even though, we have low numbers of samples, the frequency of $CD19^+$ $CD24^+$ $CD38^+$ $IL\text{-}10^+$ B cells (0-75%) were highly increased in for NSCLC. PD-1 expression on B cells were significatly increased in both blood (2,14-11,1%) and tumor tissue (3,52-28,6%) samples of NSCLC patients compared to healthy individuals (0,79-3,9%). Moreover, PD-1 and IL-10 double positive B cells were significantly increased in both blood (0,68-5,45%) and tumor tissue samples (1,58-7,04%) of patients with NSCLC compared to healthy individuals (0-0,94%). Altogether, regulatory B cels were significantly elevated in both blood and TILs of patients with NSCLC while they were significantly elevated in TILs of patients with mesothelioma. We also observed that IL-10 production levels of $PD\text{-}L1^+$ B cells in tumor microenviroment were increased. In conclusion, these results indicate an anti-inflammatory environment within tumor region both in lung cancer and mesothelioma.

KÜÇÜK HÜCRELİ DIŞI AKCİĞER KANSERİ VE MEZOTELYOMADA İMMÜN HÜCRELERİN HÜCRESEL KARAKTERİZASYONU

ÖZET

Akciğer kanseri kadın ve erkeklerdeki kanser ölümlerinin başında gelmektedir. Akciğeri çevreleyen membranlarla ilgili bir kanser türü olan mezotelyoma ise özellikle immün hücreler yönünden oldukça az çalışılmıştır. Tümör mikroçevresi immünolojik cevapları efektör hücreleri baskılayarak ya da regülatör hücre tiplerinin oluşmasına neden olarak etkiler. Regülatör hücre tipleri tarafından salgılanan immün baskılayıcı sitokinler tümör mikroçevresinde cevabın baskılanmasına katkı sağlar. Regülatör T ve B hücreleri bunu genellikle anti-enflamatuvar bir sitokin olan interlökin 10'u salgılayarak yaparlar. Bu çalışma küçük hücreli dışı akciğer kanseri ve mezotelyomalı hastaların kanlarında ve tümöre infiltre lökositlerde bulunan regülatör ve efektör hücrelerin, ifade ettikleri yüzey belirteçlerine ve salgıladıkları sitokinlere göre aydınlatılmasını amaçlamaktadır. Özellikle çalışmamız daha önce akciğer kanserinde tanımlanmamış regülatör B hücrelerinin detaylı olarak tanımlanmasını amaçlamaktadır. Bu amaçla, T hücre spesifik (CD4, CD8), regülatör B hücre (Breg) spesifik (CD19, CD24 ve CD38), PD-1 ve PD-L1 yüzey belirteçleri ile anti-enflamatuvar (IL10) ve pro-enflamatuvar (IFNγ, IL17) sitokin profillerinin incelenmiştir.

İstanbul Üniversitesi, Cerrahpaşa Tıp Fakültesi, Göğüs Cerrahisi bölümüne başvuran KHDAK ve mezotelyomalı hastalardan elde edilen periferik kan örneklerinden mononükleer kan hücreleri (PBMC) ve cerrahi operasyon sonrasında alınan tümör dokusundan Tümör infiltre lökosit (TIL) elde edilmiştir. IL10 ve Breg yüzey boyamaları öncesi PBMC ve TIL CpG ODN K3 (0.7 μg/ml) ile 24 saat uyarılmıştır. Hücre tipleri ve sitokin profilleri anti-CD4, anti-CD8, anti-CD19, anti-CD24, anti-CD38, anti-PD1, anti-IL10, anti-IFNγ ve anti-IL-17 antikorlarıyla boyanarak akan hücre ölçerde analiz edilmiştir. NSCLC mikroçevresinin etkilerini araştırmak için, $CD4^+$ T hücreleri ve B hücreleri sağlıklı PBMClerden manyetik ayırım yöntemi (Stemcell) ile izole edilmiştir. Daha sonra izole edilen T ve B hücreleri, tümör ve normal doku hücrelerinin 2 gün hücre kültüründe tutulması ile elde edilen tümör ya da normal doku besi ortamında bekletilmiştir.

7 sağlıklı kontrol, 16 KHDAK ve 3 mezotelyomalı hastada analiz yapılmıştır. $CD4^+$ ve $CD19^+$ (%0.82-24.1; %0.85-17.3) hücrelerin IL-10 ekspresyonu kontrol ile karşılaştırıldığında KHDAK hastalarının hem kan hem de TIL'lerinde (%0-23.7; %0-20) artmıştır. $CD4^+$ $IL10^+$ (%0-35.7) hücre oranları mezotelyomalı hastaların kanlarında anlamlı bir şekilde artmıştır. Ayrıca, tümörlerindeki $CD19^+$ $IL10^+$ hücreler de anlamlı bir şekilde artmıştır. Akciğer kanseri hastalarının kanlarındaki $CD19^+CD24^+CD38^+$ B hücrelerinin IL-10 ekspresyonu (%0-75) sağlıklı kontroller ile karşılaştırıldığında daha fazladır. Hem PD-1 hem IL-10 pozitif B hücreleri

sağlıklı kontroller ile karşılaştırıldığında (%0-0,94) KHDAK hastalarında (%0,68-5,45) anlamlı bir şekilde artmıştır.

Akciğer kanseri hastalarının kan örneklerinde, hem $CD4^+$ T hücreleri (%0.82-24.1) hem de $CD19^+$ B hücreleri (%0.85-17.3) tarafından artan IL-10 ekspresyonu saptanmıştır. Dahası, tümöre infiltre $CD4^+$ T hücreleri (%0-23,7) ve $CD19^+$ B hücrelerinde (%0-20) yüksek oranda IL-10 ekspresyonu vardır. Ayrıca $CD19^+$ $IL\text{-}10^+$ B hücreleri (%1,15-10) mezotelyomalı hastalarda anlamlı bir şekilde artmıştır. Sonuçlarımız $IFN\gamma^+$ sitotoksik T hücrelerinin, akciğer kanseri hastalarının TIL'lerinde kandaki miktarına göre anlamlı bir şekilde azalıp, sağlıklı kontrollerin seviyesine indiğini göstermiştir (%20,3-94,9 den %3,03-53,2 e). Buna ek olarak, IFNγ üreten $CD4^+$ T hücre oranları KHDAK hastalarının kanlarında anlamlı bir şekilde azalmıştır (%10,4-38,3 den %1,82-21,4 e). Bu nedenle, artmış $CD4^+$ $IL\text{-}10^+$ T hücre oranları, $CD4^+$ $IL\text{-}10^+$ T hücre cevabının hem sistemik hem de lokal cevaplar için anti-enflamatuvar yöne kaydığını göstermektedir. Ayrıca, *in vitro* çalışmamız $CD4^+$ T hücreleri tarafından eksprese edilen IFNγ nın normal mikroçevre ile karşılaştırıldığında tümör mikroçevresinde azaldığını göstermektedir (%15,2 den 10,7 ye). Sağlıklı kontrol B hücreleri de primer KHDAK tümör hücrelerinin süpernatantı ile muamele edildiğinde IL-10 üretimini anlamlı bir şekilde artırmıştır.

Her ne kadar örnek sayımız az olsa da, $CD19^+$ $CD24^+$ $CD38^+$ $IL\text{-}10^+$ B hücrelerinin oranı (%0-75) KHDAK'ta önemli derecede artmıştır. B hücrelerinin PD-1 ekspresyonu, sağlıklı kontroller ile karşılaştırıldığında (%0,79-3,9), KHDAK hastalarının hem kan (%2,14-11,1) hem de tümör örneklerinde (%3,52-28,6) anlamlı bir düzeyde artmıştır. Dahası kanlarındaki (%0,68-5,45) ve tümor doku örneklerindeki (%1,58-7,04) hem PD-1 hem IL-10 pozitif hücreler, sağlıklı kontroller ile karşılaştırıldığında (%0-0,94) anlamlı bir oranda artmıştır. Bu sonuçlara göre, KHDAK hastalarının hem kanlarındaki hem de TIL'lerindeki regülatör B hücreler anlamlı bir şekilde artarken mezotelyomalı hastaların TIL'lerinde anlamlı bir şekilde artmıştır. Ayrıca, tümör mikroçevresinde $PD\text{-}L1^+$ B hücrelerinin IL-10 üretimi de artmıştır. Sonuç olarak bu veriler hem akciğer kanseri hem de mezotelyomada anti-enflamatuvar bir mikroçevreye işaret etmektedir.

1. INTRODUCTION

1.1 Lung Cancer

Lung cancer is the leading cause of mortality worldwide for both women and men. It is also the most common cancer type in males in Turkey and in the first place for males and females in mortality rates (Turkey Cancer Statistics 2017, TC Ministry of Health Turkish Public Health Institution). There are two groups of lung cancer that differ from each other in terms of biological features, clinical course and treatment approaches: small cell (SCLC) and non-small cell lung cancer (NSCLC). NSCLC is also a heterogenous group of lung cancer and including three types: adenocarcinoma, squamous cell carcinoma and large cell carcinoma (Yi et al., 2014) (Figure 1.1).

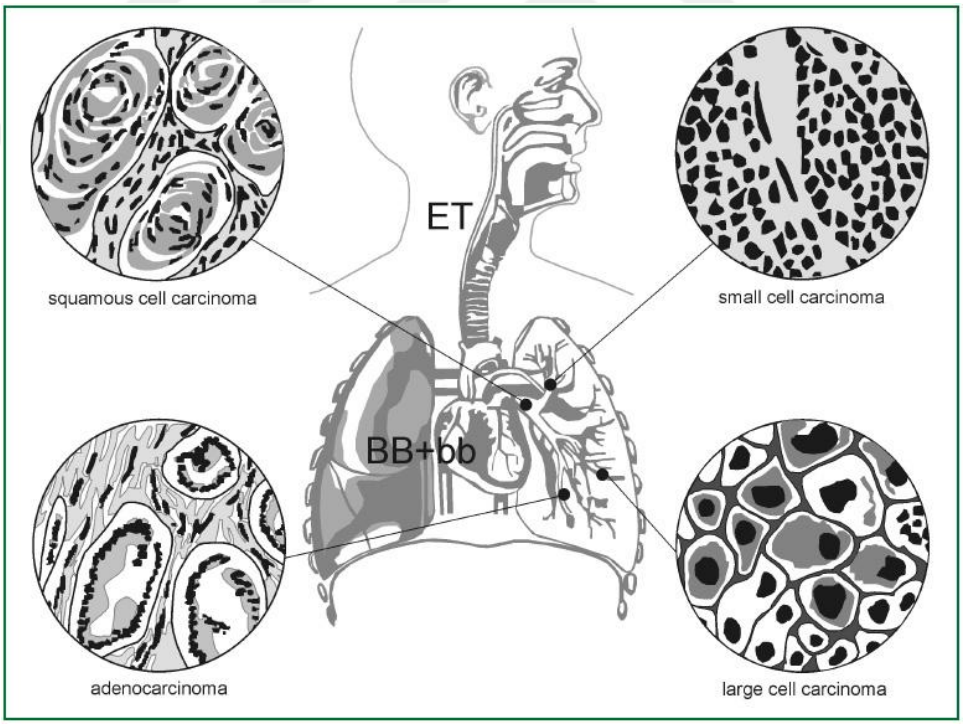

Figure 1.1 : Main types of lung cancer and their preferantial formation sites in lung, adapted from (Strum et al., 2011).

Essential immune-based cancer therapies were developed against lung cancer. There are numerous immunotherapy strategies which have clinical applications such as

immune checkpoint inhibitors. Different antibodies for instance nivolumab, atezolizumab, pembrolizumab, avelumab, tremelimumab and ipilimumab are very promising as immune checkpoint inhibitors. They function by inhibiting or a as antagonist of programmed cell death 1 (PD-1), programmed cell death ligand 1 (PD-L1) and cytotoxic T-lymphocyte–associated antigen 4 (CTLA 4) inhibitory molecules. Main idea is to reverse inhibitory mechanisms and increase the effect of immune response in anti-tumor immunity primarily by inducing anti-tumoral T cell activation (Brahmer and Pardoll, 2013, Anagnostou and Brahmer, 2015). In addition, it is also critical to know mechanisms of the anti-tumor immunity since those molecules are expressed on various cell types.

1.2 Mesothelioma

Mesothelioma is a form of cancer concerning membrane surrounding the lungs. Incidence of mesothelioma is very rare worldwide. Main cause of mesothelioma was revealed as asbestos which is a common name for silicate minerals. Asbestos can influence immunecompetent cells, so in turn incidence and progression of malignant mesothelioma. Even though there are some studies about the effects of asbestos on mesothelioma and immune cells such as natural killer (NK) cells and T helper cells (Miura et al., 2008, Nishimura et al., 2012), better characterization studies are required especially to elucidate the effects of immune cells in the tumor microenviroment.

1.3 T Cells

T cells mature in the thymus, express T cell receptor (TCR), and can express either CD8 glycoprotein on their surface and are called $CD8^+$ T cells (cytotoxic) or CD4 glycoprotein and are then called $CD4^+$ cells (helper T cells or regulatory T cells) (Figure 1.2).

Once T cells have completed their development, they circulate between blood and lymph and pass from different secondary lymphoid tissues until they are activated. Naive T cells are the cells that have not encounter any antigen yet. Activated T cells differentiate into effector and memory cells, which may remain in the lymphoid organs or migrate to non-lymphoid tissues. T cell mediated immunity is a part of

adaptive immune system which fights against microbial infections in an antigen specific manner. To induce this type of responses, antigen presenting cells (APCs) such as macrophages, dendritic cells and B cells must present specific antigens to the T cells via interaction of MHC on their surface and T cell receptor (TCR) on T cells. In addition to that, the proliferation and differentiation of naive T cells also require signals provided by costimulatory molecules expressed by APCs. B7 family is the best-defined co-stimulatory molecules that interact with CD28 on T cells. Expression of B7 co-stimulators such as CD80 (B7.1) and CD86 (B7.2) on APCs increase by encountering microbes to generate an optimum response. Although, some members of CD28 family such as transmembrane protein cytotoxic T-lymphocyte antigen-4 (CTLA4) and programmed cell death 1 (PD-1) can inhibit T cell responses to control the hyperactivation of immune responses. IL-2 is also an important player for the generation of antigen-specific clones. After activation, T cells express high levels of IL-2 receptor and IL-2 which drives the proliferation of cells (Abbas et al., 2012).

Activated T cells go through clonal expansion and proliferate rapidly. They exert their effector functions through cell mediated cytotoxicity and production of various cytokines.

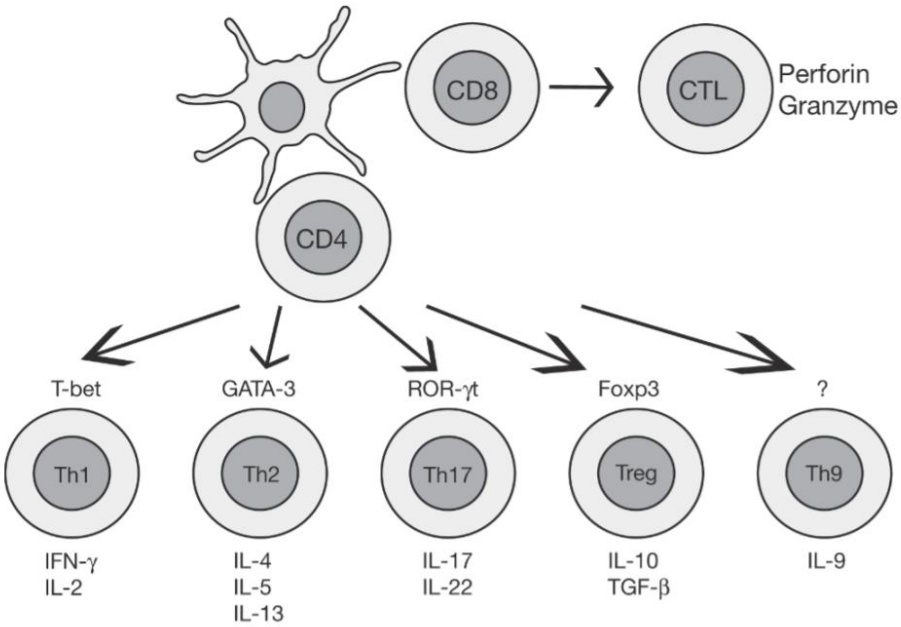

Figure 1.2 : Different types of T cells and their development adapted from (Broere et al., 2011).

1.3.1 $CD8^+$ T cells

Naive $CD8^+$ T cells differentiate into cytotoxic T cells as a result of antigenic peptide presentation by APCs. Cytotoxic $CD8^+$ T cells secrete anti-tumor and anti-viral cytokines such as TNF-α and IFNγ. They can also lead to the apoptosis of target cells either by perforin-granzyme or Fas-Fas ligand mediated pathways. Perforin makes pores in the membrane of infected or malignant cell, thereby granzyme can enter into the target cell and lead to the apoptosis of it. Another strategy for killing target cells by $CD8^+$ cytotoxic T cells is Fas-Fas ligand mediated killing. Fas is expressed on the surface of activated CD8+ T cells and interact with FasL on the target cell. This interaction leads to the activation of caspase cascade and result in apoptosis of the target cell (Broere et al., 2011).

1.3.2 $CD4^+$ T cells

$CD4^+$ T cells are classified generally as T helper cells (Th) and regulatory T cells (Treg). Th cells have roles in adaptive immunity against cancer and pathogens through activation of other effector immune cells. On the other hand, Tregs are immunosuppressive cells that supress potential harmful effects of immune cells.

T helper 1 (Th1) cells are defined as interferon gamma (IFNγ), tumor necrosis factor alpha (TNF-α) secreted $CD4^+$ T cells. They mediate immune responses against intracellular pathogens by helping to macrophages and cytotoxic T cells to kill pathogens. T helper 2 (Th2) cells are polarized by IL-4 and trigger humoral immunity including B cell proliferation, class-switching and antibody production. They produce IL-4, IL-5, IL-6, IL-10, and IL-13 cytokines and relate to inflammatory diseases such as allergy and asthma. Th17 cells are known for their protective effects against extracellular pathogens (Romagnani, 1999).

1.3.3 Regulatory T cells

Regulatory T cells (Tregs) play a crucial role in maintaining immunological unresponsiveness to self-antigens and in suppressing excessive immune responses deleterious to the host. Tregs suppress generally induction and proliferation of effector cells. Until the discovery of Foxp3, a Treg specific marker, those cells had been identified with unspecific markers such as CD25 or CD45RB (Hori et al., 2003, Fontenot et al., 2005).

Tregs have been divided into two groups: Foxp3$^+$ natural Tregs and inducible Tregs (Figure 1.3). Natural regulatory T cells express the cell-surface marker CD25 and transcription factor Foxp3. Other populations of antigen-specific Tregs can be induced from naive CD4$^+$CD25$^-$ or CD8$^+$CD25$^-$ T cells in the periphery. The inducible populations of Tregs are T regulatory 1 (Tr1) cells, which secrete high levels of IL-10, no IL-4 and no or low levels of IFNγ; and T helper 3 (Th3) cells, which secrete high levels of TGF-beta. Even though CD8$^+$ T cells are associated with cytotoxic T-lymphocyte function, there are inducible CD8$^+$ regulatory T cells which differentiate from naïve CD8$^+$CD25$^-$ T cells and can secrete IL-10 (Mills, 2004). It is well known that Foxp3 is a critical factor for Treg functions but Tr1 subtype of Tregs does not express it (Groux et al., 1997, Levings et al., 2005).

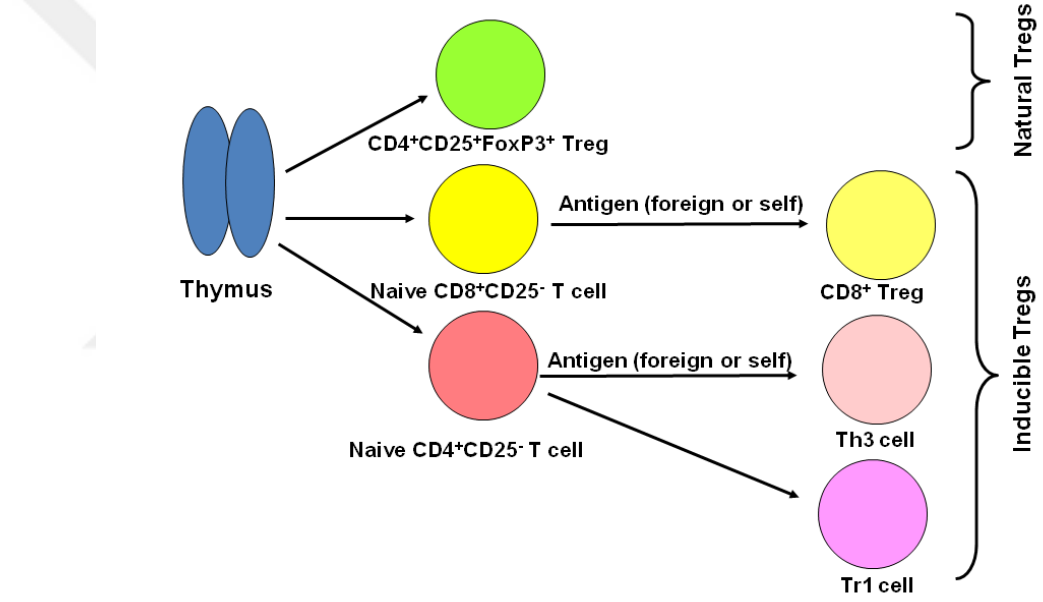

Figure 1.3 : Major subtypes of regulatory T cells, adapted from (Mills, 2004).

Some studies demonstrated that Foxp3$^+$ Tregs could differentiate into effector Th cells via down regulation of Foxp3 (Floess et al., 2007). On the other hand, it is proposed that regulatory B cells could convert Foxp3$^-$ T cells into Foxp3$^+$ Tregs or could expand Treg cell population (Lee et al., 2014).

Tregs can induce immunosuppression through contact-dependent mechanisms such as the expression of cytotoxic T-lymphocyte-associated protein 4 (CTLA-4), programmed cell death 1 (PD-1), programmed death ligand 1 (PD-L1), lymphocyte-activation protein 3 (LAG-3), CD39/73 and neuropilin 1 (Nrp1), or through contact independent mechanisms, including the sequestration of IL-2 and the production of

the soluble immunosuppressive molecules IL-10, TGF-β, adenosine, prostaglandin E2 (PGE2) or galectin-1 (Marshall et al., 2016).

1.4 B Cells

B cells are important players of adaptive immunity to fight against pathogens with the ability of antibody production, antigen presentation and generation of immunological memory. B cells originate from hematopoietic stem cells. After V(D)J gene recombinations, immature B cells originate in bone marrow. They exit from bone marrow and enter circulation as transitional B cells. Then, they enter to spleen to differentiate into either marginal zone (MZ) B cells or follicular B cells depending on their B cell receptors (BCRs) by getting survival signals through BAFF-R (Figure 1.4). First stage of development of B cells is completed in spleen. After activation with a specific antigen, they enter lymph node or other lymphoid tissues. The first activation signal occurs upon antigen binding to BCRs. Then, MZ B cells differentiate into antibody producing short-lived plasma cells in spleen. While follicular B cells develop in germinal centers into memory B cells or antibody producing long-lived plasma cells (Nelson, 2010, Pieper et al., 2013).

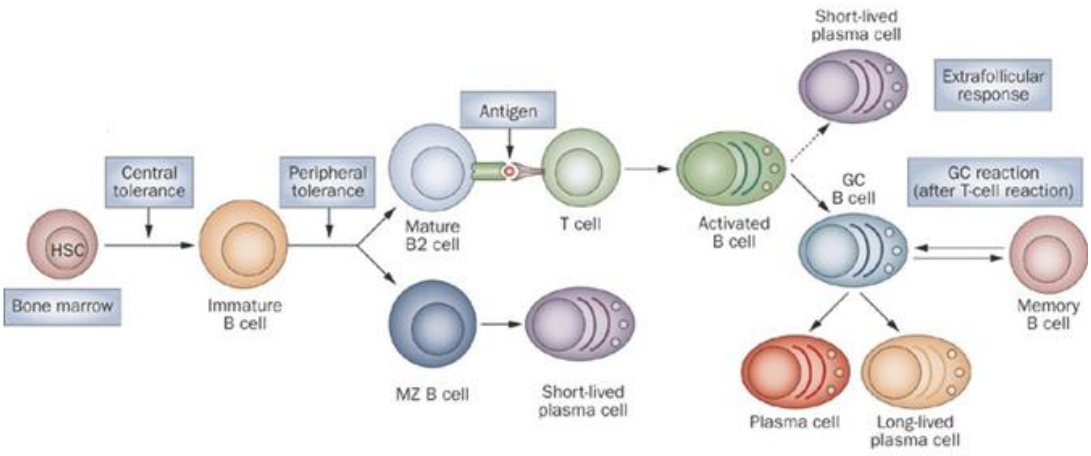

Figure 1.4 : Development of B cells, adapted from (Dorner et al., 2009).

Second activation signal occurs by either thymus independent or dependent pathways. Since B cells are antigen presenting cells (APC), they present antigens to T cells. In turn T cells provide second activation signal through their secreted cyokines and CD40-CD40L interaction. Activated T cells express CD40L which binds to the CD40 on B cells. This leads to the transcription of immunoglobulin genes, the release of cytokines from T cells and B cell proliferation. After the

completion of T dependent B cell maturation in GCs, some of antigen activated B cell develop into memory B cells that are capable of mounting rapid antibody responses.

In thymus independent mechanisms, B cells can be activated with antigens directly. Those antigens can further be subdivided into type I and type II antigens. Type I antigens are mitogenic stimuli such as lipopolysaccharide (LPS) or CpG. They activate B cells through toll-like receptors. On the other hand, type II antigens are generally polysaccharides that engage BCR and thus induce antigen specific B cell responses. Whereas TI type I antigens can activate both immature and mature B cells, TI type II antigens only activate mature B cells (Murphy, 2012).

1.4.1 Regulatory B cells

B cells with immune suppressive functions were determined in different immune contexts beside their protective role by antibody production, cytokine secretion and antigen presentation to enhance inflammatory responses. Discovery of B cells with regulatory roles happened thanks to the mouse disease models. First evidence is that B cell deficient mice did not recovered from experimental autoimmune encephalitis (EAE) (Wolf et al., 1996). Following that, studies in chronic colitis conducted by Mizoguchi et al. lead to use of "regulatory B cells" term for B cells with inhibitory features for the first time (Mizoguchi and Bhan, 2006). From that time, researchers showed those Bregs in murine autoimmune and allergic diseases such as collagen induced arthritis (CIA) (Fillatreau et al., 2002), contact hypersensitivity (CHS) (Yanaba et al., 2008), EAE (Matsushita et al., 2008), asthma (Amu et al., 2010) and lupus (Watanabe et al., 2010). Researchers also identified different phenotypes of Bregs in various studies with different disease concepts. However, phenotypes, molecular features and functions of Bregs remained to be clarified (Table 1.1).

1.4.2 Phenotypes and markers of human Bregs

To date, scientists have not revealed a unique phenotype marker to identify Bregs since all markers associated with Bregs are also expressed by other B cell subpopulations. Up to date, many Breg subsets with similar phenotypes and effector functions have been described. Several Breg subtypes were identified in mice: transitional 2 marginal-zone precursor (T2-MZP) cells, $CD5^{+}CD1d^{hi}$ B (B10) cells,

marginal-zone (MZ) B cells, Tim-1^+ B cells, $CD138^+$ plasma cells and plasmablasts (Rosser and Mauri, 2015).

First human B cell that was suggested to have a regulatory function was $CD19^+CD25^+$ B cells. They were chracterized as memory B cells ($CD27^+$) expressing high levels of immunoglobulins and IL-10 (Amu et al., 2007). Later, both transitional $CD19^+$ $CD24^{hi}$ $CD38^{hi}$ $CD1d^{hi}$ (Blair et al., 2010, Flores-Borja et al., 2013) and memory $CD19^+$ $CD24^{hi}$ $CD27^+$ (Iwata et al., 2011) Bregs were identifed in humans.

Additionally, surface antigens expressed by B cells have been shown to confer regulatory properties. Programmed death 1 ligand (PD-L1) interacts with PD-1 on T cells to induce tolerance and limit effector T cell responses. It has recently been shown to be expressed on human malignant B cells in several types of lymphoma including diffuse large B cell lymphoma (DLBCL), Hodgkin's lymphoma, and follicular lymphoma (Schwartz et al., 2016).

Recently, Xiao et al. (2016) identified a novel tumor-promoting PD-1^{high} Breg subset with $CD5^{high}$ $CD24^{-/+}$ $CD27^{high/+}$ $CD38^{dim}$ phenotype in tumor tissues of patients with hepatocellular carcinoma (HCC). They showed increased tumor infiltration of $PD1^{high}$ Bregs which produced IL-10 upon interaction with PD-L1 or anti-PD1 antibody. Increased tumor infiltration with PD-1^{high} IL-10-producing Bregs was associated with reduced number and dysfunction of $CD8^+$ cells. These findings identify a uniquely suppressive PD-1^+ B cell subset in HCC pathogenesis (Xiao et al., 2016).

Table 1.1 : Different Breg cell types in mouse and human.

Breg Subset	Mouse	Human	References
T2-MZP cells	$CD19^+CD21^{hi}$ $CD23^{hi}CD24^{hi}$	-	(Evans et al., 2007)
MZ cells	$CD19^+CD21^{hi}CD23^-$	-	(Bankoti et al., 2012)
B10 cells	$CD5^+CD1d^{hi}$	$CD24^{hi}CD27^+$	(Iwata et al., 2011, Yanaba et al., 2008)
Plasma cells	$CD138^+$MHC-$11^{lo}B220^+$	-	(Shen et al., 2014)
Tim-1^+ B cells	$CD19^+$Tim-1^+	-	(Ding et al., 2011)
Plasmablast	$CD138^+CD44^{hi}$ -	$CD19^+CD24^{hi}$ $CD27^{int}$	(Matsumoto et al., 2014)
Immature cells	-	$CD19^+CD24^{hi}CD38^{hi}$	(Blair et al., 2010)

Table 1.1 (continued) : Different Breg cell types in mouse and human.

Breg Subset	Mouse	Human	References
Br1 cells	-	-	(van de Veen et al., 2013)
PD-L1^{hi} B cells	CD19^{+}PD-L1^{hi}	CD19^{+}CD5^{hi}CD24$^{-/+}$	(Khan et al., 2015)
PD-1^{hi} B cells	-	CD27$^{hi/+}$CD38^{dim}	(Xiao et al., 2016)

Br1: B regulatory 1, MZ: marginal zone; T2-MZP: transitional 2 marginal-zone precursor, Tim-1: T cell Ig domain and mucin domain protein 1, PD-L1: Programmed death-ligand 1.

1.4.3 Regulatory mechanisms of Bregs

IL-10 is an anti-inflammatory cytokine and various immune cells such as monocytes, macrophages, dendritic cells, B cells, CD4^{+} and CD8^{+} T cells are able to produce IL-10 to suppress inflammatory responses (Couper et al., 2008). Many studies showed that Bregs suppress immune functions via interleukin-10 (IL-10) production (Mauri and Bosma, 2012). IL10, but not TGFβ, production by CD19^{+} CD24^{hi} CD38^{hi} cells inhibited production of pro-inflammatory cytokines by CD4^{+} cells (Blair et al., 2010). In addition, IL-10 secreted by CD19^{+} CD24^{hi} CD27^{+} B cells regulated cytokine production of monocytes (Iwata et al., 2011). CD19^{+} CD24^{hi} CD38^{hi} CD1d^{hi} B cells were shown to inhibit CD4^{+} T cell proliferation and enhance Foxp3 expression in regulatory T cells by through both IL10 and TGFβ (Flores-Borja et al., 2013).

Even though Bregs exert their suppressive responses mainly by producing IL-10 in both mouse and humans, there are also different subsets of Bregs that have IL-10 independent mechanisms (Floudas et al., 2016, Tedder, 2015). Rosser and Mauri (2015) reviewed that Bregs can suppress the differentiation of pro-inflammatory cells including IL12 producing dendritic cells, TNF-α producing monocytes, cytotoxic T cells, Th1 and Th17 cells through IL10, IL35 and TGFβ production. In addition, Bregs can also induce immune cells to differentiate into immunosuppressive T cells such as Foxp3^{+} Tregs and Tr1 cells (Figure 1.5).

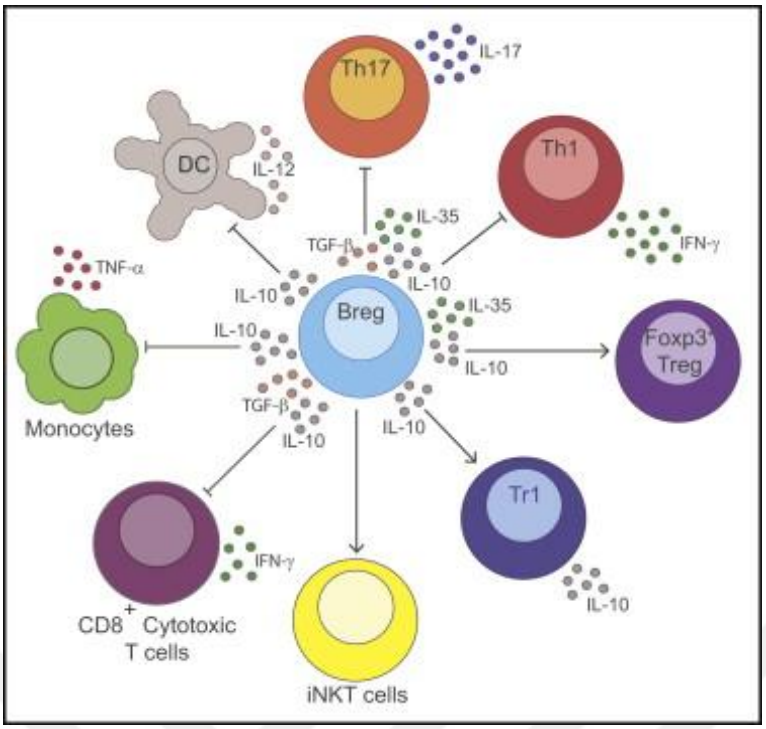

Figure 1.5 : Regulatory mechanisms of Bregs, adapted from (Rosser and Mauri., 2015).

IL-10 producing Bregs are identified in different infection, inflammation and tolerance settings, so it is likely that different stimuli and signals have important roles to induce activation of Bregs. Those signals can be distinguished into two groups: exogenous infectious stimuli and endogenous immune-mediated signals. Toll-like receptors (TLR) are pattern recognition receptors that sense the various microbial products and activate a range of immune cells. B cells express a variety of TLRs that have important functions after their activation (Vitale et al., 2010). A study used LPS treatment to induce IL-10 production by B cells and those TLR-activated B cells can suppress T-cell mediated autoimmunity in mice (Fillatreau et al., 2002). Later, the group of Fillatreau (Lampropoulou et al., 2008) showed that specific TLRs are the potent inducers of suppressive B cells and important for the induction of IL-10 secretion by B cells. LPS from Gram-negative bacteria and CpG-containing oligonucleotides that mimic bacterial DNA have been shown to inhibit disease progression in mouse model of T cell-mediated autoimmunity. The authors also showed that MyD88 dependent TLR signaling is both necessary and sufficient to stimulate IL-10 production by splenic mouse B cells. Also, immune mediated

signals such as CD40, CD80, CD86 and BAFF have been reported to induce IL-10 secretion by B cells (Yang et al., 2010, Mauri and Bosma, 2012, Mann et al., 2007).

1.5 Immune System and Tumors

Immune cells can recognize and destroy tumor cells in order to prevent tumor formation. Although, as a consequence of the tumor microenvironment, immune cells with regulatory characteristics may increase upon cancer development.

1.5.1 Tumor microenvironment

Tumor microenvironment contains immune cells along with the malignant cells and has a dynamic balance due to inhibitory and stimulatory signals. Tumor cells may express different antigens as a result of the genetic and epigenetic alterations during cancer formation (Topalian et al., 2012). Both innate and adaptive immune system have a potential to destroy cancer cells and inhibit tumor growth. Natural killer (NK) cells, and antigen presenting cells such as macrophages and dendritic cells are at the innate immunity arm. They mediate antigen non-specific and rapid responses. Adaptive immune system consists of humoral and cellular responses, B and T cells respectively, has greater effect on anti-tumor immunity for certain. In order to eliminate cancer cells, antigen presenting cells (APC) must recognize those antigens and present them to T cells to activate them. Then, activated T cells might kill the cancer cells (Liu and Zeng, 2012).

Different co-stimulatory (CD27, CD28, CD137, GITR, and OX-40) and co-inhibitory molecules (CTLA-4, PD-1, TIM3, LAG3, and KIR) expressed on the surface of effector immune cells regulate the T cell-mediated immunity. Co-stimulatory molecules promote T-cell response while co-inhibitory molecules restrain immune response to prevent autoimmunity in physiological status. The ligands of this molecules are also found on non-immune cells such as tumor cells and some normal cells of solid organs besides immune cells such as APCs (Sundar et al., 2014). Interaction between those molecules and their ligands can lead to immune tolerance. Moreover, cancer cells use those mechanisms to escape from the immune system by creating a immune suppressive microenviroment that down regulates T cell activation and cell signalling (Topalian et al., 2014).

The programmed cell death 1 (PD-1) pathway is an important way of immune resistance exerted by tumors. PD-1, which is a CD28 receptor family member was recommended as a mediator of programed cell death in lymphocytes. Recent studies showed that it was upregulated on activated B and T cells while their naive counterparts had low expression level (Yao and Chen, 2014). The role of PD-1 was understood as attenuator of the immune response. PD-1 has two known ligands: programmed death cell receptor ligand 1 (PD-L1) and programmed death cell receptor ligand 2 (PD-L2) (Figure 1.6). Upregulation and subsequent binding of PD-1 to its ligands provide an inhibitory signal during the effector phase of the T-cell response, reducing cytokine production, cell proliferation and cell survival signaling. PD-1 is also highly expressed on Treg cells and enhancing their proliferation upon binding to its ligands (Pardoll, 2012). Furthermore, in NSCLC, increased PD-1 expression on tumor infiltrating $CD8^+$ T cells was associated with impaired immune function (Zhang et al., 2010).

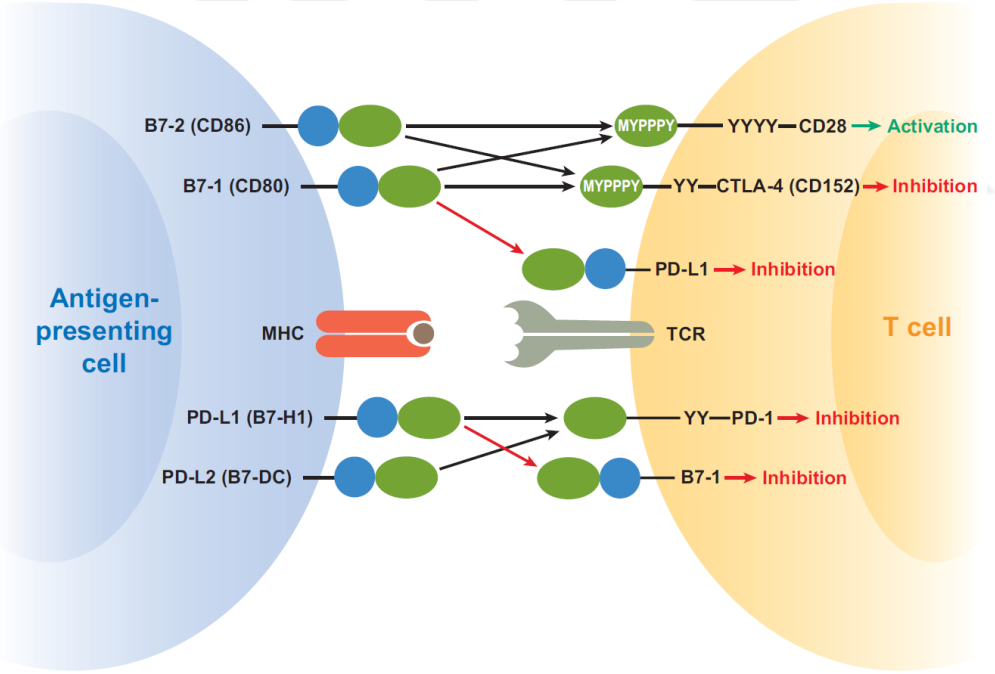

Figure 1.6 : PD-1 and its ligands, adapted from (Keir et al., 2008).

PD-L1 and PD-L2 are also expressed on tumor cells and thought to have a survival role through PD-1 pathway. PD-L1 expression on tumor cells are induced by IFNγ secretion by infiltrating T helper cells (Mellman et al., 2011, Zou, 2005). In NSCLC tumors, PD-L1 expression has been found to be upregulated (Chen et al., 2012), and

shown to be correlated with reduced tumor T cell infiltration (Konishi et al., 2004) and also an unfavorable prognosis (Chen et al., 2012, Mu et al., 2011, Sznol and Chen, 2013). Lung tumor cells may also release immune suppressive cytokines such as IL-10 and TGFβ (Domagala-Kulawik et al., 2014).

1.5.2 Infiltration of immune cells

Immune cell infiltration is a key feature of almost all cancer types, including mast cells, tumor-associated macrophages (TAMs), NK cells, NKT cells, B, and T lymphocytes. Tumor infiltrating lymphocytes (TILs) refer to the lymphocytes within and around the tumor cells. Many tumors appear to have an organizational architecture that includes B cell–T cell segregation and the presence of a high endothelial venule–like vascular structure. This architecture was named as tertiary lymphoid structures (TLSs). Dieu-Nosjean et al. (2008) also found that immune cells were organized in TLSs in NSCLC tumors, absent in nontumoral lung. It was reported to be associated with a protective immunity in NSCLC patients (Germain et al., 2014).

The immune microenvironment in lung tumors comprise T cells, B cells, natural killer cells, mature and immature dendritic cells (follicular dendritic cells), tumor-associated macrophages (TAMs, type 2), myeloid-derived suppressor cells (MDSCs), neutrophils (N1, antitumorigenic; N2, protumorigenic), and mast cells. The great majority of immune cells are found at the interface between the tumor and the normal tissue (invasive margin), and some are organized into tertiary TLSs. The latter are considered a gateway for the entrance of immune cells from the blood to the tumor (Bremnes et al., 2016) (Figure 1.7).

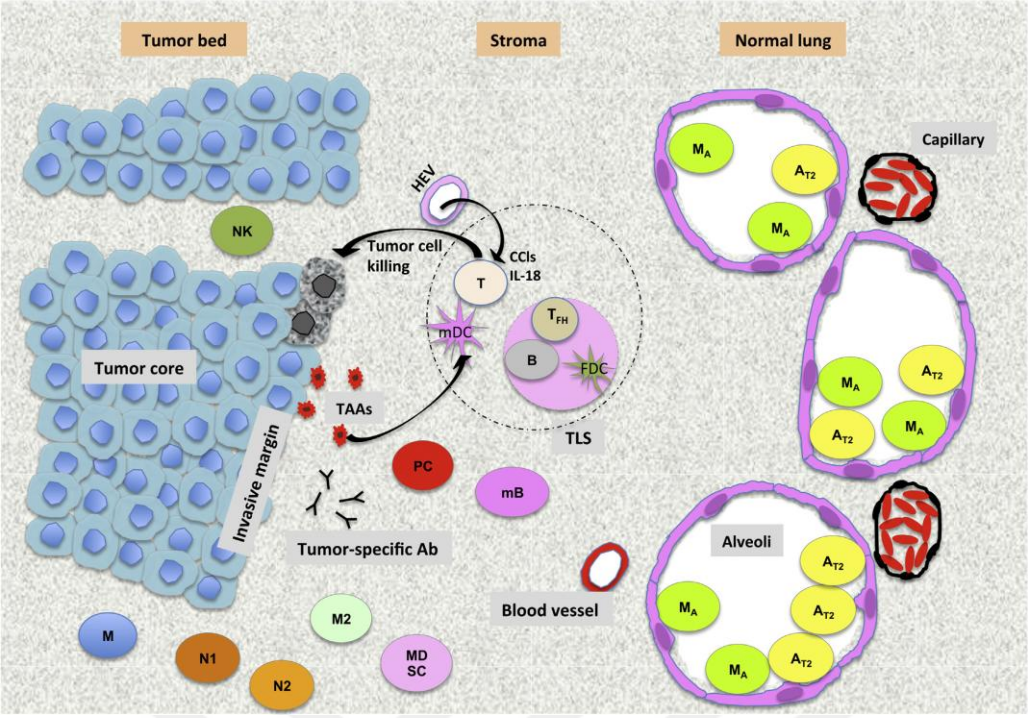

Figure 1.7 : The immune contexture in non–small cell lung cancer, adapted from (Bremnes et al., 2016).

1.5.2.1 T cell infiltration

Infiltration of $CD4^+$ and $CD8^+$ T cells have been reported to be a good prognostic factor in lung cancer. Al-Shibli et al. (2008) reported that increasing numbers of stromal $CD4^+$ cells correlated significantly with positive prognostic indicators for resected NSCLC patients. Moreover, it was reported that TILs composed mostly of $CD8^+$ T cells were significantly associated with improved survival and correlated with tumor grade, size, vascular invasion and poor levels of differentiation among NSCLC patients (Ruffini et al., 2009).

Despite the role of T lymphocytes in immune surveillance and control of early tumor growth, secretion of cytokines and other soluble molecules from tumor cells recruits Tregs to the tumor site. Tregs mediate immune tolerance and suppression of T cell mediated immunity. Increased numbers of Tregs were found in NSCLC tumors compared to normal tumor (Ishibashi et al., 2006). Tregs, which constitutively express high levels of CTLA-4 in patients with lung cancer, directly inhibit autologous T cell proliferation. In this manner, a high percentage of Tregs creates an immune suppressive microenviroment that promotes tumor growth (Woo et al.,

2002). Moreover, patients with stage I NSCLC had higher proportion of Tregs relative to cytotoxic cells, and they had a significantly higher risk of recurrence (Petersen et al., 2006).

1.5.2.2 B cell infiltration

Tumor infiltrating B (TIL-Bs) cells can have both positive and negative effects in tumor microenviroment. First of all, after antigen recognition they produce tumor specific antibodies. B cells are also antigen presenting cells, so they can present tumor antigens to T cells in order to promote anti-tumor immunity (Crawford et al., 2006). A study in NSCLC showed co-localization of tumor infiltrating B cells and $CD8^+$ T cells (Al-Shibli et al., 2008). Shen et al. (2016) speculating that $CD20^+$ B cells might have a role as APCs in tumor enviroment according to this and other studies. B cells can also influence other immune cells through cytokine production. There are some cancer studies correlate TIL-Bs with favorable clinical outcomes.

Visser et. al. (2005) found that genetic elimination of mature B and T cells limited neoplastic progression in a mouse model. The study showed that B cells may be associated with tumor promotion. TIL-Bs exert their suppressive mechanisms mainly by Bregs through IL-10, IL-35, TGFβ production and affecting other immune cell types (Figure 1.8). First indication that human Bregs may acquire malignant expansion was found in chronic lymphocytic leukemia (DiLillo et al., 2013). They found that chronic lymphocytic leukemia cells resembled Bregs in their phenotype and IL-10 secretion. In NSCLC patients, the frequency and absolute number of B10 cells are significantly elevated and further associated with the clinical stage. The number of B10 cells are significantly increased in stage IV NSCLC patients compared with healthy controls and stage II and III patients (Liu et al., 2016). Increased numbers of Bregs may lead to poor clinical prognosis in NSCLC and ovarian cancer (Wei et al., 2016). Bregs can affect the function of T cells. A study showed that Bregs could induce the anergy and apoptosis of $CD4^+$ T cells through producing TGF-β and indoleamine 2, 3-dioxygenase (Nouel et al., 2015). Bregs can also limit immune responses by $CD8^+$ T cells through TNF-α production (Schioppa et al., 2011). Moreover, they can suppress the IFNγ production by $CD8^+$ T cells in ovarian cancer (Wei et al., 2016). Another mechanism that Bregs used is the induction of regulatory mechanisms through activating Tregs. They enhance the

expression of Foxp3 and CTLA-4 in Tregs through cell to cell contact (Kessel et al., 2012). Furthermore, Bregs can suppress anti-tumor immunity by directly interacting with malignant cells. It was reported that increasing frequencies of Bregs seem to be modulated directly by tumor cells in patients with lung cancer and thus, indicate the direct interaction between Bregs and malignant cells (Zhou et al., 2014) (Figure 1.8).

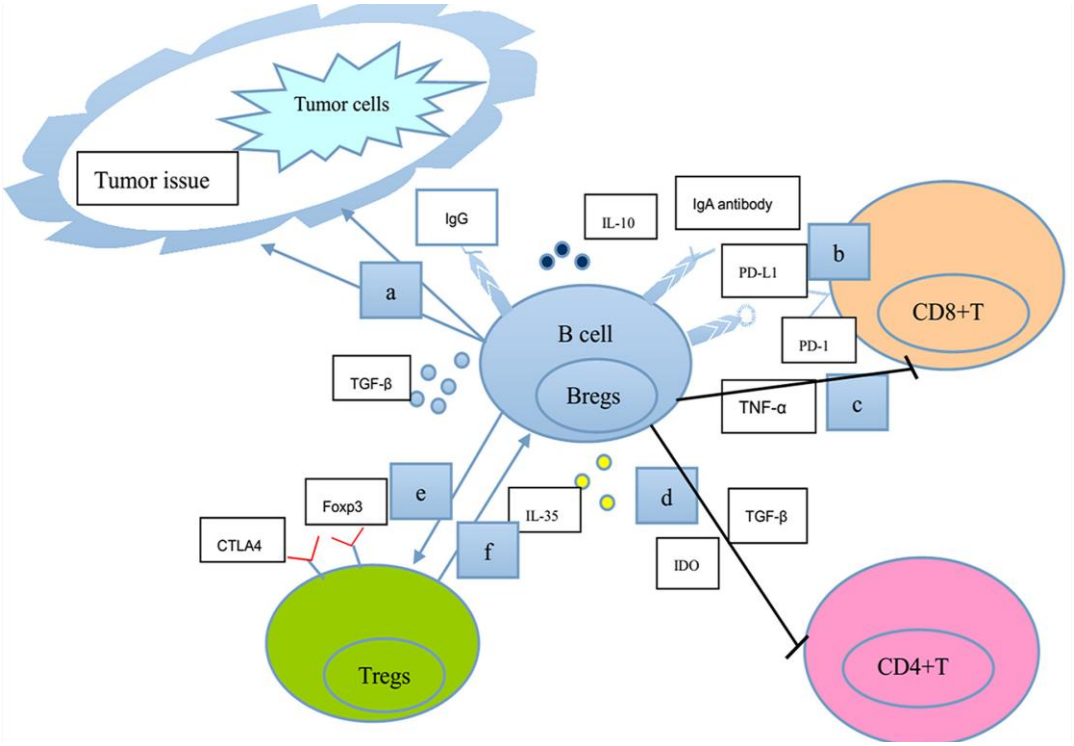

Figure 1.8 : Negative functions of B cells in tumor immunity, adapted from (Shen et al., 2016).

1.6 Aim of the Study

Lung cancer is the leading cause of cancer deaths worldwide for both women and men. Mesothelioma is a form of cancer concerning membrane surrounding the lungs. Even though there are some studies about immune cells in both lung cancer and mesothelioma, better characterization studies are required especially to elucidate the effects of immune cells in the tumor microenviroment. Tumor microenviroment mainly affects immunological responses via either supressing effector cells or converting them to the regulatory cell types. Secretion of immune suppressor cytokines by regulatory cell types contributes to suppression of immune responses within cancer microenviroment. Regulatory cell types including regulatory T and B cells contribute to the anti-inflammatory responses with their ability to secrete anti-inflammatory cytokines such as interleukin-10 (IL-10).

This study aims to characterize immune cells in non-small cell lung cancer and mesothelioma according to cell surface molecules and cytokine profiles of the cells. Cellular characterization of effector and regulatory immune cells in blood and tumor tissue samples for non-small cell lung cancer and mesothelioma patients is aimed to be performed. Our second aim was to demonstrate the effects of NSCLC microenvironment on healthy T and B cells. Overall, this study especially aims to identify types of peripheral and tumor infiltrating regulatory B cells that are not identified before in lung cancer and mesothelioma. Most of the studies in the literature regarding regulatory B cells are restricted to the studies of peripheral blood, which reflects only a systemic immune response for NSCLC. For that reason, investigating regulatory B cells within its microenvironment is necessary. To investigate the relationship among $CD4^+$ T cells, $CD19^+$ B cells and their subsets, T cell specific (CD4 and CD8), regulatory B cell specific (CD19, CD24 ve CD38), and PD-1 and PD-L1 cell surface molecules were examined along with anti-inflammatory (IL-10) and pro-inflammatory (IFNγ and IL-17) cytokine profiles.

2. MATERIALS & METHODS

2.1 Materials

2.1.1 Primary cells

2.1.1.1 Peripheral mononuclear blood cells (PBMC)

Peripheral mononuclear blood cells (PBMC) were isolated via density gradient centrifugation using Ficoll based lymphocyte separation medium (Capricorn).

2.1.1.2 Tumor infiltrating leukocytes (TIL)

Tumor infiltrating leukocytes (TIL) were isolated via enzymatic digestion using collagenase A (Millipore), hyaluronidase (MP Biomedicals) and DNase (MP Biomedicals) and later via density gradient centrifugation.

2.1.1.3 $CD4^+$ T cells

$CD4^+$ T cells were isolated from PBMCs of healthy controls via magnetic separation (Stemcell). Primary $CD4^+$ T cells were cultured in Roswell Park Memorial Institute (RPMI) medium supplemented with 10% FBS, 1% Penicillin/Streptomycin.

2.1.1.4 B cells

B cells were isolated from the spleens of PBMCs of healthy controls via magnetic separation (Stemcell). Primary B cells were cultured in Roswell Park Memorial Institute (RPMI) medium supplemented with 10% FBS, 1% Penicillin/Streptomycin.

2.1.2 Cell culture

Culture media and solutions used in cell culture studies can be seen in Table 2.1 and buffers used in cell culture studies are listed in Table 2.2.

Table 2.1 : Solutions and media used in cell culture studies.

Solution	Supplier Company
Roswell Park Memorial Institute (RPMI) Medium	Gibco
Lymphocyte Separation Medium (LSM)	Capricorn
Fetal Bovine Serum (FBS) (10%)	Gibco
Penicillin/Streptomycin (1%)	Gibco
Trypan Blue	Lonza
DMSO	Fisher-Scientific
10X Hank's Balanced Salt Solution (HBSS)	Sigma

Table 2.2 : Buffers and media used in cell culture studies.

Buffers	Content and Amount
1X PBS	9,55g in 1L ddH_2O
10X Hank's Balanced Salt Solution (HBSS)	1X with ddH_2O
Complete RPMI growth medium	RPMI medium with 10% FBS, 1% Penicillin/Streptomycin
10X Red blood cell lysis buffer	1X with ddH_2O
Cell seperation medium	PBS containing 2% FBS and 1 mM EDTA
Freezing medium	FBS:DMSO (9:1 ratio, v/v)

2.1.3 Equipments and supplies

Laboratory equipment and supplies used in this study are shown in Table 2.3 and Table 2.4 with their companies.

Table 2.3 : Laboratory equipments used in the study.

Equipment	Company
Laminar Air Flow Cabinets	FASTER BH-EN 2003
Pipettes	10 µl, 20 µl, 100 µl, 200 µl, 1000 µl Socorex and
Electronic Pipette	10 µl, 100 µl, 1000 µl Biohit CappAid
Centrifuges	Beckman Coulter Allegra ™ 25R Centrifuge Scanspeed
Incubator with CO_2	BIND
Vortex	Mixer Uzusio VTX-3000L,LMS

Table 2.3 (continued) : Laboratory equipments used in the study.

Equipment	Company
Quick spin	LMS
Magnetic stirrer	WiseStir MSH-20D, Wisd Laboratory Equipment
Light Microscope	Olympus CH30
Hemacytometer	Isolab
Ice Machine	Scotsman AF10
Freezers	Altus (+4^{o}C) Siemens (-20^{o}C) Haier (- 80^{o}C)
Flow Cytometer	BD Accuri C6

Table 2.4 : Laboratory supplies used in this study.

Supplies	Company
Scale	Precisa
Examination Gloves	Tenty
Falcons (15 ml, 50 ml)	Isolab
96-well F plate	TPP
Serological pipettes	Sarstedt
Centrifuge tubes	Sarstedt
Eppendorf tubes (0,6ml, 1,5ml, 2ml)	Interlab
Cell strainer (70 μm)	BD

2.1.4 General chemicals

General chemicals used in this study are listed with their supplier companies in Table 2.5. CpG ODN K3 was kindly provided by Professor İhsan Gürsel and PHA was kindly provided by Umut Can Küçüksezer,Ph.D.

Table 2.5 : General chemicals used in this study.

Chemical	Supplier Company	Application
EDTA	Applichem	Cell seperation
Phosphate-Buffered Saline (PBS) 10X	Lonza	Cell culture
Bovine Serum Albumin (BSA)	Santa Cruz	Cell seperation

Table 2.5 (continued) : General chemicals used in the study.

Chemical	Supplier Company	Application
Ionomycin (stock concentration:1 mg/ml)	Calbiochem	Treatment
PMA (stock concentration:1 mg/ml)	Sigma Aldrich	Treatment
Collegenase A	Millipore	TIL isolation
DNase	MP Biomedicals	TIL isolation
Hyaluronidase	MP Biomedicals	TIL isolation
Gentamicin	Thermo-fisher	TIL isolation
Fixation Buffer (4%)	Biolegend	Intracellular staining
Permeabilization Buffer (10X)	Biolegend	Intracellular staining
Isopropanol	Sigma-Aldrich	Cell freezing
Polymyxin B sulfate	HiMedia Laboratories	Tumor cell isolation
CFSE	Molecular probes	Proliferation assay
Monensin (stock concentration: 50 mg/ml)	Calbiochem	Intracellular staining
1000X Brefeldin A (stock concentration: 3 mg/ml)	e-bioscience	Intracellular staining
Recombinant CD40L	R&D systems	B cell culture

2.1.5 Antibodies

Antibodies used in this study are given in table 2.6.

Table 2.6 : Antibodies used in this study.

Antibody	Supplier	Stock Concentration
Mouse anti-human CD19 APC	Biolegend	50 µg/ml
Mouse anti-human CD4 PerCP	Biolegend	200 µg/ml
Mouse anti- human CD4 FITC	Biolegend	200 µg/ml
Mouse anti- human CD4 PE	Biolegend	100 µg/ml
Mouse anti-human CD8 FITC	BD	200 µg/ml
Rat anti-human CD24 PE	Biolegend	200 µg/ml
Mouse anti-human CD38 PerCP	Biolegend	400 µg/ml
Anti-human IL-10 Alexa Fluor 488	Biolegend	50 µg/ml
Rat anti-human IL-10 PE	Biolegend	25 µg/ml
Mouse anti-human IFNγ PE	Biolegend	40 µg/ml
Mouse anti-human IL-17A FITC	Biolegend	25 µg/ml
Mouse anti-human PD-L1 APC	Biolegend	400 µg/ml
Mouse purified anti-human PD-1	Biolegend	500 µg/ml
Anti-mouse IgG PE	Santa Cruz	400 µg/ml

2.2 Methods

2.2.1 Determination of immune cell types in blood and TIL

2.2.1.1 Patients

7 healthy controls (3 females and 4 males, median age was 36 years; range, 25 to 52 years), 16 non-small lung cancer (3 females and 13 males, median age was 59 years; range, 42 to 69) and 3 mesothelioma (3 males, median age was 66 years; range 55 to 78) patients from Istanbul University, Cerrahpaşa Medical School, Thoracic Surgery Department were included in this study. Tissue and blood samples were taken from patients with operable non-small lung cancer and mesothelioma. Only blood samples were taken from healthy controls. Blood samples were collected into EDTA tubes. Normal tissue samples taken from the region close to the tumor region and tumor tissue samples were obtained from patients during surgery. Tissue samples were placed into tubes containing cold Roswell Park Memorial Institute (RPMI) 1640 culture medium and transferred to the cell culture laboratory on ice.

2.2.1.2 Isolation of peripheral mononuclear blood cells (PBMC)

Peripheral Mononuclear Blood Cells (PBMC) were isolated from blood samples by Ficoll gradient centrifugation. Briefly, blood was diluted with the equal volume of phosphate buffered saline (PBS). Diluted blood was layered onto Ficoll based lymphocyte separation medium (LSM) in a falcon tube and centrifuged at 1200 g for 20 minutes. The interface between plasma and medium was collected and diluted with RPMI 1640 and then centrifuged at 300 g for 10 minutes. Supernatant was discarded. Cell pellet was dissolved in 2-3 ml of red blood cell lysis buffer and incubated at room temperature for 10 minutes. Then, 5 ml RPMI 1640 was added and centrifuged. Supernatant was discarded and cell pellet was dissolved in 1 ml RPMI 1640. Cells were counted and cell viability was assessed with trypan blue staining and cryopreserved in freezing medium until used for the experiments.

2.2.1.3 Isolation of tumor infiltrating lymphocytes (TIL)

Tumor infiltrating lymphocytes (TIL) were isolated separately from normal (tumor-free) and tumor tissue by mechanic and enzymatic digestion. Firstly, tissues were washed in Hanks' Balanced Salt Solution (HBSS) supplemented with gentamicin (50

µg/ml). Then they were minced into small fragments. Those fragments were digested in a mixture of 0,5 mg/ml Collagenase A, 0,1mg/ml Hyaluronidase and 0,01mg/ml Dnase at 37 °C for 1-2 hours. The volume of enzymatic solution and the time required for tissue dissociation were dependent on specimen characteristics. After incubation, the cell suspension was filtered through a 70 µm cell strainer and washed twice with HBSS. Cells were counted and cell viability was assessed with trypan blue staining. Discontinuous density gradient centrifugation was conducted to further separate lymphocytes from erythrocytes, dead cells and tumor cells. 100% of LSM, 75% of LSM and cell suspension was layered from bottom to top in a falcon tube to make discontinuous density gradient. Cell suspension was centrifuged at 1200 g for 20 minutes. The lower interface suspended on 100% of LSM contained TIL and upper interface suspended on 75% of LSM contained tumor cells. Both interfaces were collected, washed with HBSS by centrifuging at 300g for 8 minutes. Supernatants were discarded. Cell pellets were dissolved in 2-3 ml of red blood cell lysis buffer to lyse remaining erythrocytes. TIL and tumor cells were counted and cell viability was assessed with Trypan blue staining and cryopreserved in freezing medium until used for the experiments (Figure 2.1).

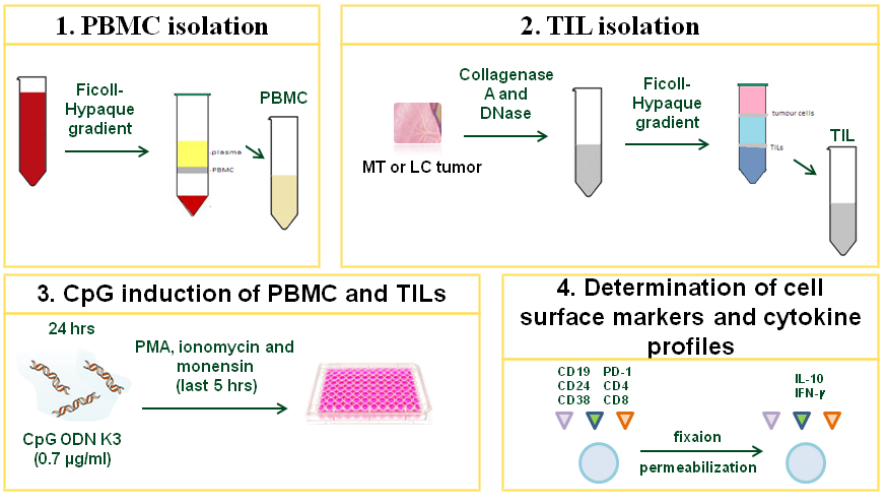

Figure 2.1 : Isolation, treatment and analysis of PBMC and TILs.

2.2.1.4 CpG ODN K3 treatment of PBMC and TILs

After seperation of PBMC and TILs from blood and biopsies of patients, cells were distrubuted into a 96 well plate as 500.000 cells/ml. In order to induce IL-10 expression, PBMC and TILs were stimulated with 0,7 μg/ml CpG ODN K3. CpG treatment was not performed for IFNγ and IL-17 stainings. 50 ng/ml PMA, 500 ng/ml ionomycin and 3 μg/ml monensin to stop cytokine secretion were added at the last 5 hours of culture for each staining group (Figure 2.1).

2.2.1.5 Flow cytometric analysis of PBMC and TILs

To characterize different cell types within the blood and biopsies of LC and MT patients, various combinations of surface and intracellular stainings were performed for different cell types. Staining groups were: CD4, CD19, IL10; CD19, CD24, CD38; CD19, CD24, CD38, IL10; CD19, PD-1, IL10; CD4, CD8, CD19, IFNγ; and CD4, CD19, IL17.

Surface antigen staining

At the end of the 24 hours of incubation, cells were harvested and washed with FACS buffer. Firstly, they were stained for 1 hour on ice in 25 μl FACS buffer with 0,15 μl of the following fluorophore conjugated surface antibodies: anti-CD4-PerCP, anti-CD8-FITC, anti-CD19-APC, anti-CD24-PE, anti-CD38-PerCP, purified anti-PD-1 (stock concentrations: 200 μg/ml, 200 μg/ml, 50 μg/ml, 200 μg/ml, 400 μg/ml, and 500 μg/ml, respectively). Then, they were washed with FACS buffer by centrifugation at 3000 rpm for 5 minutes at +4^{o}C. Supernatants were discarded and proceeded to the intracellular staining. For PD-1 and CD19 staining; cells were first incubated with purified anti-PD-1 for 1 hour on ice. Then 25 μl FACS buffer containing anti-mouse PE secondary antibody was added and incubated for 40 minutes on ice. After PD-1 staining was completed, proceeded to the CD19 staining as both of our surface antibodies were produced in mouse. Surface staining with anti-CD19-APC were performed in the same manner and cells were washed with FACS buffer before intracellular staining.

Intracellular staining

Intracellular staining was carried out with: anti-IL10-Alexa Fluor 488, anti-IFNγ-PE and anti-IL17-FITC antibodies. After surface staining and washing, cells were fixed with 100 μl of 1X Fixation buffer (Biolegend) for 15 minutes on ice. 1X Fixation

buffer containing paraformaldehyde was diluted from 4X with 1X PBS. Cells were washed with 350 µl of FACS buffer by centrifugation at 3000 rpm for 5 minutes following fixation. Supernatant was discarded and pellets were resuspended in 300 µl of 1X permeabilization buffer containing Saponin (diluted from 10X with ddH_2O) to permeabilize the cell membrane for entrance of antibodies. Saponin interacts with membrane to make holes on it. After 10 minutes incubation on ice with 1X permeabilization buffer, cells were centrifuged at 3000 rpm for 5 minutes. Since permeabilizaiton buffer makes transient pores on the cell membrane, it is added to subsequent steps of staining. Then cells were resuspended in 25 µl of permeabilization buffer containing either 0,3 µl anti-IL10-Alexa Fluor 488, anti-IFNγ-PE or anti-IL17-FITC (stock concentrations: 50 µg/ml, 40 µg/ml, 25 µg/ml, respectively) and incubated for 2 hours on ice in dark. Then cells were washed with 300 µl 1X permeabilization buffer by centrifugation at 300 rpm 5 minutes. Supernatant were discarded and pellet was dissolved in 200 µl FACS buffer to analyzed with Accuri C6 Flow Cytometry and later analysis were done with Flow Jo software. Color compensation was performed by using single antibody stained samples. Additively, the cells that were not stained were used as unstained control group.

2.2.2 Effect of tumor microenvironment on immune cells

2.2.2.1 Conditioned medium preperation from tumor and normal tissue

Culture supernatants were acquired by culture of completely digested lung tumor or normal tissue biopsy specimens. Digestion was performed as described in Section 2.2.1.3. After incubation, mixture was filtered through a 70 µm cell strainer and washed twice with RPMI medium containing polymyxin B (20 µg/ml) to exclude endotoxin contamination. Thereafter, digested cells were resuspended in complete medium as 10^6 cells per ml and cultured in a 6 well plate. After 2 days, the supernatants were harvested, centrifuged, and stored at −80 °C.

2.2.2.2 PBMC isolation

Whole blood was collected from healthy individuals and PBMC isolation from peripheral bloods of healthy control individuals was performed by Ficoll gradient centrifugation as described in Section 2.2.1.2.

2.2.2.3 Magnetic isolation of $CD4^+$ T and B cells

$CD4^+$ T and B cells were purified from the PBMCs by magnetic cell sorting with a column free commercial reagent kit (Stemcell EasySep™ Human $CD4^+$ Selection Kit and Human B Cell Enrichment Kit, respectively) following the manufacturer's instructions. Firstly, positive selection of $CD4^+$ T cells were performed. 10^8 cells per ml were resuspended in cell seperation buffer and transfered into 5 ml polystren falcon tube. Selection cocktail that labels $CD4^+$ T cells was added as 100 µl per ml of sample, mixed and incubated for 15 minute at room temperature. Then, magnetic particles were added as 50 µl per ml of sample, mixed and incubated for 10 minute at room temperature. After incubation, cell seperation buffer was added up to 2.5 ml, mixed gently and placed into the EasySep™ magnet without the lid and incubated for 5 minute at room temperature. After that, supernatant containing non-$CD4^+$ T cells were transfered into a new falcon tube for B cell enrichment. For the tube containing magnetically labeled $CD4^+$ T cells, selection procedure with magnet was repeated for 2 more times.

For B cell enrichment, remaining PBMCs were resuspended with cell seperation buffer as $5x10^7$ cells per ml. Enrichment coctail that labels non-B cells was added as 50 µl per ml of sample, mixed and incubated for 10 minute at room temperature. Then, magnetic particles were added as 75 µl per ml of sample, mixed and incubated for 5 minute at room temperature. After incubation, cell seperation buffer was added up to 2.5 ml, mixed gently and placed into the EasySep™ magnet without the lid and incubated for 5 minute at room temperature. After that, supernatant containing enriched B cells were transfered into a new falcon tube. Isolated B and $CD4^+$ T cells were resuspended in tumor or normal tissue conditioned mediums and plated into 96 well plate. Some of the isolated cells were seperated to check the purity and viability. Also 10^6 $CD4^+$ T cells were seperated for proliferation assay.

Flow staining for CD4 and CD19 surface markers

Purity of freshly purified $CD4^+$ T cells and B cells was determined using flow cytometer. $5x10^5$ $CD4^+$ T cells were stained with 0.1 µl PE conjugated anti-CD4 antibody (stock concentration: 100 µg/ml) while B cells were stained with 0.1 µl APC conjugated anti-CD19 antibody (stock concentration: 50 µg/ml) in 25 µl FACS Buffer in the dark on ice for 1 hour. A fraction of $CD4^+$ T cells and B cells were left as unstained controls. Then, cells were washed once with 300 µl FACS Buffer by centrifugation at 3000 rpm for 5 minutes. Supernatant was discarded and pellet was resuspended in 200 µl of FACS Buffer and samples were analyzed with flow cytometer.

2.2.2.4 B cell culture

B cells were resuspended in either tumor or normal tissue conditioned mediums as 10^6 cells per ml. For optimal detection of IL-10 production by using intracellular staining, CpG ODN K3 (0,7 µg/ml) and recombinant human CD40 ligand (1 µg/ml) were also used. B cells were cultured for 24 hours and 50 ng/ml PMA, 500 ng/ml ionomycin and 0,3 mg/ml 1X Brefeldin A to stop cytokine secretion were added at the last 5 hours of culture. After 1 day of incubation, cells were harvested for surface and intracellular staining.

2.2.2.5 $CD4^+$ T cell culture

T cells were resuspended in either tumor or normal tissue conditioned mediums as 10^6 cells per ml. PHA (2 µg/ml) and CpG ODN K3 (0,7 µg/ml) were also used. T cells were cultured for 24 hours and 50 ng/ml PMA, 500 ng/ml ionomycin and 3 µg/ml 1X Brefeldin A to stop cytokine secretion were added at the last 5 hours of culture. After 1 day of incubation, cells were harvested for surface and intracellular staining.

2.2.2.6 Flow cytometric analysis of B and $CD4^+$ T cells

At the end of the 24 hours of incubation, cells were harvested and washed with FACS buffer. Firstly, they were stained for 1 hour on ice in 25 µl FACS buffer with 0,15 µl of the purified anti-PD-1 (stock concentration: 500 µg/ml). Then, they were washed with FACS buffer by centrifugation at 3000 rpm for 5 minutes at $+4^oC$. Supernatants were discarded and 25 µl FACS buffer containing anti-mouse PE

secondary antibody (stock concentration: 400 µg/ml) was added and incubated for 40 minutes on ice. After PD-1 staining was completed, proceeded to the PD-L1 staining as both of our surface antibodies were produced in mouse. Surface staining with anti-PD-L1-APC (stock concentration: 400 µg/ml) were performed in the same manner and cells were washed with FACS buffer before intracellular staining.

Intracellular staining was carried out with: anti-IL10-PE for B and $CD4^+$ T cells and anti-IFNγ-PE for $CD4^+$ T cells. After surface staining and washing, cells were fixed with 100 µl of 1X Fixation buffer (Biolegend) for 15 minutes on ice. 1X Fixation buffer containing paraformaldehyde was diluted from 4X with 1X PBS. Cells were washed with 350 µl of FACS buffer by centrifugation at 3000 rpm for 5 minutes following fixation. Supernatant was discarded and pellets were resuspended in 300 µl of 1X permeabilization buffer containing Saponin (diluted from 10X with ddH_2O) to permeabilize the cell membrane for enterence of antibodies. After 10 minutes incubation on ice with 1X permeabilization buffer, cells were centrifuged at 3000 rpm for 5 minutes. Since permeabilizaiton buffer makes transient pores on the cell membrane, all staining steps were performed with it after this stage. Because of that cells were resuspended in 25 µl of permeabilization buffer containing either 0,3 µl anti-IL10-PE (stock concentration: 25 µg/ml) or anti-IFNγ-PE (stock concentration: 40 µg/ml) and incubated for 2 hours on ice in dark. Then cells were washed with 300 µl 1X Permeabilization buffer by centrifugation at 300 rpm 5 minutes. Suprnatant were discarded and pellet was dissoleved in 200 µl FACS buffer to analyzed with Accuri C6 Flow Cytometry and later analysis were done with Flow Jo software.

2.2.2.7 CFSE proliferation assay

For CFSE labeling, 10^6 $CD4^+$ T cells were resuspended in a 1 ml volume of PBS containing 5% FBS in a fresh tube. The tube was laid horizontally. 110 µl of PBS was added to the non-wetted portion of the plastic at the top of the tube ensuring that was not mix with the cells, and in that 1 µl of the 5 mM stock of CFSE was resuspended. The tube was capped and inverted quickly several times and vortexed. The cells were left to label with CFSE by incubating for 5 min at room temperature. Then, they were washed by diluting with ten volumes of PBS containing 5% FBS, centrifuged at 300g for 5 min and the supernatant was discarded. Cells were washed once more in the same manner.

Then, labeled cells were resuspended in either tumor conditioned medium 1, tumor conditioned medium 2, normal tissue conditioned medium 1 or normal tissue conditioned medium 2. To stimulate the basal-level of T-cell proliferation, 2 μg/ml PHA was added into all experimental groups. Non-PHA-induced but CFSE labelled T cells were left to be used as the control of the proliferation. Stimulated and unstimulated control cells were culltured in different conditioned mediums for 3 days.

2.2.3 Statistical analysis

All *p* values were calculated using GraphPad Prism 6.0 software. Significancies were determined by Student *t* test. In all analyses, a two-tailed *p*-value of less than 0.05 was considered statistically significant. In column bar graphs, vertical bars indicate standard deviations of the mean.

3. RESULTS

3.1 $CD4^+$ T Cells in Patients with NSCLC and MT

3.1.1 $CD4^+$ T cell frequencies in patients with NSCLC and MT

Inflammation mediated by infiltrating immune cells plays a key role in cancer pathogenesis. T cells display critical and diverse roles in the establishment and suppression of inflammation within the tumor microenvironment. $CD4^+$ T cells include T helper cells and Tregs. The frequencies of $CD4^+$ T cells were examined by surface staining of CD4 which was afterwards detected by flow cytometry. For this purpose, PBMCs were isolated from blood of healthy controls (n=6), LC patients (n= 12) and MT patients (n=2) by Ficoll density gradient centrifugation. TILs were also isolated from tumor tissue samples of LC (n=10) and MT (n=2) patients after enzymatic digestion. Then, PBMC and TILs were labeled with anti-CD4-PerCP and analyzed with Flow Cytometry. Percentages of $CD4^+$ T cells were determined compared to unstained control within lymphocyte population.

The frequency of $CD4^+$ T cells decreased in NSCLC patients' blood (7,36-67,8% *P=0,07*) compared to healthy individuals (31,6-47,9%). $CD4^+$ T cells also tended to decrease in MT patients' blood (21,1; 34,3% *P=0,07*). A few $CD4^+$ T cell infiltration was observed in LC (0,17-6,06%) and in MT (0,71; 2,34%) patients' tumors (Figure 3.1).

3.1.2 IFNγ producing $CD4^+$ T cells in NSCLC and MT

Th1 cells are defined as IFNγ and TNF-α secreted $CD4^+$ T cells. They mediate immune responses against intracellular pathogens by helping macrophages and cytotoxic T cells to kill pathogens (Romagnani,1999). The IFNγ production of $CD4^+$ T cells was examined by intracellular IFNγ staining which was afterwards detected by flow cytometry. For this purpose, PBMCs were isolated from blood of healthy controls (n=6), LC patients (n= 12) and MT patients (n=3) by Ficoll gradient centrifugation.

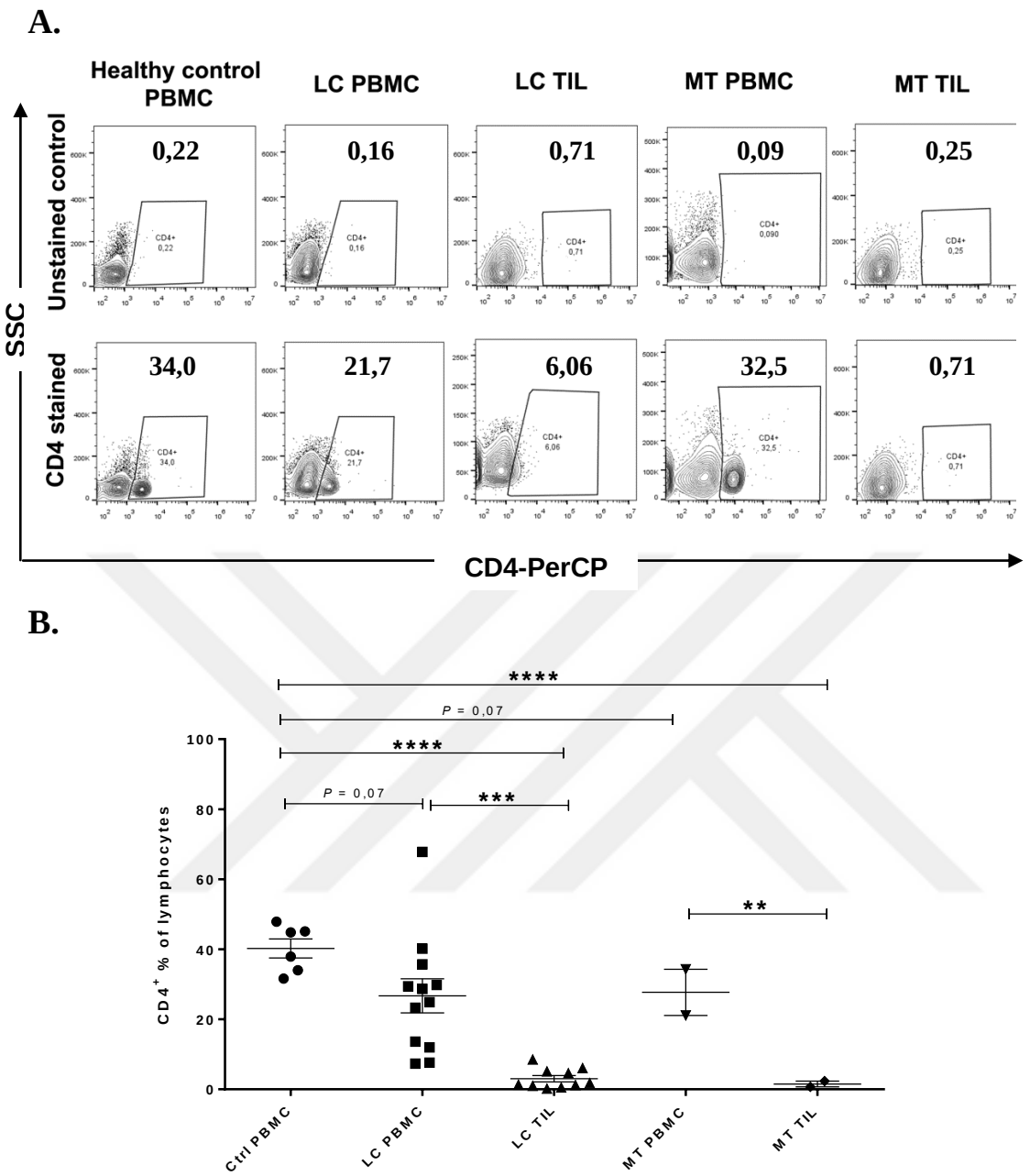

Figure 3.1 : $CD4^+$ T cell percentages gated on lymphocytes for LC and MT patients' blood and TILs. A) CD4 staining representative quadrant plots for one blood sample from a healthy person, as well as one blood sample and one tumor tissue sample (TIL) from LC and MT. B)Frequencies of $CD4^+$ T cells in 6 blood samples of healthy controls; 12 blood samples, 10 lung tissue samples of LC patients and 2 blood samples, 2 lung tissue samples for MT patients. Each dot represents one individual. Graphs were prepared using Graphpad Prism 6. Student's *t* test were used for statistical analysis. **p*<0.05, ***p*<0.01, ****p*<0.001, *****p*<0.0001. Ctrl, control; LC, lung cancer; MT, mesothelioma; PBMC, peripheral blood mononuclear cell; TIL, tumor infiltrating leukocytes.

TILs were also isolated from tumor biopsies of LC (n=5) and MT (n=3) patients. Then, cells were stimulated with PMA and ionomycin for 5 h in the presence of Monensin to keep the cytokines accumulated inside the golgi complex.

Percentages of $CD4^+IFN\gamma^+$ T cells were determined compared to unstained control and $CD4^+$ cells within lymphocyte population. IFNγ expression of $CD4^+$ T cells were significantly decreased in blood of NSCLC patients compared to healthy controls (10,4-38,3% to 1,82-21,4%). However, IFNγ expression of $CD4^+$ T cells were highly increased for blood sample of one patient with MT. IFNγ producing T cells were also observed in LC and MT tumors. There was a trend of decrease of IFNγ producing T cells in tumor tissues of patients with NSCLC and MT. (Figure 3.2).

3.1.3 IL-17 producing $CD4^+$ T cells in NSCLC and MT

IL-17 producing Th17 cells with Tregs modulate cytokine and chemokine production, promote immune cell recruitment and help regulate anti-tumor and pro-tumor immune cell activation states in the tumor microenvironment (Marshall et al., 2016) . The IL-17 production of $CD4^+$ T cells was examined by intracellular IL-17 staining which was afterwards detected by flow cytometry. For this purpose, PBMCs were isolated from blood of healthy controls (n=6), LC patients (n= 10) and MT patients (n=4) by density gradient centrifugation. TILs were also isolated from tumor biopsies of LC (n=4) and MT (n=4) patients.

Percentages of $CD4^+IL\text{-}17^+$ T cells were determined compared to unstained control and $CD4^+$ cells within lymphocyte population. IL-17 expression by $CD4^+$ T cells was not alternated among patient groups and control with slight increase in blood and TILs of patients with NSCLC (Figure 3.3).

3.1.4 IL-10 producing $CD4^+$ T cells in NSCLC and MT

Tregs influence the tumor microenvironment during the progression of lung cancers. The IL-10 production of $CD4^+$ T cells was examined by intracellular IL-10 antibody staining which was afterwards detected by flow cytometry. For this purpose, PBMCs were isolated from blood of healthy controls (n=6), LC patients (n= 12) and MT patients (n=3) by density gradient centrifugation. TILs were also isolated from tumor tissue samples of LC (n=5) and MT (n=3) patients.

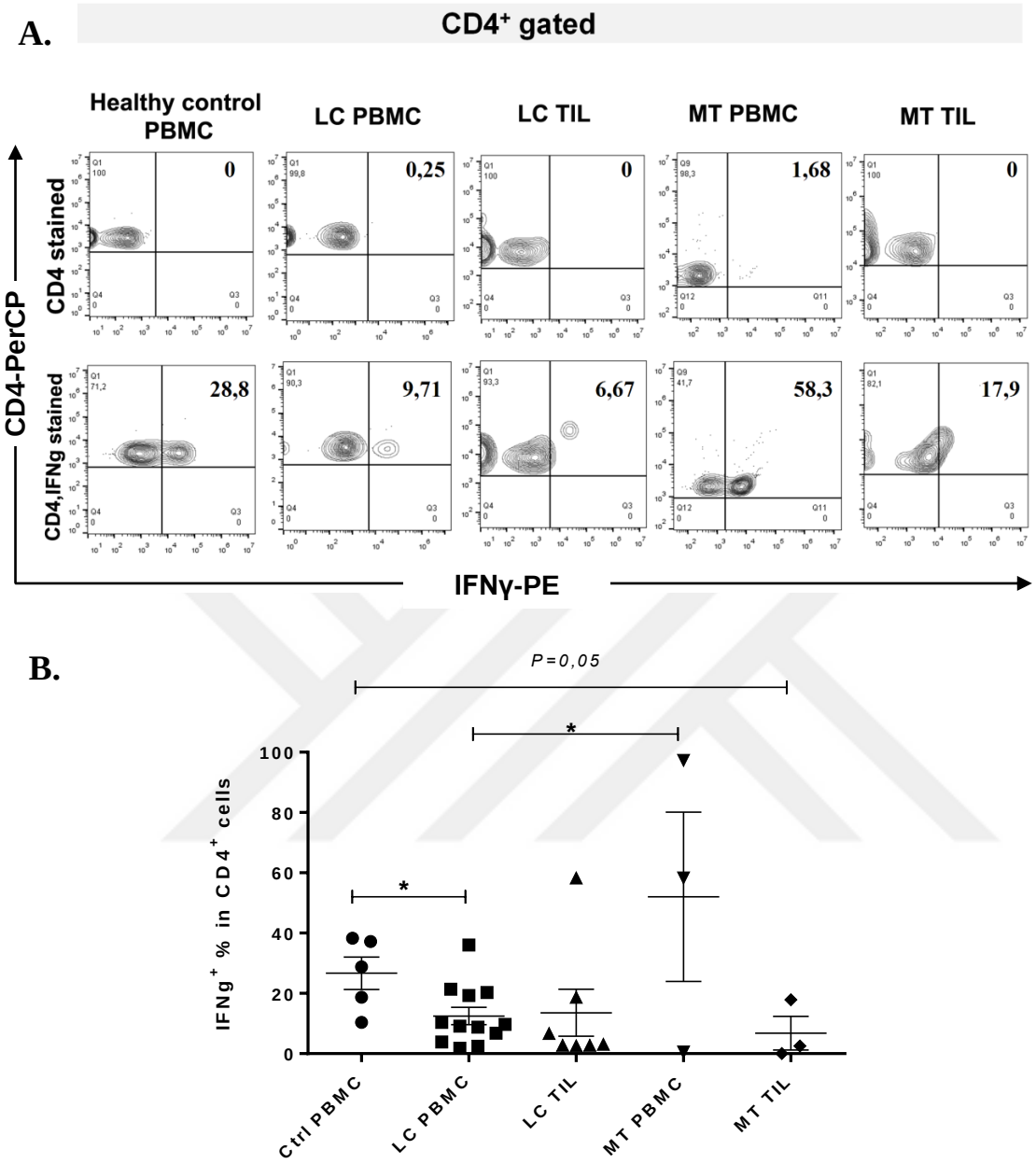

Figure 3.2 : $CD4^+IFN\gamma^+$ cell percentages in $CD4^+$ T lymphocytes of LC and MT patients' blood and TILs. A) Representative quadrant plots of IFNγ intracellular staining gated on $CD4^+$ cells for one blood sample from a healthy person, as well as one blood sample and one tumor tissue sample (TIL) from LC and MT. B)Frequencies of $CD4^+IFN\gamma^+$ T cells in 5 blood samples of healthy controls; 12 blood samples, 7 lung tissue samples of LC patients and 3 blood samples, 3 lung tissue samples of MT patients. Each dot represents one individual. Graphs were prepared using Graphpad Prism 6. Student's *t* test were used for statistical analysis. *p<0.05, **p<0.01, ***p<0.001, ****p<0.0001. LC, lung cancer; MT, mesothelioma; PBMC, peripheral blood mononuclear cell; TIL, tumor infiltrating leukocytes.

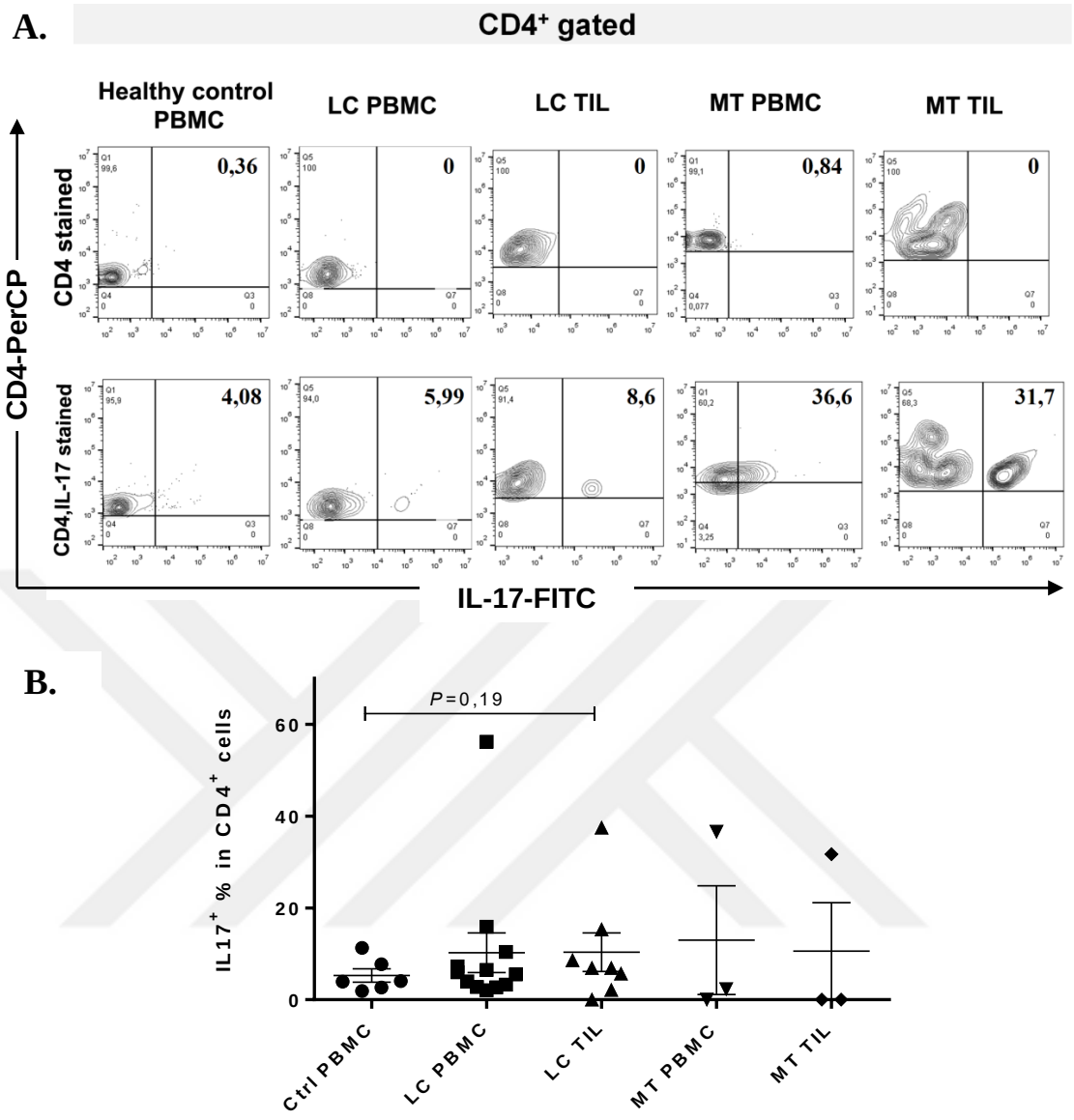

Figure 3.3 : $CD4^+IL\text{-}17^+$ cell percentages in $CD4^+$ T lymphocytes of LC and MT patients' blood and TILs. A) Representative quadrant plots of IL-17 intracellular staining gated on $CD4^+$ cells for one blood sample from a healthy person, as well as one blood sample and one tumor tissue sample (TIL) from LC and MT. B)Frequencies of $CD4^+IL\text{-}17^+$ T cells in 6 blood samples of healthy controls; 11 blood samples, 8 lung tissue samples of LC patients and 3 blood samples, 3 lung tissue samples of MT patients. Each dot represents one individual. Graphs were prepared using Graphpad Prism 6. Student's *t* test were used for statistical analysis. **p*<0.05, ***p*<0.01, ****p*<0.001, *****p*<0.0001. LC, lung cancer; MT, mesothelioma; PBMC, peripheral blood mononuclear cell; TIL, tumor infiltrating leukocytes.

Then, cells were stimulated with 0,7 µg/ml CpG for 24 h, and PMA and ionomycin for 5 h in the presence of Monensin to keep the cytokines accumulated inside the Golgi complex. First, cells were labeled with anti-CD4-PerCP. After that, the cells were fixed and permeabilized. Lastly, they were incubated with Alexa Fluor 488-coupled anti-IL-10 antibody that was prepared inside the permeabilization buffer.

Percentages of $CD4^+IL\text{-}10^+$ T cells were determined compared to unstained control and $CD4^+$ cells within lymphocyte population. IL-10 expression of $CD4^+$ T cells were highly increased in PBMCs (0,82-24,1%) and TILs (0-23,7%) of NSCLC patients compared with healthy individuals (0-2,77%). In addition, IL-10 production by $CD4^+$ T cells in MT patients' blood (0;35,7%) were higher compared to blood of healthy people (0-2,77%) (Figure 3.4).

3.2 $CD8^+$ T Cells in Patients with NSCLC and MT

3.2.1 $CD8^+$ T cell frequencies in patients with NSCLC and MT

The frequencies of $CD8^+$ Cytotoxic T cells were examined by surface staining of CD8 which was afterwards detected by flow cytometry. For this purpose, PBMCs were isolated from blood of healthy controls (n=6), LC patients (n= 13) and MT patients (n=3) by Ficoll density gradient centrifugation. TILs were also isolated from tumor tisuue samples of LC (n=8) and MT (n=3) patients. PBMC and TILs were labeled with anti-CD8-FITC and analyzed with flow cytometry. Percentages of $CD8^+$ T cells were determined compared to unstained control within lymphocyte population. The frequency of $CD8^+$ T cells tended to decrease in LC and MT patients' blood compared to healthy individuals. $CD8^+$ T cell infiltration was observed in tumor samples of LC (0,09-27,8%) and MT (3-31,9%) patients (Figure 3.5).

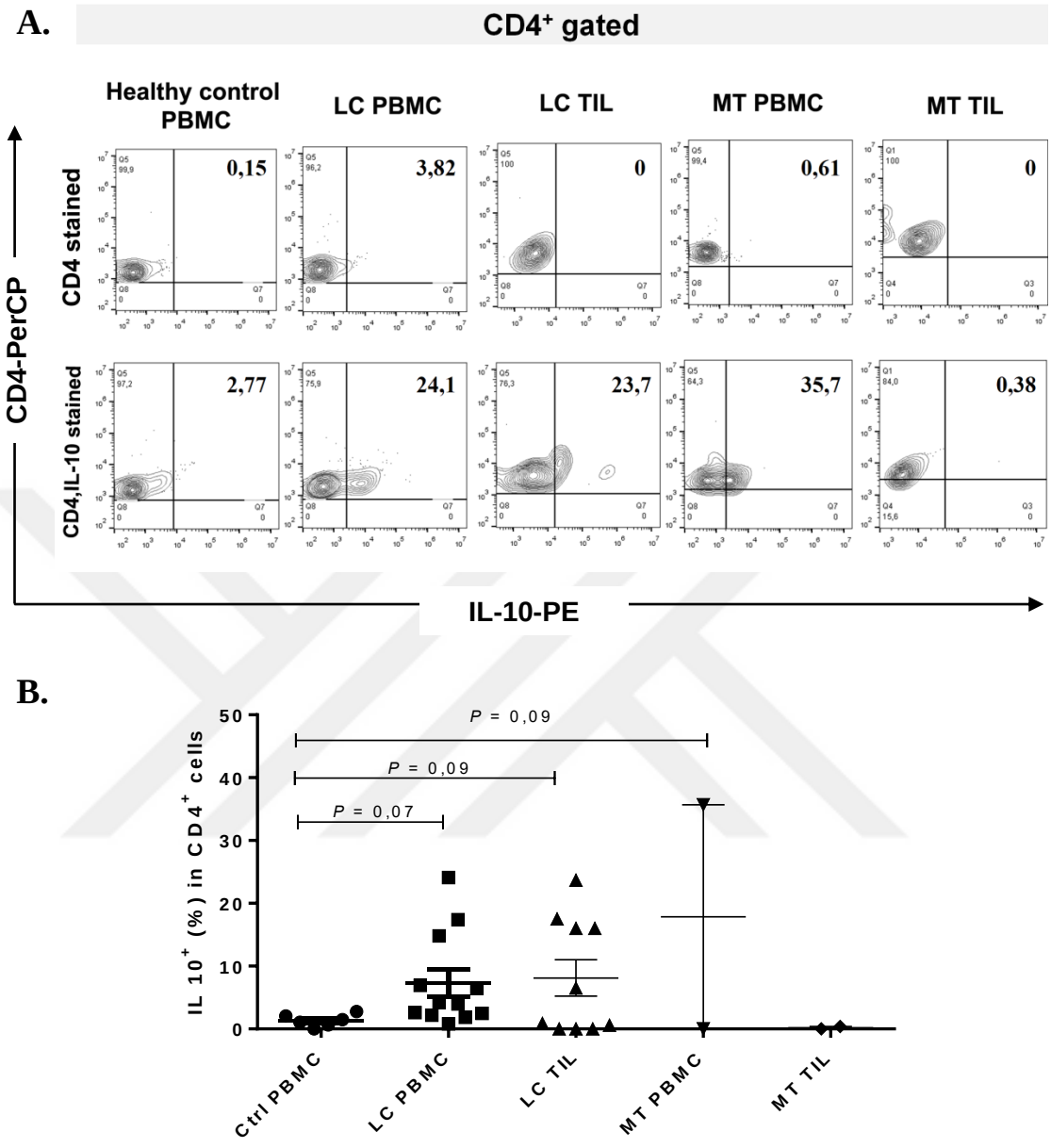

Figure 3.4 : $CD4^+IL\text{-}10^+$ cell percentages gated on $CD4^+$ T lymphocytes for LC and MT patients' blood and TILs. A) Representative quadrant plots of IL-10 intracellular staining gated on $CD4^+$ cells for one blood sample from a healthy person, as well as one blood sample and one tumor tissue sample (TIL) from LC and MT. B)Frequencies of $CD4^+IL10^+$ T cells in 6 blood samples of healthy controls; 12 blood samples, 10 lung tissue samples of LC patients and 2 blood samples, 2 lung tissue samples of MT patients. Each dot represents one individual. Graphs were prepared using Graphpad Prism 6. Student's *t* test were used for statistical analysis. **p*<0.05, ***p*<0.01, ****p*<0.001, *****p*<0.0001. LC, lung cancer; MT, mesothelioma; PBMC, peripheral blood mononuclear cell; TIL, tumor infiltrating leukocytes.

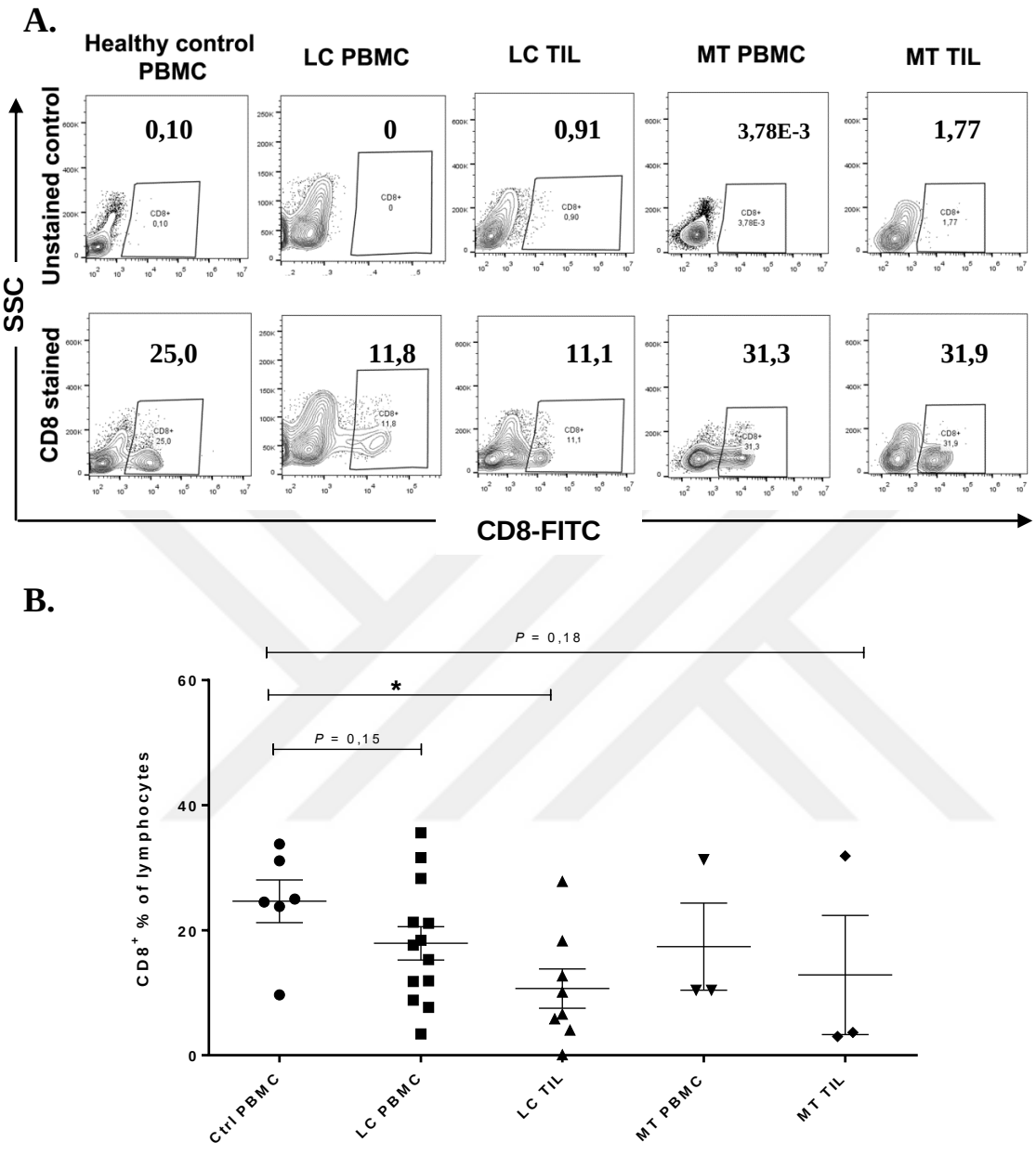

Figure 3.5 : $CD8^+$ cell percentages gated on lymphocytes for LC and MT patients' blood and TILs. A) CD8 staining representative quadrant plots for one blood sample from a healthy person, as well as one blood sample and one tumor tissue sample (TIL) from LC and MT. B)Frequencies of $CD8^+$ T cells in 6 blood samples of healthy controls; 13 blood samples, 8 lung tissue samples of LC patients and 3 blood samples, 3 lung tissue samples of MT patients. Each dot represents one individual. Graphs were prepared using Graphpad Prism 6. Student's *t* test were used for statistical analysis. **p*<0.05, ***p*<0.01, ****p*<0.001, *****p*<0.0001. Ctrl, control; LC, lung cancer; MT, mesothelioma; PBMC, peripheral blood mononuclear cell; TIL, tumor infiltrating leukocytes.

3.2.2 IFNγ producing $CD8^+$ T cells in NSCLC and MT

It is known that cytotoxic T cells secrete anti-tumor cytokines such as IFNγ. The IFNγ production of $CD8^+$ T cells was examined by intracellular IFNγ staining which was afterwards detected by flow cytometry. For this purpose, PBMCs were isolated from blood of healthy controls (n=6), LC patients (n=12) and MT patients (n=3) by density gradient centrifugation. TILs were also isolated from tumor biopsies of LC (n=5) and MT (n=3) patients.

Percentages of $CD8^+IFN\gamma^+$ T cells were determined compared to unstained control and $CD8^+$cells within lymphocyte population. IFNγ expression of $CD8^+$ T cells were significantly increased (15,2-68,9% to 20,3-94,9%) in blood of patients with NSCLC compared to healthy controls. IFNγ producing T cells were also observed in LC and MT tumors in lower levels, $CD8^+IFN\gamma^+$ cells constituted almost 80% of $CD8^+$ T cells in tumor for one NSCLC patient (Figure 3.6).

3.3 $CD19^+$ B Cells in Patients with NSCLC and MT

3.3.1 $CD19^+$ B cell frequencies in patients with NSCLC and MT

Accumulating evidence is pointing to a role of B cells in modulating the immune response to solid tumors. Because of this, frequencies of $CD19^+$ B cells were examined by surface staining of CD19 which was afterwards detected by flow cytometry. For this purpose, PBMCs were isolated from blood of healthy controls (n=6), LC patients (n= 13) and MT patients (n=3). TILs were also isolated from tumor biopsies of LC (n=10) and MT (n=3) patients. PBMC and TILs were labeled with anti-CD19-APC and analyzed with flow cytometry. Percentages of $CD19^+$ B cells were determined compared to unstained control within lymphocyte population. B cell numbers were seem to be similar between controls' and patients' blood sample. Although, increased $CD19^+$ B cell infiltration to the tumors of MT (0,98-17,4%) and LC (0,09-33,3%) patients can be observed (Figure 3.7).

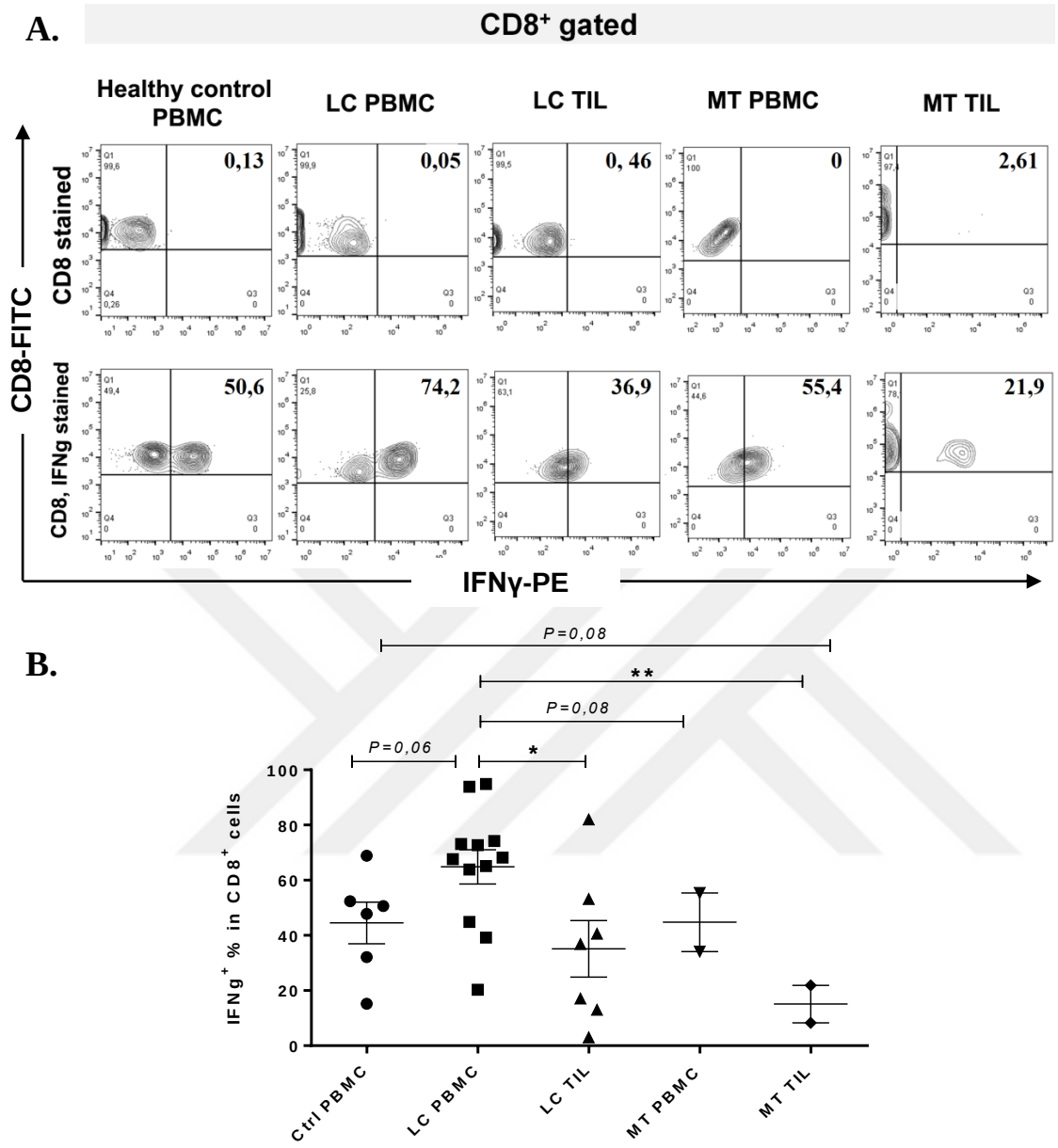

Figure 3.6 : $CD8^+IFN\gamma^+$ cell percentages in $CD8^+$ T lymphocytes of LC and MT patients' blood and TILs. A) Representative quadrant plots of IFNγ intracellular staining gated on $CD8^+$ cells for one blood sample from a healthy person, as well as one blood sample and one tumor tissue sample (TIL) from LC and MT. B)Frequencies of $CD8^+IFN\gamma^+$ T cells in 6 blood samples of healthy controls; 12 blood samples, 7 lung tissue samples of LC patients and 2 blood samples, 2 lung tissue samples of MT patients. Each dot represents one individual. Graphs were prepared using Graphpad Prism 6. Student's *t* test were used for statistical analysis. **p*<0.05, ***p*<0.01, ****p*<0.001, *****p*<0.0001. LC, lung cancer; MT, mesothelioma; PBMC, peripheral blood mononuclear cell; TIL, tumor infiltrating leukocytes.

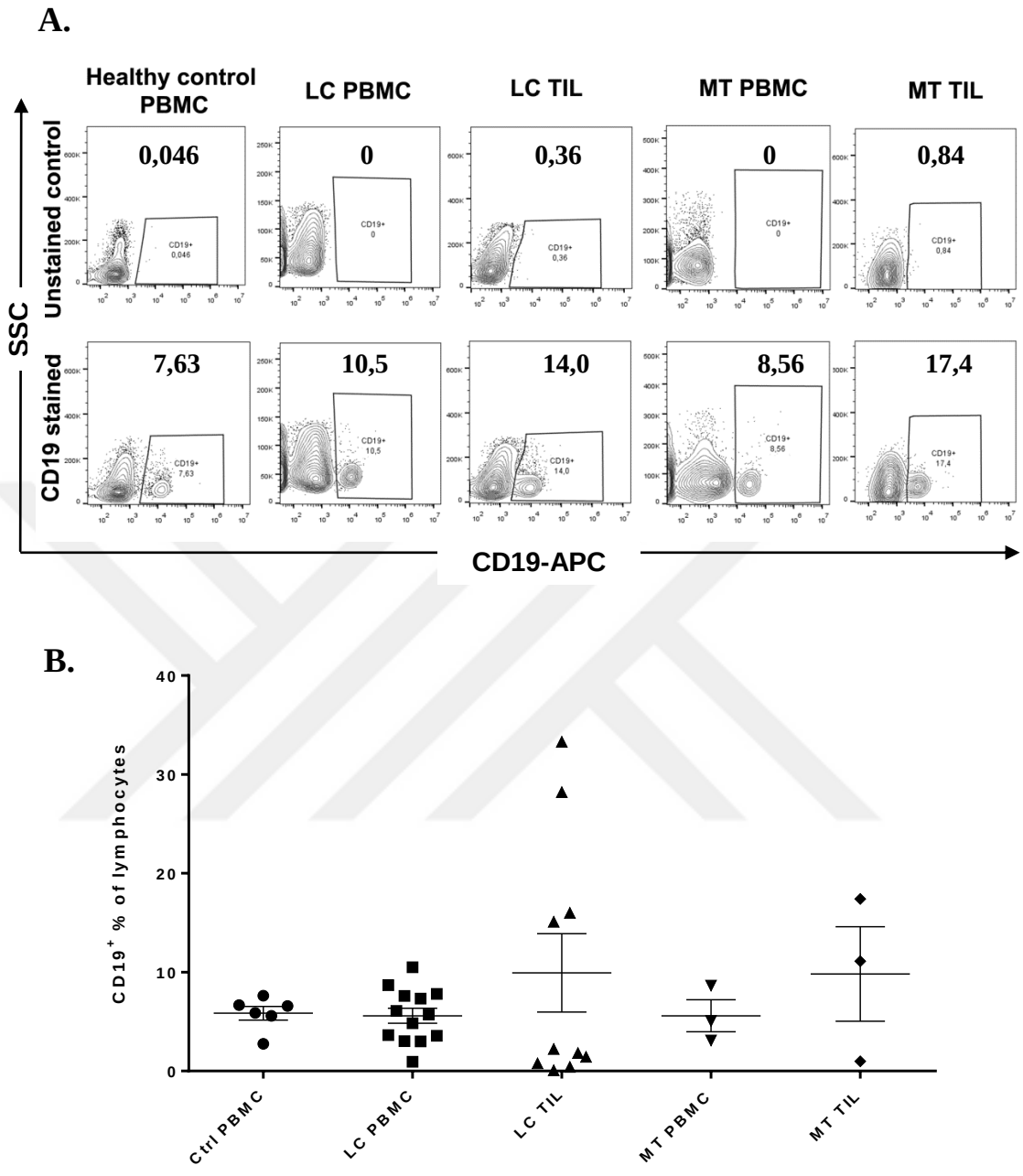

Figure 3.7 : $CD19^+$ cell percentages gated on lymphocytes for LC and MT patients' blood and TILs. A) CD19 staining representative quadrant plots for one blood sample from a healthy person, as well as one blood sample and one tumor tissue sample (TIL) from LC and MT. B)Frequencies of $CD19^+$ B cells in 6 blood samples of healthy controls; 13 blood samples, 10 lung tissue samples of LC patients and 3 blood samples, 3 lung tissue samples of MT patients. Each dot represents one individual. Graphs were prepared using Graphpad Prism 6. Student's *t* test were used for statistical analysis. **p*<0.05, ***p*<0.01, ****p*<0.001, *****p*<0.0001. Ctrl, control; LC, lung cancer; MT, mesothelioma; PBMC, peripheral blood mononuclear cell; TIL, tumor infiltrating leukocytes.

3.3.2 IFNγ producing $CD19^+$ B cells in NSCLC and MT

The IFNγ production of $CD19^+$ B cells was examined by intracellular IFNγ staining which was afterwards detected by flow cytometry. For this purpose, PBMCs were isolated from blood of healthy controls (n=6), LC patients (n= 12) and MT patients (n=3). TILs were also isolated from tumor biopsies of LC (n=5) and MT (n=3) patients. Then, cells were stimulated with PMA and ionomycin for 5 h in the presence of monensin to keep the cytokines accumulated inside the golgi complex. First, cells were labeled with anti-CD19-APC. After that, the cells were fixed. After that, the cells were fixed and permeabilized. Lastly, they were incubated with PE-coupled anti-IFNγ antibody that was prepared inside the permeabilization buffer.

Percentages of $CD19^+$ $IFN\gamma^+$ B cells were determined compared to unstained control and $CD19^+$ cells within lymphocyte population. $CD19^+IFN\gamma^+$ cells were also tend to be but not significantly increased in bloods of LC patients (2,31-56,5% to 1,01-81,6%) (Figure 3.8).

3.3.3 IL-17 producing $CD19^+$ B cells in NSCLC and MT

The IL-17 production of $CD19^+$ B cells was examined by intracellular IL-17 antibody staining which was afterwards detected by flow cytometry. For this purpose, PBMCs were isolated from blood of healthy controls (n=6), LC patients (n= 10) and MT patients (n=4). TILs were also isolated from tumor biopsies of LC (n=4) and MT (n=4) patients. Then, cells were stimulated with PMA and ionomycin for 5 h in the presence of monensin to keep the cytokines accumulated inside the golgi complex. First, cells were labeled with anti-CD19-APC. After that, the cells were fixed and permeabilized. Lastly, they were incubated with FITC-coupled anti-IL-17 antibody that was prepared inside the permeabilization buffer.

Percentages of $CD19^+IL\text{-}17^+$ B cells were determined compared to unstained control and $CD19^+$ cells within lymphocyte population. IL-17 expression by $CD19^+$ B cells (0,44-9,7%) had a trend of increase in LC patients' blood compared to control (0,76-3,72%) (Figure 3.9).

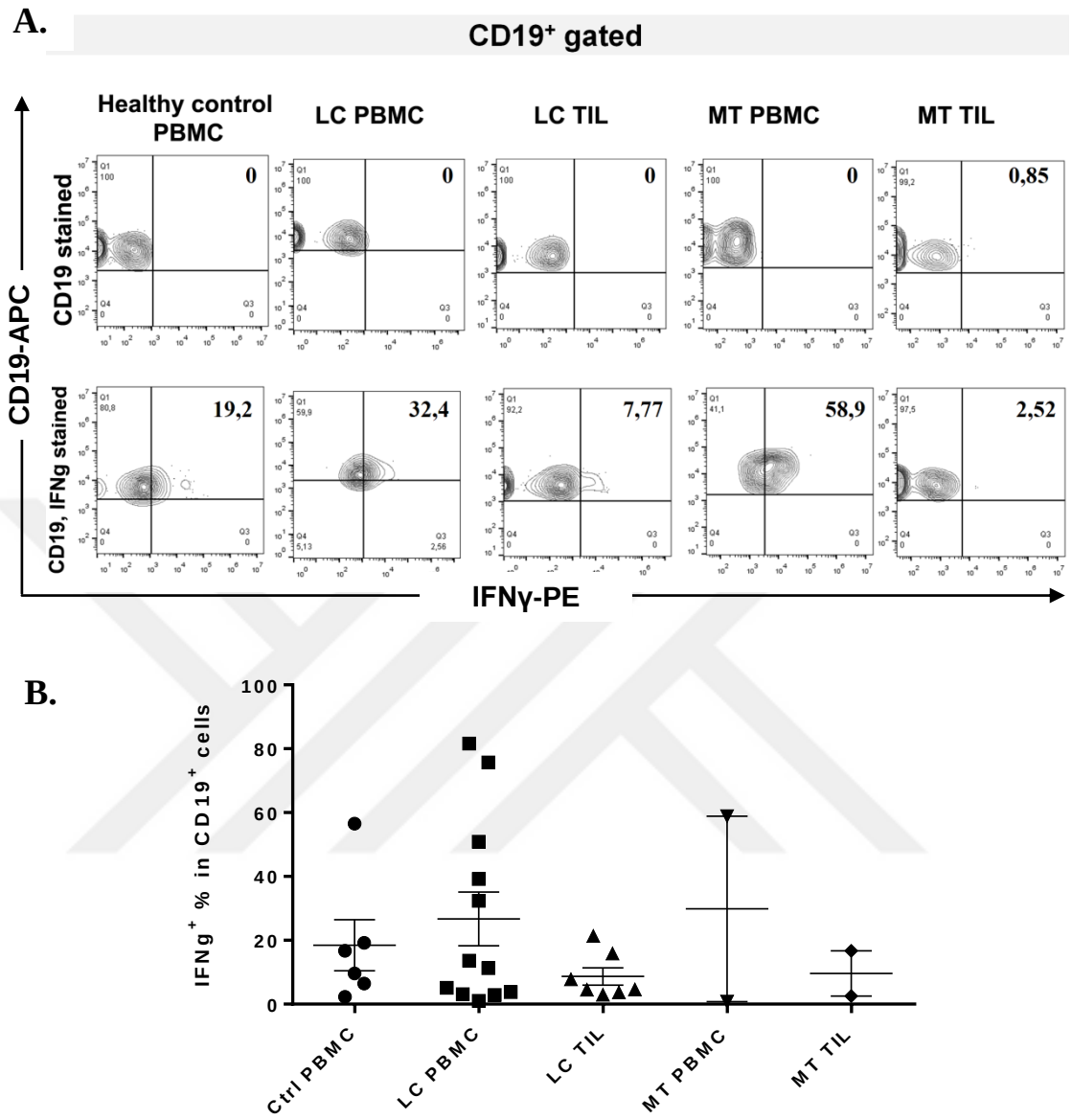

Figure 3.8 : $CD19^+IFN\gamma^+$ cell percentages in $CD19^+$ B lymphocytes of LC and MT patients' blood and TILs. A) Representative quadrant plots of IFNγ intracellular staining gated on $CD19^+$ cells for one blood sample from a healthy person, as well as one blood sample and one tumor tissue sample (TIL) from LC and MT. B)Frequencies of $CD19^+IFN\gamma^+$ T cells in 6 blood samples of healthy controls; 12 blood samples, 7 lung tissue samples of LC patients and 2 blood samples, 2 lung tissue samples of MT patients. Each dot represents one individual. Graphs were prepared using Graphpad Prism 6. Student's *t* test were used for statistical analysis. **p*<0.05, ***p*<0.01, ****p*<0.001, *****p*<0.0001. LC, lung cancer; MT, mesothelioma; PBMC, peripheral blood mononuclear cell; TIL, tumor infiltrating leukocytes.

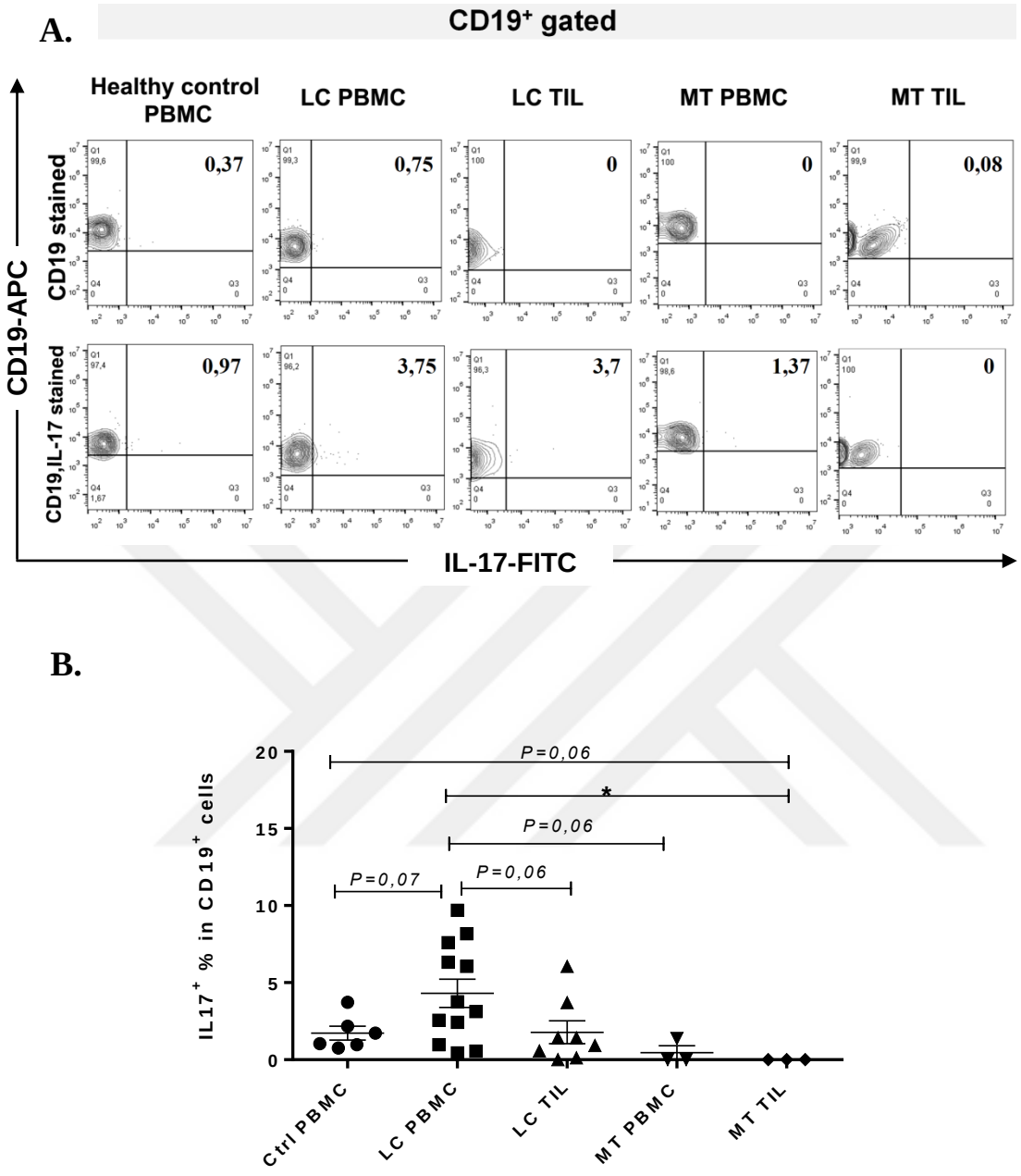

Figure 3.9 : $CD19^{+}IL\text{-}17^{+}$ cell percentages in $CD19^{+}$ B lymphocytes of LC and MT patients' blood and TILs. A) Representative quadrant plots of IL-17 intracellular staining gated on $CD19^{+}$ cells for one blood sample from a healthy person, as well as one blood sample and one tumor tissue sample (TIL) from LC and MT. B)Frequencies of $CD19^{+}IL\text{-}17^{+}$ T cells in 6 blood samples of healthy controls; 12 blood samples, 8 lung tissue samples of LC patients and 3 blood samples, 3 lung tissue samples of MT patients. Each dot represents one individual. Graphs were prepared using Graphpad Prism 6. Student's *t* test were used for statistical analysis. **p*<0.05, ***p*<0.01, ****p*<0.001, *****p*<0.0001. LC, lung cancer; MT, mesothelioma; PBMC, peripheral blood mononuclear cell; TIL, tumor infiltrating leukocytes.

3.3.4 IL-10 producing $CD19^+$ B cells in NSCLC and MT

Bregs are generated in response to signals from the tumor microenvironment and in turn promote tumor growth mainly with secreting IL-10. The IL-10 production of $CD19^+$ B cells was examined by intracellular IL-10 staining which was afterwards detected by flow cytometry. For this purpose, PBMCs were isolated from blood of healthy controls (n=6), LC patients (n= 12) and MT patients (n=3). TILs were also isolated from tumor tissue samples of LC (n=5) and MT (n=3) patients. Then, cells were stimulated with 0,7 μg/ml CpG for 24 h, and PMA and ionomycin for 5 h in the presence of monensin to keep the cytokines accumulated inside the golgi complex. First, cells were labeled with anti-CD19-APC. After that, the cells were fixed and permeabilized. Lastly, they were incubated with Alexa Fluor 488-coupled anti-IL-10 antibody that was prepared inside the permeabilization buffer.

Percentages of $CD19^+IL\text{-}10^+$ B cells were determined compared to unstained control and $CD19^+$ cells within lymphocyte population. IL-10 expression of $CD19^+$ B cells increased significantly in bloods (0,85-17,3%) and TILs (0-20%) of patients with NSCLC compared with healthy individuals (0-1,46%). Moreover, IL-10 production by MT tumor infiltrating $CD19^+$ B cells (1,15-10%) were significantly higher compared to blood of healthy people (0-1,46%) (Figure 3.10).

3.4 $CD19^+CD24^+CD38^+$ B Cells in Patients with NSCLC and MT

3.4.1 $CD19^+CD24^+CD38^+$ B cell frequencies in patients with NSCLC and MT

IL-10 producing $CD19^+CD24^+CD38^+$ B cells have been characterized as a type of regulatory B cells in literature (Blair et al., 2010, Flores-Borja et al., 2013). The frequencies of $CD19^+CD24^+CD38^+$ B cells were examined by surface staining of CD19, CD24 and CD38 which was afterwards detected by flow cytometry. For this purpose, PBMCs were isolated from blood of healthy controls (n=6), LC patients (n= 11) and MT patients (n=3). TILs were also isolated from tumor biopsies of LC (n=4) and MT (n=4) patients. PBMC and TILs were labeled with anti-CD19-APC, anti-CD24-PE and anti-CD38-PerCP; analyzed with flow cytometry. Percentages of $CD19^+CD24^+CD38^+$, $CD19^+CD24^+CD38^-$, and $CD19^+CD24^-CD38^+$ B cells were determined compared to unstained control and $CD19^+$ cells within lymphocyte population. In each group, $CD19^+CD24^+CD38^-$ B cells were most common type of B

cells. Moreover, $CD19^{+}CD24^{-}CD38^{+}$ B cells were tend to be increased in bloods of LC patients (0,36-16,3%) compared to healthy controls (1,4-3,85%) (Figure 3.11).

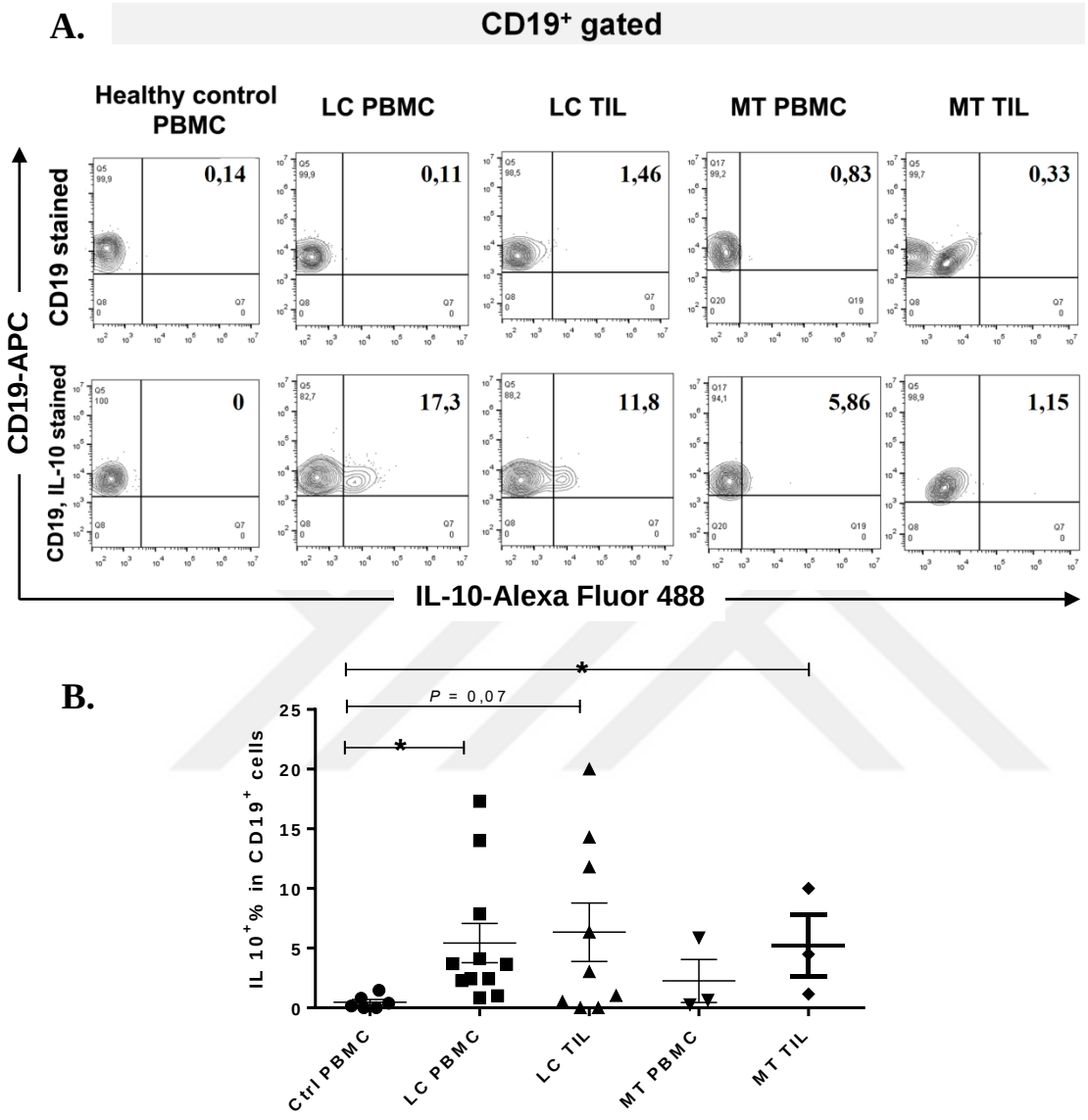

Figure 3.10 : $CD19^{+}IL\text{-}10^{+}$ cell percentages gated on $CD19^{+}$ B lymphocytes for LC and MT patients' blood and TILs. A) Representative quadrant plots of IL-10 intracellular staining gated on $CD19^{+}$ cells for one blood sample from a healthy person, as well as one blood sample and one tumor tissue sample (TIL) from LC and MT. B)Frequencies of $CD19^{+}IL10^{+}$ B cells in 6 blood samples of healthy controls; 11 blood samples, 9 lung tissue samples of LC patients and 3 blood samples, 3 lung tissue samples of MT patients. Each dot represents one individual. Graphs were prepared using Graphpad Prism 6. Student's *t* test were used for statistical analysis. **p*<0.05, ***p*<0.01, ****p*<0.001, *****p*<0.0001. LC, lung cancer; MT, mesothelioma; PBMC, peripheral blood mononuclear cell; TIL, tumor infiltrating leukocytes.

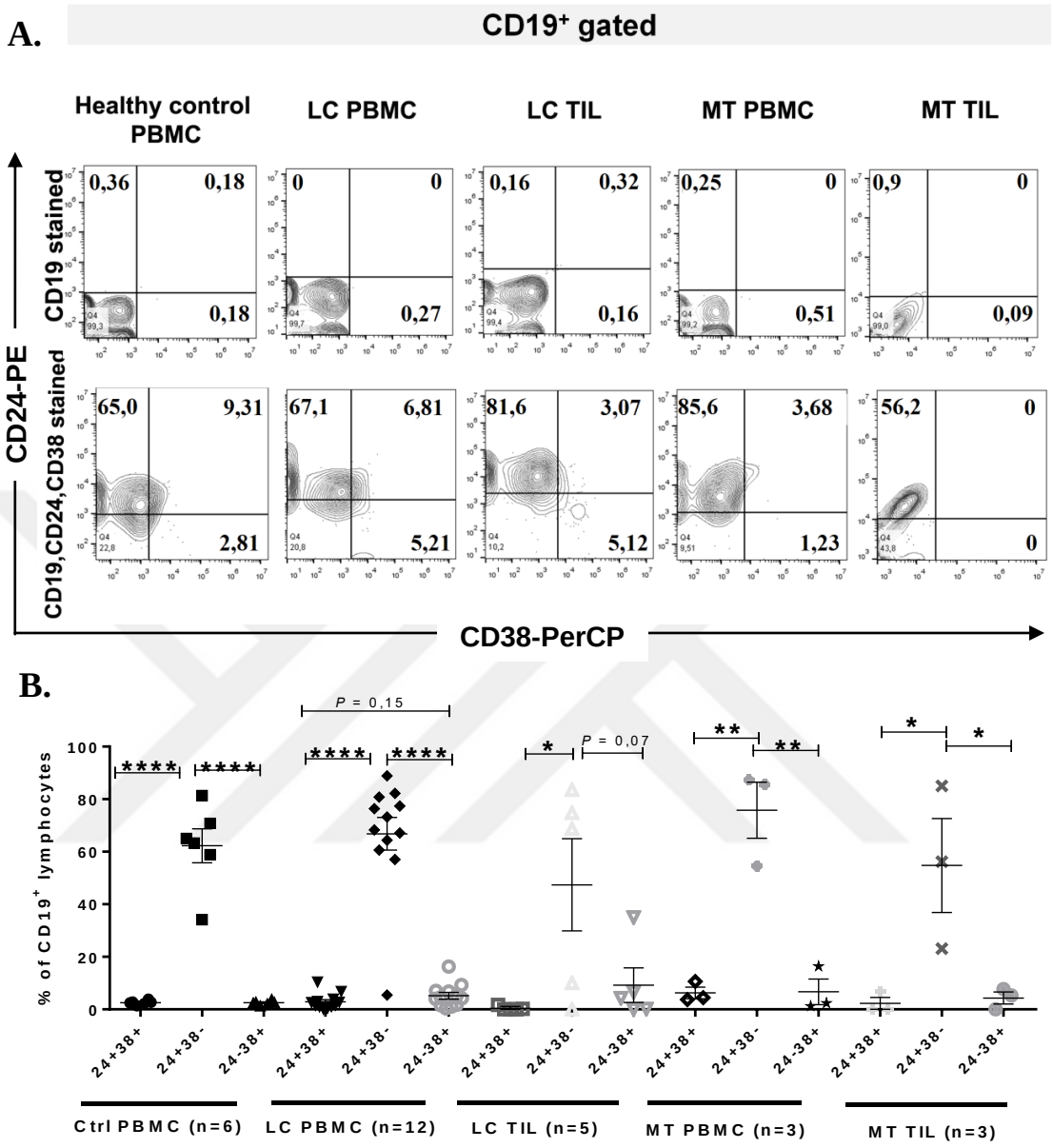

Figure 3.11 : $CD19^+CD24^+CD38^+$/ $CD19^+CD24^+CD38^-$/ $CD19^+CD24^-$ $CD38^+$ cell percentages gated on $CD19^+$ B lymphocytes of LC patients' blood and TILs. A) Representative quadrant plots of CD19,CD24,CD38 staining gated on $CD19^+$ cells for one blood sample for a healthy person, as well as one blood sample and one tumor tissue sample (TIL) from LC and MT.. B)Frequencies of $CD19^+CD24^+CD38^+$/ $CD19^+CD24^+CD38^-$/ $CD19^+CD24^-CD38^+$ B cells in 6 blood samples for healthy controls, 10 blood samples for LC patients, 5 tumor tissue samples for LC patients, 3 blood samples and tissue samples for MT patients. Each dot represents one individual. Graphs were prepared using Graphpad Prism 6. Student's *t* test were used for statistical analysis. **p*<0.05, ***p*<0.01, ****p*<0.001, *****p*<0.0001. LC, lung cancer; MT, mesothelioma; PBMC, peripheral blood mononuclear cell; TIL, tumor infiltrating lymphocytes.

3.4.2 IL-10 producing $CD19^+CD24^+CD38^+$ B cells in NSCLC

The IL-10 production of $CD19^+CD24^+CD38^+$ B cells was examined by intracellular IL-10 antibody staining which was afterwards detected by flow cytometry. For this purpose, PBMCs were isolated from blood of healthy controls (n=6) and LC patients (n= 11). Then, cells were stimulated with 0,7 μg/ml CpG for 24 h, and PMA and ionomycin for 5 h in the presence of monensin to keep the cytokines accumulated inside the golgi complex. First, cells were labeled with anti-CD19-APC, anti-CD24-PE and anti-CD38-PerCP. After that, the cells were fixed and permeabilized. Lastly, they were incubated with Alexa Fluor-coupled anti-IL-10 antibody that was prepared inside the permeabilization buffer.

Percentages of $CD19^+CD24^+CD38^+$ $IL\text{-}10^+$, $CD19^+CD24^+CD38^-$ $IL\text{-}10^+$ and $CD19^+CD24^-CD38^+$ $IL\text{-}10^+$ B cells were determined compared to unstained control and $CD19^+$ cells within lymphocyte population. IL-10 expression in $CD19^+CD24^+CD38^+$ B cells (0-4,35% and 0-75%) were significantly higher than $CD19^+CD24^+CD38^-$ B cells (0-0,77% and 0-4,82%) in both blood samples of healthy controls and LC patients. Also, $CD19^+CD24^+CD38^+$ $IL\text{-}10^+$ B cells were significantly more than $CD19^+CD24^-CD38^+$ $IL\text{-}10^+$ B cells (0-13,3%) in blood of LC patients. Above all, IL-10 expression by $CD19^+CD24^+CD38^+$ B cells from blood of LC patients were greater than $CD19^+CD24^+CD38^+$ B cells of healthy controls (P=0,07) (Figure 3.12).

3.5 $CD19^+PD\text{-}1^+$ B Cells in Patients with NSCLC and MT

3.5.1 $CD19^+PD\text{-}1^+$ B cell frequencies in patients with NSCLC and MT

Recently, novel tumor-promoting $PD\text{-}1^{high}$ Breg subset in tumor tissues of patients with hepatocellular carcinoma were identified (Xiao et al., 2016). Therefore, frequencies of $CD19^+PD\text{-}1^+$ B cells were examined by surface staining of CD19 and PD-1 which was afterwards detected by flow cytometry. For this purpose, PBMCs were isolated from blood of healthy controls (n=6) and LC patients (n=4). TILs were also isolated from tumor biopsies of LC patients (n=4). After 24 hours of CpG and 5 hours PMA and ionomycin treatment, PBMCs were labeled with anti-CD19-APC and anti-PD-1-PE. Samples were analyzed with flow cytometry.

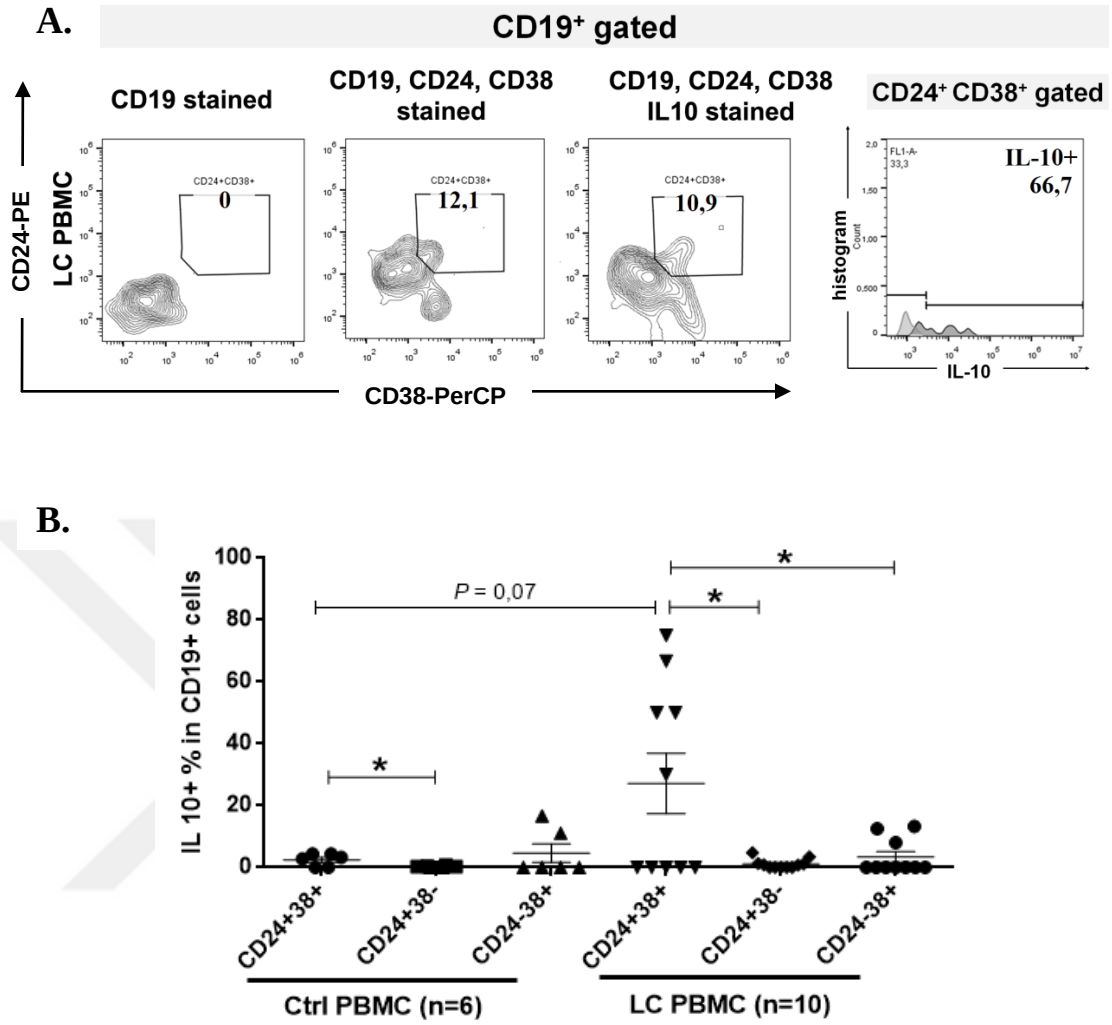

Figure 3.12 : $CD19^+CD24^+CD38^+IL\text{-}10^+$/ $CD19^+CD24^+CD38^-IL\text{-}10$/ $CD19^+CD24^-CD38^+IL\text{-}10^+$ cell percentages gated on $CD19^+CD24^+CD38^+$ / $CD19^+CD24^+CD38^-$ / $CD19^+CD24^-CD38^+$ B lymphocytes of LC patients' blood and TILs. A) Representative quadrant plots of IL-10 intracellular staining gated on $CD19^+CD24^+CD38^+$ / $CD19^+CD24^+CD38^-$ / $CD19^+CD24^-CD38^+$ cells for one blood sample from LC. B)Frequencies of $CD19^+CD24^+CD38^+IL\text{-}10^+$/ $CD19^+CD24^+CD38^-IL\text{-}10$/ $CD19^+CD24^-CD38^+IL\text{-}10^+$ B cells in 6 blood samples of healthy controls and 10 blood samples of LC patients. Each dot represents one individual. Graphs were prepared using Graphpad Prism 6. Student's *t* test were used for statistical analysis. **p*<0.05, ***p*<0.01, ****p*<0.001, *****p*<0.0001. LC, lung cancer; MT, mesothelioma; PBMC, peripheral blood mononuclear cell; TIL, tumor infiltrating leukocytes.

Percentages of $CD19^+PD\text{-}1^+$ B cells were determined compared to unstained control and $CD19^+$ cells within lymphocyte population. PD-1 expression of B cells were significantly increased in blood (2,14-11,1%) and tumor tissues (3,52-28,6%) of patients with NSCLC compared to healthy individuals (0,79-3,9%) (Figure 3.13).

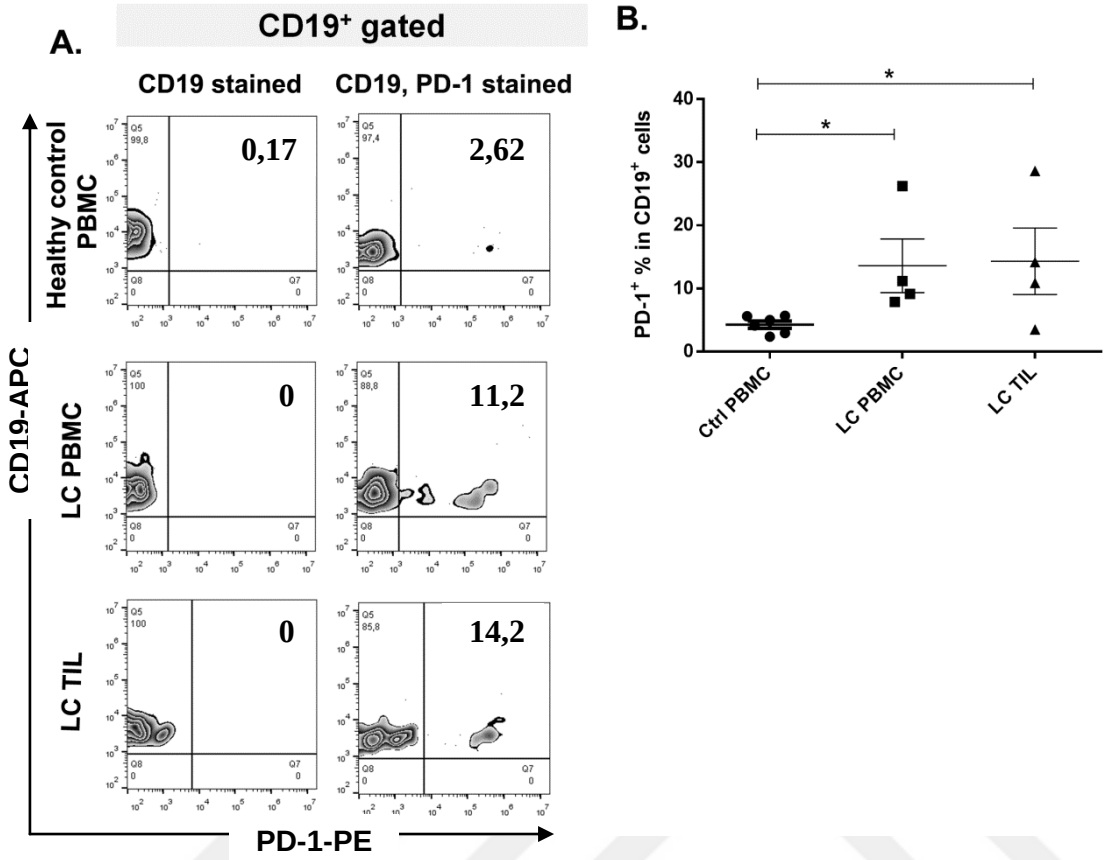

Figure 3.13 : $CD19^+PD\text{-}1^+$ cell percentages gated on $CD19^+$ B lymphocytes for LC patients' blood and TILs. A) Representative quadrant plots of PD-1 staining gated on $CD19^+$ cells for one blood sample from a healthy person, as well as one blood sample and one tumor tissue sample (TIL) from LC. B)Frequencies of CD19 $PD\text{-}1^+$ B cells in 6 blood samples of healthy controls; 4 blood samples and 4 lung tissue samples of LC patients. Each dot represents one individual. Graphs were prepared using Graphpad Prism 6. Student's *t* test were used for statistical analysis. **p*<0.05, ***p*<0.01, ****p*<0.001, *****p*<0.0001. LC, lung cancer; PBMC, peripheral blood mononuclear cell; TIL, tumor infiltrating leukocytes.

3.5.2 IL-10 producing $CD19^+PD\text{-}1^+$ B cells in NSCLC and MT

The IL-10 production of $CD19^+PD\text{-}1^+$ B cells was examined by intracellular IL-10 staining which was afterwards detected by flow cytometry. For this purpose, PBMCs were isolated from blood of healthy controls (n=6) and LC patients (n=4). Then, cells were stimulated with 0,7 μg/ml CpG for 24 h, and PMA and ionomycin for 5 h in the presence of monensin to keep the cytokines accumulated inside the Golgi complex. First, cells were labeled with anti-CD19-APC and anti-PD-1-PE. After that, the cells were fixed and permeabilized. Lastly, they were incubated with Alexa Fluor-coupled anti-IL-10 antibody that was prepared inside the permeabilization buffer.

Percentages of $CD19^+$ $PD\text{-}1^+$ $IL\text{-}10^+$ B cells were determined compared to unstained control and $CD19^+$ cells within lymphocyte population. PD-1 and IL-10 double positive B cells were significantly increased in blood samples of patients with NSCLC (0,68-5,45%) in comparison to healthy individuals (0-0,94%) (Figure 3.14).

3.6 Effect of Tumor Microenvironment on Immune Cells

3.6.1 $CD19^+$ B and $CD4^+$ T cell isolation from peripheral blood

B and $CD4^+$ T cells were isolated from PBMCs by using Human B Cell Enrichment Kit and $CD4^+$ Selection Kit, (see Materials&Methods, Section 2.2.3.3). Isolation of $CD4^+$ T cells and enrichment of B cells were performed by positive and negative selection, respectively, using magnetic separation method. Following the separation, to detect their purity, $CD4^+$ T cells were labeled with PE-coupled anti-CD4 antibody; B cells were labeled with APC-coupled anti-CD19 antibody and compared to unstained control. Flow cytometry analyses showed that the $CD4^+$ T cells were isolated with purities of 98,2% and 99,4%; the B cells were isolated with purities of 92,2% and 89,4% (Figure 3.15).

3.6.2 $CD4^+$ T cells

3.6.2.1 Tumor microevironment increases IL-10 expression of $CD4^+$ T cells

The IL-10 production of $CD4^+$T cells was examined by intracellular IL-10 staining which was afterwards detected by flow cytometry (Figure 3.16). For this purpose, the cells were cultured with either tumor conditioned medium or normal tissue conditioned medium and stimulated with 2 μg/ml PHA for 24 h compared to unstained control is given. $CD4^+$ T cells were also stimulated with PMA and ionomycin for 5 h in the presence of 1X Brefeldin A to keep the cytokines accumulated inside the Golgi complex. After that, the cells were fixed and permeabilized. Lastly, they were incubated with PE-coupled anti-IL-10 antibody that was prepared inside the permeabilization buffer.

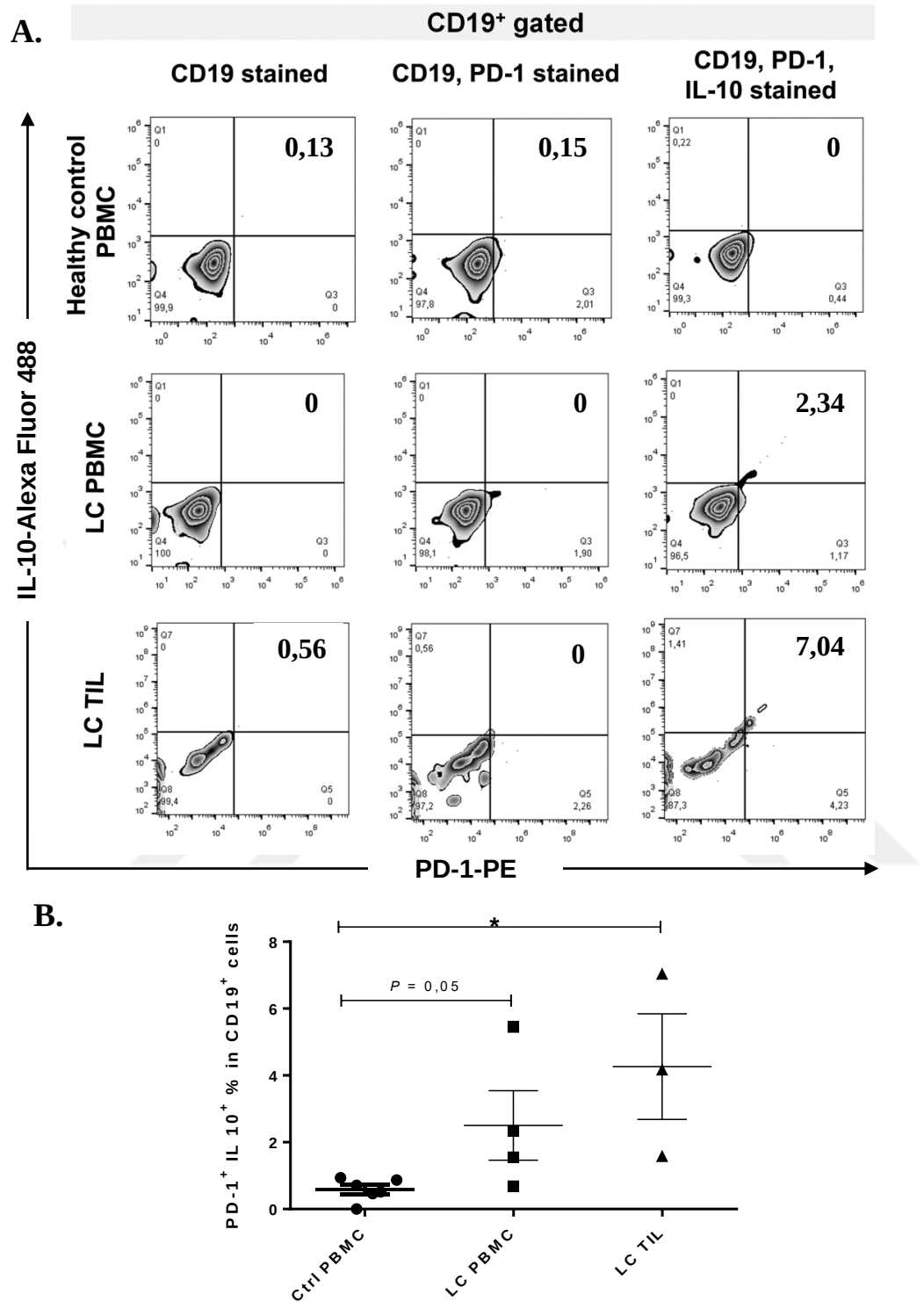

Figure 3.14 : $CD19^+PD\text{-}1^+IL\text{-}10^+$ cell percentages gated on $CD19^+$ B lymphocytes for LC patients' blood and TILs. A) Representative quadrant plots of IL-10 intracellular staining gated on $CD19^+$ cells for one blood sample from a healthy person, as well as one blood sample and one tumor tissue sample (TIL) from LC and MT. B) Frequencies of $CD19^+IL10^+$ B cells in 6 blood samples of healthy controls; 11 blood samples, 9 lung tissue samples of LC patients and 3 blood samples, 3 lung tissue samples of MT patients. Each dot represents one individual. Graphs were prepared using Graphpad Prism 6. Student's *t* test were used for statistical analysis. **p*<0.05, ***p*<0.01, ****p*<0.001, *****p*<0.0001. LC, lung cancer; PBMC, peripheral blood mononuclear cell; TIL, tumor infiltrating leukocytes.

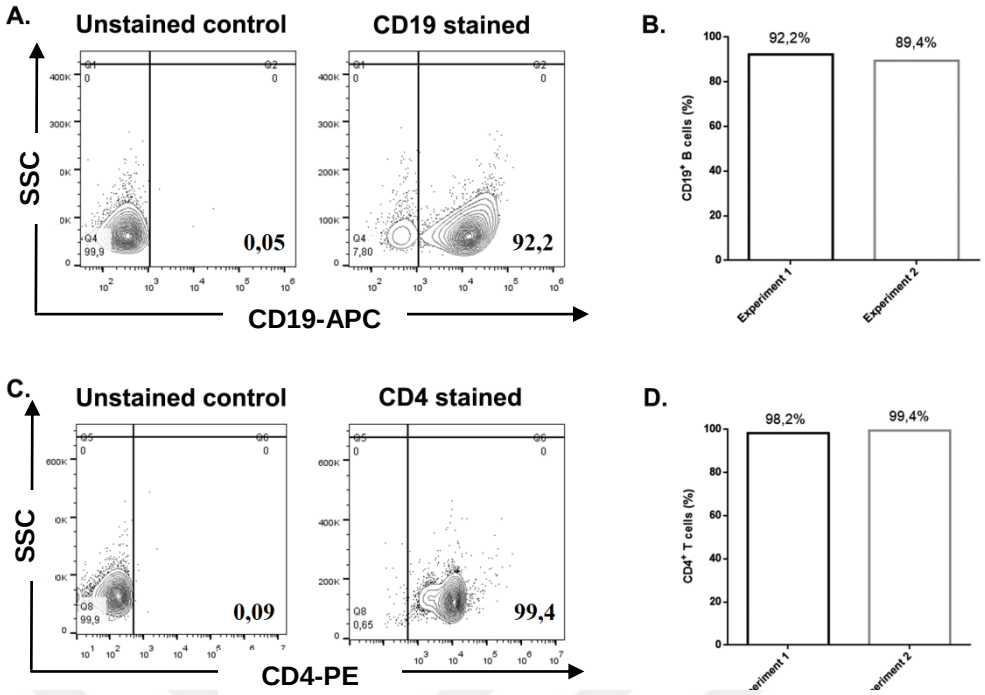

Figure 3.15 : Purity of B and $CD4^+$ T cells isolated from PBMCs of healthy controls. A.) Representative flow cytometry quadrant plot of purified B cells compared to unstained control. B cells were magnetically isolated from PBMCs by negative selection. Cells were either stained with APC-coupled anti-CD19 antibody or left unstained (unstained control) in order to detect the percentage of cells expressing B cell-specific surface marker CD19. B.) B cell purities of each experiment are shown in the graph. C.) Representative flow cytometry quadrant plot of purified $CD4^+$ T cells compared to unstained control. $CD4^+$ T cells were magnetically isolated from PBMCs by positive selection. Cells were either stained with PE-coupled anti-CD4 antibody or left unstained (unstained control) in order to detect the percentage of cells expressing $CD4^+$ T cell-specific surface marker CD4. B.) $CD4^+$ T cell purities of each experiment are shown in the graph. For the measurements BD ACCURI C6 flow cytometer and for the analyses FlowJo Software is used. Graphs are prepared with Graphpad Prism 6 software.

As shown in Figure 3.16, when compared with the normal tissue conditioned culture, $CD4^+$T cells had higher levels of IL-10 production when cultured with tumor conditioned medium. 3,71% and 2,94% of T cells cultured with tumor conditioned medium produced IL-10 while 1,54% and 1,93% of the T cell population was IL-10 positive when T cells were cultured with normal tissue conditioned medium. Even though there were some deviations within the two experimental data sets in the result graph (Figure 3.16B), the IL-10 cytokine production levels of T cells in tumor microenviroment were increased according to normal tissue microenvironment for both of the experiments. It could be suggested that in both experiments there was a trend of differentiation of $CD4^+$ T cells into $IL10^+$ $CD4^+$ Tregs.

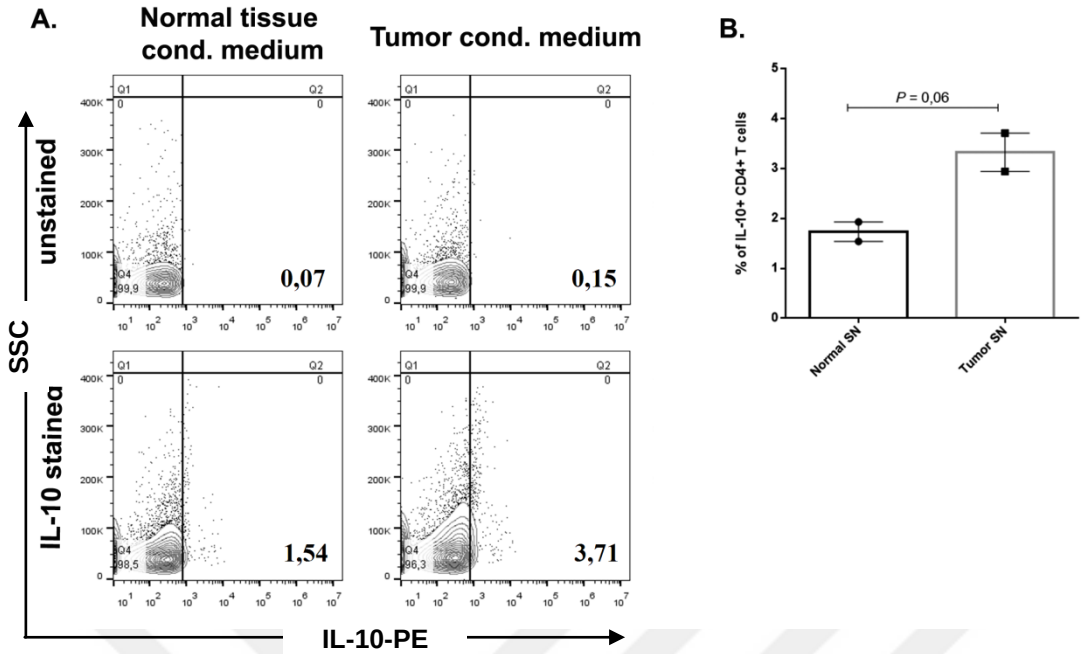

Figure 3.16 : IL-10 Levels of $CD4^+$ T cells cultured with either tumor conditioned medium or normal tissue conditioned medium for 24 h. A.) Representative flow cytometry quadrant plot of $CD4^+IL\text{-}10^+$ T cells cultured with either tumor conditioned medium or normal tissue conditioned medium and stimulated with 2 µg/ml PHA and 0,7 µg/ml CpG for 24 h compared to unstained control is given. $CD4^+$ T cells were also stimulated with PMA and ionomycin for 5 h in the presence of 1X Brefeldin A. Intracellular staining was done for IL-10 cytokine using anti-IL10-PE antibody. B.) A graphical expression of the $CD4^+IL\text{-}10^+$ T cells cultured with either tumor conditioned medium (tumor SN) or normal tissue conditioned medium (normal SN). For the measurements BD ACCURI C6 flow cytometer and for the analyses FlowJo Software was used. Graphs were prepared with Graphpad Prism 6 software. Student's *t* test were used for statistical analysis. **p*<0.05.

3.6.2.2 Tumor microevironment decreases IFNγ expression of $CD4^+$ T cells

The IFNγ production of $CD4^+$ T cells was examined by intracellular IFNγ staining which was afterwards detected by flow cytometry (Figure 3.17). For this purpose, the cells cultured with either tumor conditioned medium or normal tissue conditioned medium and stimulated with 2 µg/ml PHA for 24 h compared to unstained control is given. $CD4^+$ T cells were also stimulated with PMA and ionomycin for 5 h in the presence of 1X Brefeldin A to keep the cytokines accumulated inside the Golgi complex. After that, the cells were fixed and permeabilized. Lastly, they were incubated with PE-coupled anti-IFNγ antibody.

As shown in Figure 3.17, when compared to culturing with the normal tissue conditioned medium, $CD4^+$ T cells had lower levels of IFNγ production when cultured with tumor conditioned medium. 8,21% and 10,7% of T cells cultured with

tumor conditioned medium produced IFNγ while 8,21% and 15,2% of the T cell population was IFNγ positive when T cells were cultured with normal tissue conditioned medium. Even though for one of the experiments IFNγ level was the same for both of the conditioned mediums, tumor microenvironment was likely to suppress almost half of the IFNγ production (Figure 3.16B). Altogether, it could be suggested that there was a trend of suppression of IFNγ production by tumor microenvironment.

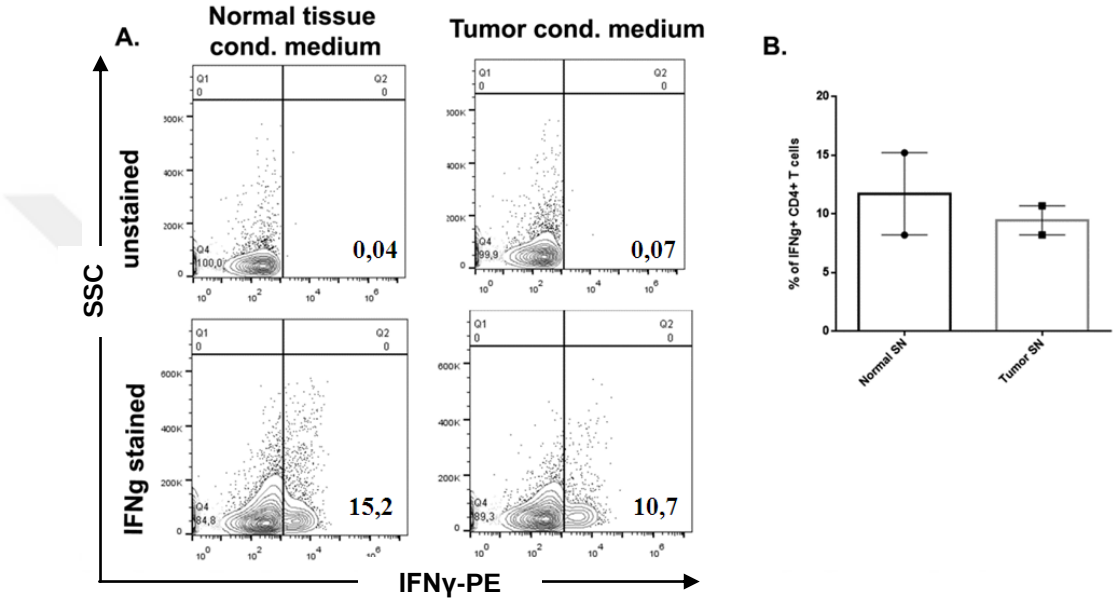

Figure 3.17 : IFNγ Levels of $CD4^+$ T cells cultured with either tumor conditioned medium or normal tissue conditioned medium for 24 h. A.) Representative flow cytometry quadrant plot of $CD4^+IFN\gamma^+$ T cells cultured with either tumor conditioned medium or normal tissue conditioned medium and stimulated with 2 µg/ml PHA and 0,7 µg/ml CpG for 24 h compared to unstained control is given. $CD4^+$ T cells were also stimulated with PMA and ionomycin for 5 h in the presence of 1X Brefeldin A. Intracellular staining was done for IFNγ cytokine using anti-IFNγ-PE antibody. B.) A graphical expression of the $CD4^+IFN\gamma^+$ T cells cultured with either tumor conditioned medium (tumor SN) or normal tissue conditioned medium (normal SN). For the measurements BD ACCURI C6 flow cytometer and for the analyses FlowJo Software was used. Graphs were prepared with Graphpad Prism 6 software. Student's *t* test were used for statistical analysis.

3.6.2.3 Tumor microevironment enhances proliferation of $CD4^+$ T cells

To monitor an immune response, it is important to follow lymphocyte proliferation with minimal disruption to cell viability and function. The intracellular fluorescent dye, CFSE, has been shown to be particularly effective at monitoring lymphocyte division in many experimental situations. CFSE has the ability to stably label molecules within cells, with each cell division resulting in a sequential halving of

fluorescence (Quah et al., 2007). After T cells were labeled with CFSE, they were cultured with either tumor or normal tissue conditioned medium. To stimulate the basal-level T-cell proliferation, PHA was added into all experimental groups including: tumor conditioned medium 1, tumor conditioned medium 2, normal tissue conditioned medium 1 and normal tissue conditioned medium 2. Non-PHA-induced T cells were used as controls.

As shown in Figure 3.18, when compared with the normal tissue conditioned medium culturing, $CD4^+$ T cells had higher proliferation capacity when cultured with tumor conditioned medium. At least 15,2% of T cells cultured with tumor conditioned medium were proliferated while at least 5,69% of the T cell population was proliferated when T cells were cultured with normal tissue conditioned medium.

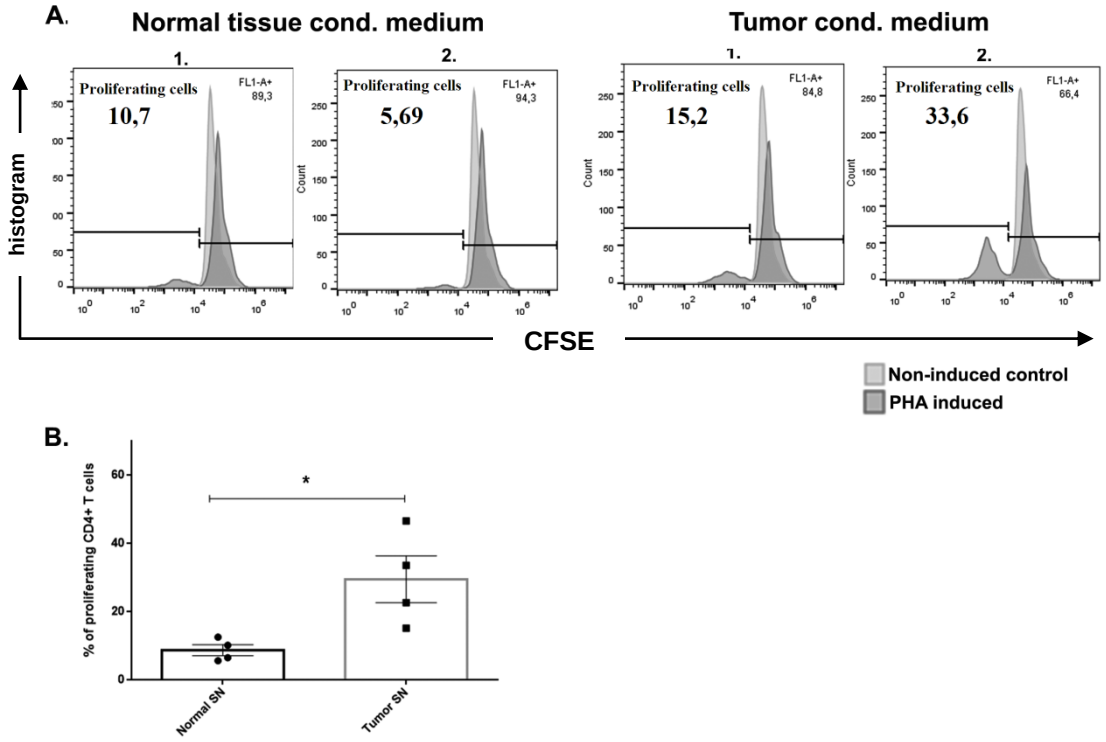

Figure 3.18 : Proliferation of $CD4^+$ T cells cultured with either tumor conditioned medium 1, 2 or normal tissue conditioned medium 1,2 for 3 d. A.) Representative flow cytometry graphs for each experimental group, with the percentage of proliferating T cells (cells left to the unstimulated $CFSE^+$ cells) labeled in the graph. T cells were cultured with either tumor conditioned medium or normal tissue conditioned medium and stimulated with 2 µg/ml PHA for 3 d,. B.) A graphical expression of the proliferating T cells cultured with either tumor conditioned medium (tumor SN) or normal tissue conditioned medium (normal SN). For the measurements BD ACCURI C6 flow cytometer and for the analyses FlowJo Software was used. Graphs were prepared with Graphpad Prism 6 software. Student's *t* test were used for statistical analysis. *p<0.05.

3.6.3 B cells

3.6.3.1 Tumor microevironment increases IL-10 expression by $CD19^+$ B cells

The IL-10 production of B cells was examined by intracellular IL-10 staining which was afterwards detected by flow cytometry (Figure 3.19). For this purpose, the cells cultured with either tumor conditioned medium or normal tissue conditioned medium and stimulated with 1 μg/ml recombinant CD40L and 0,7 μg/ml CpG for 24 h compared to unstained control is given. B cells were also stimulated with PMA and ionomycin for 5 h in the presence of 1X Brefeldin A to keep the cytokines accumulated inside the Golgi complex. After that, the cells were fixed and permeabilized. Lastly,they were incubated with PE-coupled anti-IL-10 antibody that was prepared inside the permeabilization buffer.

As shown in Figure 3.19, when compared with the normal tissue conditioned culture, B cells had significantly higher levels of IL-10 production when cultured with tumor conditioned medium. 9,21% and 6,51% of B cells cultured with tumor conditioned medium produced IL-10 while 0,34% and 1,26% of the B cell population was IL-10 positive when B cells were cultured with normal tissue conditioned medium. The IL-10 cytokine production levels of B cells in tumor microenviroment were significantly increased according to normal tissue microenvironment for both of the experiments. It could be suggested that in both experiments there is a differentiation of B cells into $IL10^+$ regulatory B cells.

3.6.3.2 Tumor microevironment increases numbers of PD-$L1^+$ IL-10^+ B cells

PD-L1 as a ligand of PD-1 is constitutively expressed on B lymophocytes, macrophages and DC. A number of studies have indicated that PD-1/PD-L1 pathway is a crucial modulator of host immune responses in regulation tumor immunity (Guan et al., 2016). The IL-10 production of PD-$L1^+$ B cells was examined by intracellular IL-10 antibody staining which was afterwards detected by flow cytometry (Figure 3.19). For this purpose, the cells cultured with either tumor conditioned medium or normal tissue conditioned medium and stimulated with 1 μg/ml recombinant CD40L and 0,7 μg/ml CpG for 24 h compared to unstained control is given. B cells were also stimulated with PMA and ionomycin for 5 h in the presence of 1X Brefeldin A to keep the cytokines accumulated inside the Golgi complex. First, cells were labeled with anti-PD-L1-APC. After that, the cells were fixed and permeabilized. Lastly,

they were incubated with PE-coupled anti-IL-10 antibody that was prepared inside the permeabilization buffer.

As shown in Figure 3.20, when compared with the normal tissue conditioned medium culturing, B cells had higher numbers of PD-L1 and IL-10 double positive B cells when cultured with tumor conditioned medium. 4,59 and 1,68% of PD-L1^{+} B cells cultured with tumor conditioned medium produced IL-10 while 2,33% and 1,21% of the PD-L1^{+} B cell population was IL-10 positive when they were cultured with normal tissue conditioned medium. The IL-10 cytokine production levels of PD-L1^{+} B cells in tumor microenviroment were increased according to normal tissue microenvironment for both of the experiments. It could be suggested that in both experiments there is a differentiation of B cells into PD-L1^{+}IL10^{+} regulatory B cells.

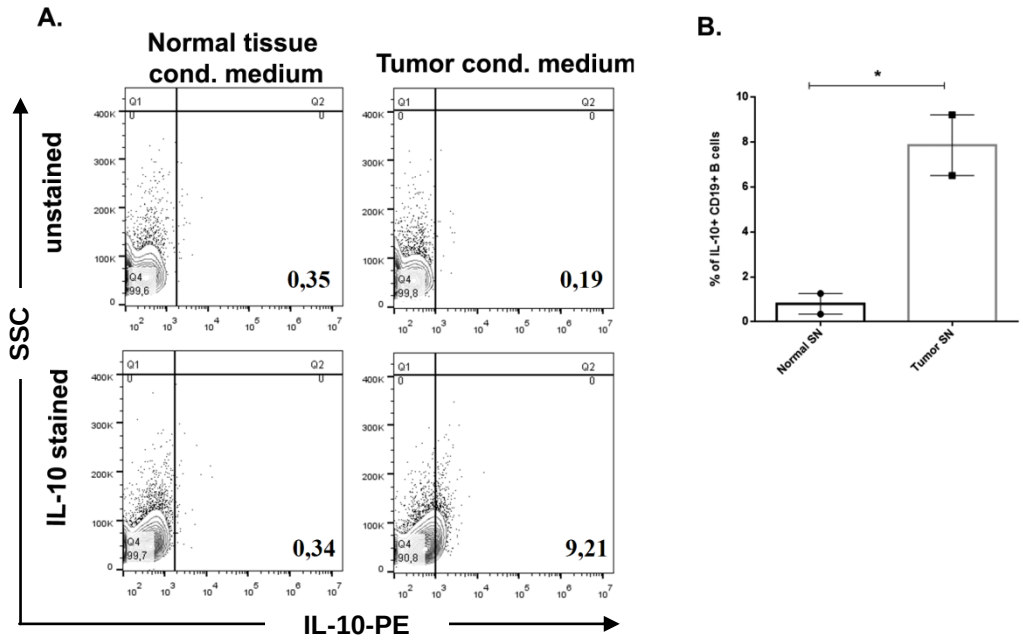

Figure 3.19 : IL-10 Levels of B cells cultured with either tumor conditioned medium or normal tissue conditioned medium for 24 h. A.) Representative flow cytometry quadrant plot of IL-10^{+} B cells cultured with either tumor conditioned medium or normal tissue conditioned medium and stimulated with 1 µg/ml recombinant CD40L and 0,7 µg/ml CpG for 24 h compared to unstained control is given. B cells were also stimulated with PMA and ionomycin for 5 h in the presence of 1X Brefeldin A. Intracellular staining was done for IL-10 cytokine using anti-IL10-PE antibody. B.) A graphical expression of the IL-10^{+} B cells cultured with either tumor conditioned medium (tumor SN) or normal tissue conditioned medium (normal SN). For the measurements BD ACCURI C6 flow cytometer and for the analyses FlowJo Software was used. Graphs were prepared with Graphpad Prism 6 software. Student's *t* test were used for statistical analysis. **p*<0.05.

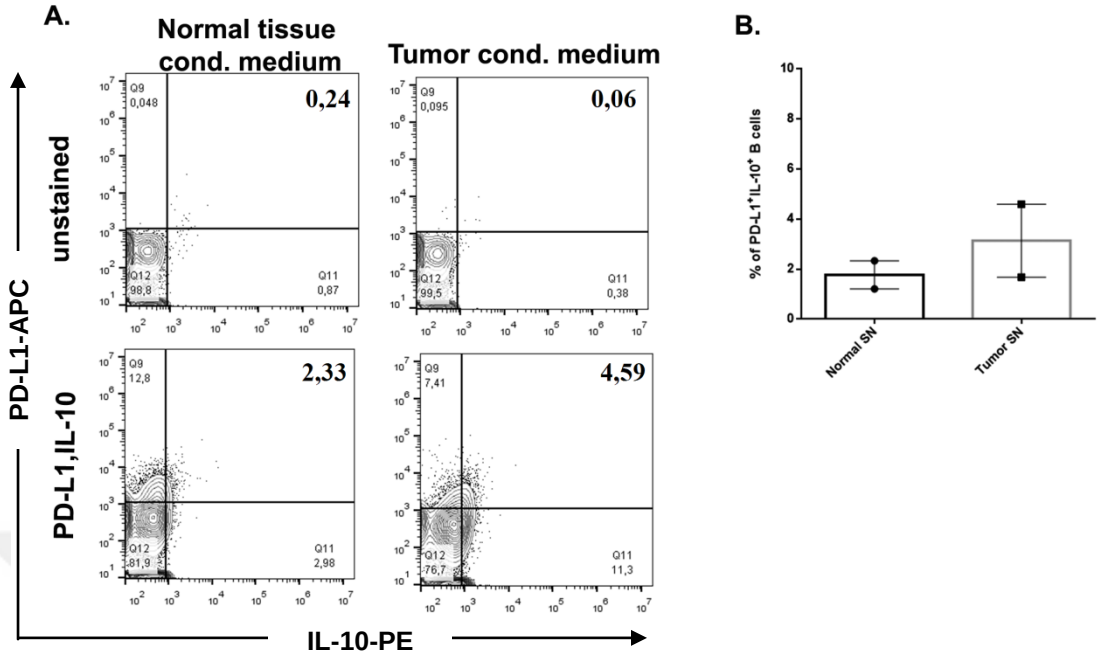

Figure 3.20 : IL-10 Levels of PD-L1^{+} B cells cultured with either tumor conditioned medium or normal tissue conditioned medium for 24 h. A.) Representative flow cytometry quadrant plot ofPD-L1^{+} IL-10^{+} B cells cultured with either tumor conditioned medium or normal tissue conditioned medium and stimulated with 1 µg/ml recombinant CD40L and 0,7 µg/ml CpG for 24 h compared to unstained control is given. B cells were also stimulated with PMA and ionomycin for 5 h in the presence of 1X Brefeldin A. Intracellular staining was done for IL-10 cytokine using anti-IL10-PE antibody. B.) A graphical expression of the IL-10^{+} B cells cultured with either tumor conditioned medium (tumor SN) or normal tissue conditioned medium (normal SN). For the measurements BD ACCURI C6 flow cytometer and for the analyses FlowJo Software was used. Graphs were prepared with Graphpad Prism 6 software. Student's *t* test were used for statistical analysis. **p*<0.05.

4. DISCUSSION AND CONCLUSION

Lung cancer is the main cause of the cancer deaths worldwide, for this reason understanding the immunological effector and regulator mechanims are crucial for applying appropriate immunotherapies. The inflammatory response depends on innate and adaptive immune cell activities to maintain tissue homeostasis. Although, immune cell composition in the tumor microenvironment may contribute to immune evasion and cancer development. Immune cell infiltration is a key feature of almost all cancer types, and TILs refer to the lymphocytes within and around the tumor cells. We observed more $CD8^+$ and $CD19^+$ cell infiltration compared to $CD4^+$ cells both in NSCLC and mesothelioma by flow cytometry analysis (Figure 1; Figure 5; Figure 7).

Tumor microenviroment mainly affects immunological responses via either supressing effector cells or converting them to the regulatory cell types. Those regulatory cell types including regulatory T and B cells contribute to the anti-inflammatory responses with their ability to secrete anti-inflammatory cytokines such as IL-10, IL-35, TGFβ, etc. IL-10 production by immune cells is the key factor of anti-inflammatory responses. To detect IL-10 production by $CD4^+$ T cells and B cells, 24 hours CpG and 5 hours of PMA/ionomycin stimulation were performed. Activation with CpG and PMA/ionomycin cocktail is important for the optimal detection of IL-10 production of B cells by using intracellular cytokine staining (de Masson et al., 2014). Flow cytometry results showed that IL-10 expression was increased in both $CD4^+$ T cells (0.82-24.1%) and $CD19^+$ B cells (0.85-17.3%) for blood samples of the patients with lung cancer compared to healthy individuals. Moreover, there was a high incidence of IL-10 expression in their tumor infiltrating $CD4^+$ T cells (0-23,7%) and $CD19^+$ B cells (0-20%). In addition, tumor infiltrating $CD19^+$ $IL\text{-}10^+$ B cells (1,15-10%) were significantly increased in mesothelioma patients. These results indicate an anti-inflammatory environment within tumor region both in lung cancer and mesothelioma (Figure 3.4; Figure 3.10).

Regulatory T cells have been relatively well studied compared to regulatory B cells in NSCLC. Ishibashi et al. (2006) showed that Tregs numbers were increased in

NSCLC by checking Foxp3 expression in tumor tissues by real time PCR. Also, increased Treg levels in peripheral blood relative to the stage of the disease were highest in patients with metastatic tumors (Erfani et al., 2012). Shigematsu et al. (2012) found a higher proportion of Tregs ($CD4^+$ $CD25^+$ $Foxp3^+$) in TIL and lymph nodes than in blood and presented that Tregs suppressed the induction of cytotoxic T lymphocytes against lung cancer cells. Our results also showed that $IFN\gamma^+$ cytotoxic T cells were significantly decreased in TIL of lung cancer patients to the healthy control level compared with their blood samples (20,3-94,9% to 3,03-53,2%). Same trend can also be observed for MT patients (34,1; 55,4% to 8,33; 21,9%) (Figure 3.6).

It is known that Th1 cells secrete IL-2 and IFNγ that suppress Th2 responses, whereas Th2 cells secrete IL-4 and IL-10 that inhibit Th1 responses (Mosmann et al., 1986). Researchers have shown that peripheral blood lymphocytes from NSCLC patients with recurrence showed an unfavorable imbalance between Th1 and Th2 cells, with significantly depressed Th1 to Th2 ratios (Ito et al., 1999). Later, Th1/Th2 balance in the lung cancer studies were shifted to the Treg/Th17 balance. Peripheral blood of NSCLC patients is characterized by a significantly higher percentage of Th17 and Treg cells compared to healthy individuals. However, in NSCLC patients, the levels of these two $CD4^+$ T cell subsets were inversely correlated in peripheral blood (Duan et al., 2015). Even though, we did not check Th2 response, we showed that IFNγ producing $CD4^+$ T cell frequencies were significantly decreased in PBMCs of LC patients (10,4-38,3% to 1,82-21,4%) and Th17 percentages did not change significantly in both blood and tumor tissue compared to healthy individuals (Figure 2; Figure 3). In turn, increased $CD4^+$ $IL\text{-}10^+$ T cell frequencies suggests that $CD4^+$ T cell response shift to the anti-inflammatory responses for both systemic and local responses. Highly pure B and $CD4^+$ T cells were isolated from healthy individuals to study effects of tumor microenvironment on B and T cells (Figure 3.15). Moreover, our *in vitro* studies showed that IFNγ expression by $CD4^+$ T cells decreased (15,2 to 10,7%) whereas IL-10 expression was increased (1,54 to 3,71%) when they were cultured with tumor conditioned medium compared to normal tissue conditioned medium. (Figure 3.16; Figure 3.17). However, the experiment must be repeated with different tumor conditioned mediums since we need to come to an exact conclusion. In order to determine effects of tumor microenvironment on proliferation of $CD4^+$ T

cells, CFSE labelling was performed prior to treatment with tumor supernatant for 3 days. The intracellular fluorescent dye, CFSE, has been found to be particularly effective at monitoring lymphocyte division in many experimental situations via sequential halving of fluorescence (Quah et al., 2007). According to CFSE assay, analyzed with flow cytometry, proliferating $CD4^+$ T cells were significantly increased in tumor microenvironment compared with the normal tissue microenvironment. Those proliferating $CD4^+$ T cells might be Tregs (Figure 18). However, further investigation of those proliferating cells with Treg specific transcription factor, Foxp3 are required. Altogether, this results confirm the suppressing ability of NSCLC tumor microenvironment.

Most of the studies in the literature regarding regulatory B cells are restricted to the studies using peripheral blood, which reflects only a systemic immune responses for NSCLC. For that reason, investigating regulatory B cells within its microenviroment is necessary. Liu et al. (2016) identified IL-10 producing B cells were upregulated in peripheral blood of NSCLC patients without an increase of $CD19^+$ B cells which is consistent with our results. In this study, we both checked blood and tumor tissue of the NSCLC and mesothelioma patients. Regulatory B cels were significantly elevated in both blood and TILs of patients with NSCLC while they were significantly elevated in TILs of patients with mesothelioma (Figure 3.10). Also, healthy control B cells were significantly elevated IL-10 production when they cultured with supernatant of primary NSCLC tumor cells (Figure 3.19). IFNγ and IL-17 production were also measured in B cells but no difference was detected among experimental groups (Figure 3.7; Figure 3.8).

Even though there are different studies showing that IL-10 producing B cells are significantly increased in NSCLC, their phenotypes have not been identified in detail to the date. Our aim was to identify regulatory B cells in detail for NSCLC and also for mesothelioma. IL-10 producing $CD19^+CD24^+CD38^+$ B cells has been characterized as a type of regulatory B cells in literature (Blair et al., 2010, Flores-Borja et al., 2013). Firstly, the frequency of $CD19^+CD24^+CD38^+$IL-10^+ B cells (0-75%) were highly increased in blood compared to $CD19^+CD24^+CD38^-$ and $CD19^+CD24^-CD38^+$ B cells for NSCLC (Figure 3.12) despite that $CD19^+CD24^+CD38^+$ cell percentages were low and significantly did not change within blood and TILs of patient groups compaired with healthy controls (Figure

3.11). This results suggest that $CD19^{+}CD24^{+}CD38^{+}IL\text{-}10^{+}$ B cells might have an important role for immunosuppresive mechanisms for NSCLC.

There are numerous studies that analyzed relation of PD-L1 and PD-L2 expression and fewer studies that analyzed the role of PD-1 in patient survival. However, previously published reports using different methods such as immunohistochemistry, microarray and flow cytometry have been controversial about PD-1 and PD-L1 prognostic value in patients with NSCLC (Lafuente-Sanchis et al., 2017). Zheng et al. (2016) reported that PD-1 expression in blood $CD4^{+}$ T cells were associated with poor clinical outcome. However, there is no study to investigate PD-1 expression of B cells in NSCLC. Recently, novel tumor-promoting $PD\text{-}1^{high}$ Breg subset in tumor tissues of patients with hepatocellular carcinoma were identified (Xiao et al., 2016). For these reasons, to investigate the role of PD-1 and IL10 expressions on B cells in NSCLC, both blood and tumor tissue samples were analyzed with flow cytometry. Even though we had low numbers of samples, we demonstrated that PD-1 expression on B cells were significatly increased in both blood (2,14-11,1%) and tumor tissue (3,52-28,6%) samples of NSCLC patients compared to healthy individuals (0,79-3,9%). Moreover, PD-1 and IL-10 double positive B cells were significantly increased in both blood (0,68-5,45%) and tumor tissue samples (1,58-7,04%) of patients with NSCLC compared to healthy individuals (0-0,94%) (Figure 13; Figure 14). Altogether, we speculate that high PD-1 expression may contribute to the immunosuppressive role of both peripheral and regional Bregs in NSCLC.

PD-L1 as a ligand of PD-1 is constitutively expressed on B lymophocytes, macrophages and DCs. The PD-1/PD-L1 interaction exerts inhibitory effects that limit effector cells response and regulate the balance between T cell activation and tolerance. (Guan et al., 2016). We wanted to detect effects of tumor microenvironment on PD-L1 expression of B cells and observed that IL-10 production levels of $PD\text{-}L1^{+}$ B cells in tumor microenviroment were increased. Therefore we speculate that high PD-L1 expression may also contribute to the immunosuppressive role of Bregs (Figure 3.20). We also investigated PD-1 expression on B and T cells from healthy individuals in tumor microenvironment, however elevated PD-1 expression cannot be detected in tumor microenvironment *in vitro*. This could be because of the short incubation time.

The recognition of mechanisms of anticancer immune response may have important therapeutic implications. For that reason, we aimed to identify immune cells in NSCLC and under-eximined mesothelioma. Even though we have low number of samples for mesothelioma because of its low incidence, IL10 producing regulatory B cells were identified in cancer microenvironment. For NSCLC, peripheral and regional Bregs that express high levels of PD-1 were identified. Moreover, IL-10 producing peripheral $CD19^{+}CD24^{+}CD38^{+}$ regulatory B cells were determined. However, number of samples taken from lung cancer and mesothelioma patients must be increased for better characterization. In addition, different techniques can be used to detect PD-1, PD-L1 and IL10 in samples taken from patients. Immunohistochemistry staining of PD-1, PD-L1, CD20 and CD4 can be performed for NSCLC patients' tumor and normal tissues to detect PD-1 and PD-L1 expressing B and T cells. PD-1, PD-L1 and IL10 can be detected at mRNA level in B and T cells from tumor and normal tissues by using real time PCR. Altogether, our results contributed to the literature through identifing different immune cells in NSCLC and mesothelioma.

REFERENCES

Abbas, A. K., Lichtman, A. H., and Pillai, S. (2012). *Cellular and Molecular Immunology* Elsevier Saunders.

Al-Shibli, K. I., Donnem, T., Al-Saad, S., Persson, M., Bremnes, R. M., and Busund, L. T. (2008). Prognostic effect of epithelial and stromal lymphocyte infiltration in non-small cell lung cancer. *Clin Cancer Res,* 14**,** 5220-7.

Amu, S., Saunders, S. P., Kronenberg, M., Mangan, N. E., Atzberger, A., and Fallon, P. G. (2010). Regulatory B Cells prevent and reverse allergic Airway inflammation via Foxp3-positive T regulatory cells in a murine model. *J Allergy Clin Immunol,* 125**,** 1114-1124.e8.

Amu, S., Tarkowski, A., Dorner, T., Bokarewa, M., and Brisslert, M. (2007). The human immunomodulatory CD25+ B cell population belongs to the memory B cell pool. *Scand J Immunol,* 66**,** 77-86.

Anagnostou, V. K., and Brahmer, J. R. (2015). Cancer immunotherapy: a future paradigm shift in the treatment of non-small cell lung cancer. *Clin Cancer Res,* 21**,** 976-84.

Bankoti, R., Gupta, K., Levchenko, A., and Stager, S. (2012). Marginal zone B cells regulate antigen-specific T cell responses during infection. *J Immunol,* 188**,** 3961-71.

Blair, P. A., Norena, L. Y., Flores-Borja, F., Rawlings, D. J., Isenberg, D. A., Ehrenstein, M. R., and Mauri, C. (2010). CD19(+)CD24(hi)CD38(hi) B cells exhibit regulatory capacity in healthy individuals but are functionally impaired in systemic lupus erythematosus patients. *Immunity,* 32**,** 129-40.

Brahmer, J. R., and Pardoll, D. M. (2013). Immune checkpoint inhibitors: making immunotherapy a reality for the treatment of lung cancer. *Cancer Immunol Res,* 1**,** 85-91.

Bremnes, R. M., Busund, L. T., Kilvaer, T. L., Andersen, S., Richardsen, E., Paulsen, E. E., Hald, S., Khanehkenari, M. R., Cooper, W. A., Kao, S. C., and Donnem, T. (2016). The role of tumor-infiltrating lymphocytes in development, progression, and prognosis of non-small cell lung cancer. *J Thorac Oncol,* 11**,** 789-800.

Broere, F., Apasov, S. G., Sitkovsky, M. V., and Van Eden, W. (2011). A2 T cell subsets and T cell-mediated immunity. 15-27.

Chen, Y. B., Mu, C. Y., and Huang, J. A. (2012). Clinical significance of programmed death-1 ligand-1 expression in patients with non-small cell lung cancer: a 5-year-follow-up study. *Tumori,* 98**,** 751-5.

Couper, K. N., Blount, D. G., and Riley, E. M. (2008). IL-10: the master regulator of immunity to infection. *J Immunol,* 180**,** 5771-7.

De Masson, A., Le Buanec, H., and Bouaziz, J. D. (2014). Purification and immunophenotypic characterization of human B cells with regulatory functions. *Methods Mol Biol,* 1190**,** 45-52.

Dilillo, D. J., Weinberg, J. B., Yoshizaki, A., Horikawa, M., Bryant, J. M., Iwata, Y., Matsushita, T., Matta, K. M., Chen, Y., Venturi, G. M., Russo, G., Gockerman, J. P., Moore, J. O., Diehl, L. F., Volkheimer, A. D., Friedman, D. R., Lanasa, M. C., Hall, R. P., and Tedder, T. F. (2013).

Chronic lymphocytic leukemia and regulatory B cells share IL-10 competence and immunosuppressive function. *Leukemia,* 27**,** 170-82.

Ding, Q., Yeung, M., Camirand, G., Zeng, Q., Akiba, H., Yagita, H., Chalasani, G., Sayegh, M. H., Najafian, N., and Rothstein, D. M. (2011). Regulatory B cells are identified by expression of TIM-1 and can be induced through TIM-1 ligation to promote tolerance in mice. *J Clin Invest,* 121**,** 3645-56.

Domagala-Kulawik, J., Osinska, I., and Hoser, G. (2014). Mechanisms of immune response regulation in lung cancer. *Transl Lung Cancer Res,* 3**,** 15-22.

Dorner, T., Radbruch, A., and Burmester, G. R. (2009). B-cell-directed therapies for autoimmune disease. *Nat Rev Rheumatol,* 5**,** 433-41.

Duan, M. C., Han, W., Jin, P. W., Wei, Y. P., Wei, Q., Zhang, L. M., and Li, J. C. (2015). Disturbed Th17/Treg balance in patients with non-small cell lung cancer. *Inflammation,* 38**,** 2156-65.

Erfani, N., Mehrabadi, S. M., Ghayumi, M. A., Haghshenas, M. R., Mojtahedi, Z., Ghaderi, A., and Amani, D. (2012). Increase of regulatory T cells in metastatic stage and CTLA-4 over expression in lymphocytes of patients with non-small cell lung cancer (NSCLC). *Lung Cancer,* 77**,** 306-11.

Evans, J. G., Chavez-Rueda, K. A., Eddaoudi, A., Meyer-Bahlburg, A., Rawlings, D. J., Ehrenstein, M. R., and Mauri, C. (2007). Novel suppressive function of transitional 2 B cells in experimental arthritis. *The Journal of Immunology,* 178**,** 7868-7878.

Fillatreau, S., Sweenie, C. H., Mcgeachy, M. J., Gray, D., and Anderton, S. M. (2002). B cells regulate autoimmunity by provision of IL-10. *Nat Immunol,* 3**,** 944-50.

Floess, S., Freyer, J., Siewert, C., Baron, U., Olek, S., Polansky, J., Schlawe, K., Chang, H. D., Bopp, T., Schmitt, E., Klein-Hessling, S., Serfling, E., Hamann, A., and Huehn, J. (2007). Epigenetic control of the foxp3 locus in regulatory T cells. *PLoS Biol,* 5**,** e38.

Flores-Borja, F., Bosma, A., Ng, D., Reddy, V., Ehrenstein, M. R., Isenberg, D. A., and Mauri, C. (2013). CD19+CD24hiCD38hi B cells maintain regulatory T cells while limiting TH1 and TH17 differentiation. *Sci Transl Med,* 5**,** 173ra23.

Floudas, A., Amu, S., and Fallon, P. G. (2016). New Insights into IL-10 Dependent and IL-10 Independent Mechanisms of Regulatory B Cell Immune Suppression. *J Clin Immunol,* 36 Suppl 1**,** 25-33.

Fontenot, J. D., Rasmussen, J. P., Williams, L. M., Dooley, J. L., Farr, A. G., and Rudensky, A. Y. (2005). Regulatory T cell lineage specification by the forkhead transcription factor foxp3. *Immunity,* 22**,** 329-41.

Germain, C., Gnjatic, S., Tamzalit, F., Knockaert, S., Remark, R., Goc, J., Lepelley, A., Becht, E., Katsahian, S., Bizouard, G., Validire, P., Damotte, D., Alifano, M., Magdeleinat, P., Cremer, I., Teillaud, J. L., Fridman, W. H., Sautes-Fridman, C., and Dieu-Nosjean, M. C. (2014). Presence of B cells in tertiary lymphoid structures is associated with a protective immunity in patients with lung cancer. *Am J Respir Crit Care Med,* 189**,** 832-44.

Groux, H., O'garra, A., Bigler, M., Rouleau, M., Antonenko, S., De Vries, J. E., and Roncarolo, M. G. (1997). A CD4+ T-cell subset inhibits antigen-specific T-cell responses and prevents colitis. *Nature,* 389**,** 737-42.

Guan, H., Wan, Y., Lan, J., Wang, Q., Wang, Z., Li, Y., Zheng, J., Zhang, X., Wang, Z., Shen, Y., and Xie, F. (2016). PD-L1 is a critical mediator of regulatory B cells and T cells in invasive breast cancer. *Sci Rep,* 6**,** 35651.

Hori, S., Nomura, T., and Sakaguchi, S. (2003). Control of regulatory T cell development by the transcription factor Foxp3. *Science,* 299**,** 1057-61.

Ishibashi, Y., Tanaka, S., Tajima, K., Yoshida, T., and Kuwano, H. (2006). Expression of Foxp3 in non-small cell lung cancer patients is significantly higher in tumor tissues than in normal tissues, especially in tumors smaller than 30 mm. *Oncol Rep,* 15**,** 1315-9.

Ito, N., Nakamura, H., Tanaka, Y., and Ohgi, S. (1999). Lung carcinoma: analysis of T helper type 1 and 2 cells and T cytotoxic type 1 and 2 cells by intracellular cytokine detection with flow cytometry. *Cancer,* 85**,** 2359-67.

Iwata, Y., Matsushita, T., Horikawa, M., Dilillo, D. J., Yanaba, K., Venturi, G. M., Szabolcs, P. M., Bernstein, S. H., Magro, C. M., Williams, A. D., Hall, R. P., St Clair, E. W., and Tedder, T. F. (2011). Characterization of a rare IL-10-competent B-cell subset in humans that parallels mouse regulatory B10 cells. *Blood,* 117**,** 530-41.

Keir, M. E., Butte, M. J., Freeman, G. J. and Sharpe, A. H. (2008). PD-1 and its ligands in tolerance and immunity. *Annu Rev Immunol,* 26**,** 677-704.

Kessel, A., Haj, T., Peri, R., Snir, A., Melamed, D., Sabo, E., and Toubi, E. (2012). Human CD19(+)CD25(high) B regulatory cells suppress proliferation of CD4(+) T cells and enhance Foxp3 and CTLA-4 expression in T-regulatory cells. *Autoimmun Rev,* 11**,** 670-7.

Khan, A. R., Hams, E., Floudas, A., Sparwasser, T., Weaver, C. T., and Fallon, P. G. (2015). PD-L1hi B cells are critical regulators of humoral immunity. *Nat Commun,* 6**,** 5997.

Konishi, J., Yamazaki, K., Azuma, M., Kinoshita, I., Dosaka-Akita, H., and Nishimura, M. (2004). B7-H1 expression on non-small cell lung cancer cells and its relationship with tumor-infiltrating lymphocytes and their PD-1 expression. *Clin Cancer Res,* 10**,** 5094-100.

Lafuente-Sanchis, A., Zuniga, A., Estors, M., Martinez-Hernandez, N. J., Cremades, A., Cuenca, M., and Galbis, J. M. (2017). Association of PD-1, PD-L1, and CTLA-4 Gene Expression and Clinicopathologic Characteristics in Patients With Non-Small-Cell Lung Cancer. *Clin Lung Cancer,* 18**,** e109-e116.

Lampropoulou, V., Hoehlig, K., Roch, T., Neves, P., Calderon Gomez, E., Sweenie, C. H., Hao, Y., Freitas, A. A., Steinhoff, U., Anderton, S. M., and Fillatreau, S. (2008). TLR-activated B cells suppress T cell-mediated autoimmunity. *J Immunol,* 180**,** 4763-73.

Lee, K. M., Stott, R. T., Zhao, G., Soohoo, J., Xiong, W., Lian, M. M., Fitzgerald, L., Shi, S., Akrawi, E., Lei, J., Deng, S., Yeh, H., Markmann, J. F., and Kim, J. I. (2014). TGF-beta-producing regulatory B cells induce regulatory T cells and promote transplantation tolerance. *Eur J Immunol,* 44**,** 1728-36.

Levings, M. K., Gregori, S., Tresoldi, E., Cazzaniga, S., Bonini, C., and Roncarolo, M. G. (2005). Differentiation of Tr1 cells by immature dendritic cells requires IL-10 but not CD25+CD4+ Tr cells. *Blood,* 105**,** 1162-9.

Liu, J., Wang, H., Yu, Q., Zheng, S., Jiang, Y., Liu, Y., Yuan, G., and Qiu, L. (2016). Aberrant frequency of IL-10-producing B cells and its association

with Treg and MDSC cells in Non Small Cell Lung Carcinoma patients. *Hum Immunol,* 77**,** 84-9.

Liu, Y., and Zeng, G. (2012). Cancer and innate immune system interactions: translational potentials for cancer immunotherapy. *J Immunother,* 35**,** 299-308.

Mann, M. K., Maresz, K., Shriver, L. P., Tan, Y., and Dittel, B. N. (2007). B cell regulation of CD4+CD25+ T regulatory cells and IL-10 via B7 is essential for recovery from experimental autoimmune encephalomyelitis. *J Immunol,* 178**,** 3447-56.

Marshall, E. A., Ng, K. W., Kung, S. H., Conway, E. M., Martinez, V. D., Halvorsen, E. C., Rowbotham, D. A., Vucic, E. A., Plumb, A. W., Becker-Santos, D. D., Enfield, K. S., Kennett, J. Y., Bennewith, K. L., Lockwood, W. W., Lam, S., English, J. C., Abraham, N., and Lam, W. L. (2016). Emerging roles of T helper 17 and regulatory T cells in lung cancer progression and metastasis. *Mol Cancer,* 15**,** 67.

Matsumoto, M., Baba, A., Yokota, T., Nishikawa, H., Ohkawa, Y., Kayama, H., Kallies, A., Nutt, Stephen L., Sakaguchi, S., Takeda, K., Kurosaki, T., and Baba, Y. (2014). Interleukin-10-Producing Plasmablasts Exert Regulatory Function in Autoimmune Inflammation. *Immunity,* 41**,** 1040-1051.

Matsushita, T., Yanaba, K., Bouaziz, J. D., Fujimoto, M., and Tedder, T. F. (2008). Regulatory B cells inhibit EAE initiation in mice while other B cells promote disease progression. *J Clin Invest,* 118**,** 3420-30.

Mauri, C., and Bosma, A. (2012). Immune regulatory function of B cells. *Annu Rev Immunol,* 30**,** 221-41.

Mellman, I., Coukos, G., and Dranoff, G. (2011). Cancer immunotherapy comes of age. *Nature,* 480**,** 480-9.

Mills, K. H. (2004). Regulatory T cells: friend or foe in immunity to infection? *Nat Rev Immunol,* 4**,** 841-55.

Miura, Y., Nishimura, Y., Maeda, M., Murakami, S., Hayashi, H., Fukuoka, K., Kishimoto, T., Nakano, T., and Otsuki, T. (2008). Immunological alterations found in mesothelioma patients and supporting experimental evidence. *Environ Health Prev Med,* 13**,** 55-9.

Mizoguchi, A., and Bhan, A. K. (2006). A Case for Regulatory B Cells. *The Journal of Immunology,* 176**,** 705-710.

Mosmann, T. R., Cherwinski, H., Bond, M. W., Giedlin, M. A., and Coffman, R. L. (1986). Two types of murine helper T cell clone. I. Definition according to profiles of lymphokine activities and secreted proteins. *J Immunol,* 136**,** 2348-57.

Mu, C. Y., Huang, J. A., Chen, Y., Chen, C., and Zhang, X. G. (2011). High expression of PD-L1 in lung cancer may contribute to poor prognosis and tumor cells immune escape through suppressing tumor infiltrating dendritic cells maturation. *Med Oncol,* 28**,** 682-8.

Murphy, K. 2012. *Janeway's Immunobiology*, Garland Science.

Nelson, B. H. (2010). CD20+ B cells: the other tumor-infiltrating lymphocytes. *J Immunol,* 185**,** 4977-82.

Nishimura, Y., Maeda, M., Kumagai-Takei, N., Matsuzaki, H., Lee, S., Fukuoka, K., Nakano, T., Kishimoto, T., and Otsuki, T. (2012). Effect of asbestos on anti-tumor immunity and immunological alteration in patients with malignant mesothelioma.

Nouel, A., Pochard, P., Simon, Q., Segalen, I., Le Meur, Y., Pers, J. O., and Hillion, S. (2015). B-Cells induce regulatory T cells through TGF-beta/IDO production in A CTLA-4 dependent manner. *J Autoimmun,* 59**,** 53-60.

Pardoll, D. M. (2012). The blockade of immune checkpoints in cancer immunotherapy. *Nat Rev Cancer,* 12**,** 252-64.

Petersen, R. P., Campa, M. J., Sperlazza, J., Conlon, D., Joshi, M. B., Harpole, D. H., Jr., and Patz, E. F., Jr. (2006). Tumor infiltrating Foxp3+ regulatory T-cells are associated with recurrence in pathologic stage I NSCLC patients. *Cancer,* 107**,** 2866-72.

Pieper, K., Grimbacher, B., and Eibel, H. (2013). B-cell biology and development. *J Allergy Clin Immunol,* 131**,** 959-71.

Quah, B. J., Warren, H. S., and Parish, C. R. (2007). Monitoring lymphocyte proliferation in vitro and in vivo with the intracellular fluorescent dye carboxyfluorescein diacetate succinimidyl ester. *Nat Protoc,* 2**,** 2049-56.

Romagnani, S. (1999). Th1/Th2 cells. *Inflamm Bowel Dis,* 5**,** 285-94.

Rosser, E. C., and Mauri, C. (2015). Regulatory B cells: origin, phenotype, and function. *Immunity,* 42**,** 607-12.

Ruffini, E., Asioli, S., Filosso, P. L., Lyberis, P., Bruna, M. C., Macri, L., Daniele, L., and Oliaro, A. (2009). Clinical significance of tumor-infiltrating lymphocytes in lung neoplasms. *Ann Thorac Surg,* 87**,** 365-71; discussion 371-2.

Schioppa, T., Moore, R., Thompson, R. G., Rosser, E. C., Kulbe, H., Nedospasov, S., Mauri, C., Coussens, L. M., and Balkwill, F. R. (2011). B regulatory cells and the tumor-promoting actions of TNF-alpha during squamous carcinogenesis. *Proc Natl Acad Sci U S A,* 108**,** 10662-7.

Schwartz, M., Zhang, Y., and Rosenblatt, J. D. (2016). B cell regulation of the anti-tumor response and role in carcinogenesis. *J Immunother Cancer,* 4**,** 40.

Shen, M., Sun, Q., Wang, J., Pan, W., and Ren, X. (2016). Positive and negative functions of B lymphocytes in tumors. *Oncotarget,* 7**,** 55828-55839.

Shen, P., Roch, T., Lampropoulou, V., O'connor, R. A., Stervbo, U., Hilgenberg, E., Ries, S., Dang, V. D., Jaimes, Y., Daridon, C., Li, R., Jouneau, L., Boudinot, P., Wilantri, S., Sakwa, I., Miyazaki, Y., Leech, M. D., Mcpherson, R. C., Wirtz, S., Neurath, M., Hoehlig, K., Meinl, E., Grutzkau, A., Grun, J. R., Horn, K., Kuhl, A. A., Dorner, T., Bar-Or, A., Kaufmann, S. H., Anderton, S. M., and Fillatreau, S. (2014). IL-35-producing B cells are critical regulators of immunity during autoimmune and infectious diseases. *Nature,* 507**,** 366-70.

Sundar, R., Soong, R., Cho, B. C., Brahmer, J. R., and Soo, R. A. (2014). Immunotherapy in the treatment of non-small cell lung cancer. *Lung Cancer,* 85**,** 101-9.

Sznol, M., and Chen, L. (2013). Antagonist antibodies to PD-1 and B7-H1 (PD-L1) in the treatment of advanced human cancer--response. *Clin Cancer Res,* 19**,** 5542.

Tedder, T. F. (2015). Introduction: Regulatory B Cell Special Issue-making all the pieces fit. *Int Immunol,* 27**,** 467-70.

Topalian, S. L., Drake, C. G., and Pardoll, D. M. (2012). Targeting the PD-1/B7-H1(PD-L1) pathway to activate anti-tumor immunity. *Curr Opin Immunol,* 24**,** 207-12.

Topalian, S. L., Sznol, M., Mcdermott, D. F., Kluger, H. M., Carvajal, R. D., Sharfman, W. H., Brahmer, J. R., Lawrence, D. P., Atkins, M. B.,

Powderly, J. D., Leming, P. D., Lipson, E. J., Puzanov, I., Smith, D. C., Taube, J. M., Wigginton, J. M., Kollia, G. D., Gupta, A., Pardoll, D. M., Sosman, J. A., and Hodi, F. S. (2014). Survival, durable tumor remission, and long-term safety in patients with advanced melanoma receiving nivolumab. *J Clin Oncol,* 32**,** 1020-30.

Van De Veen, W., Stanic, B., Yaman, G., Wawrzyniak, M., Sollner, S., Akdis, D. G., Ruckert, B., Akdis, C. A., and Akdis, M. (2013). IgG4 production is confined to human IL-10-producing regulatory B cells that suppress antigen-specific immune responses. *J Allergy Clin Immunol,* 131**,** 1204-12.

Vitale, G., Mion, F., and Pucillo, C. (2010). Regulatory B cells: evidence, developmental origin and population diversity. *Mol Immunol,* 48**,** 1-8.

Watanabe, R., Ishiura, N., Nakashima, H., Kuwano, Y., Okochi, H., Tamaki, K., Sato, S., Tedder, T. F., and Fujimoto, M. (2010). Regulatory B cells (B10 cells) have a suppressive role in murine lupus: CD19 and B10 cell deficiency exacerbates systemic autoimmunity. *J Immunol,* 184**,** 4801-9.

Wei, X., Jin, Y., Tian, Y., Zhang, H., Wu, J., Lu, W., and Lu, X. (2016). Regulatory B cells contribute to the impaired antitumor immunity in ovarian cancer patients. *Tumour Biol,* 37**,** 6581-8.

Wolf, S. D., Dittel, B. N., Hardardottir, F., and Janeway, C. A., Jr. (1996). Experimental autoimmune encephalomyelitis induction in genetically B cell-deficient mice. *J Exp Med,* 184**,** 2271-8.

Woo, E. Y., Yeh, H., Chu, C. S., Schlienger, K., Carroll, R. G., Riley, J. L., Kaiser, L. R., and June, C. H. (2002). Cutting edge: Regulatory T cells from lung cancer patients directly inhibit autologous T cell proliferation. *J Immunol,* 168**,** 4272-6.

Xiao, X., Lao, X. M., Chen, M. M., Liu, R. X., Wei, Y., Ouyang, F. Z., Chen, D. P., Zhao, X. Y., Zhao, Q., Li, X. F., Liu, C. L., Zheng, L., and Kuang, D. M. (2016). PD-1hi Identifies a Novel Regulatory B-cell Population in Human Hepatoma That Promotes Disease Progression. *Cancer Discov,* 6**,** 546-59.

Yanaba, K., Bouaziz, J. D., Haas, K. M., Poe, J. C., Fujimoto, M., and Tedder, T. F. (2008). A regulatory B cell subset with a unique CD1dhiCD5+ phenotype controls T cell-dependent inflammatory responses. *Immunity,* 28**,** 639-50.

Yang, M., Sun, L., Wang, S., Ko, K. H., Xu, H., Zheng, B. J., Cao, X., and Lu, L. (2010). Novel function of B cell-activating factor in the induction of IL-10-producing regulatory B cells. *J Immunol,* 184**,** 3321-5.

Yao, S., and Chen, L. (2014). PD-1 as an immune modulatory receptor. *Cancer J,* 20**,** 262-4.

Zhang, Y., Huang, S., Gong, D., Qin, Y., and Shen, Q. (2010). Programmed death-1 upregulation is correlated with dysfunction of tumor-infiltrating CD8+ T lymphocytes in human non-small cell lung cancer. *Cell Mol Immunol,* 7**,** 389-95.

Zhou, J., Min, Z., Zhang, D., Wang, W., Marincola, F., and Wang, X. (2014). Enhanced frequency and potential mechanism of B regulatory cells in patients with lung cancer. *J Transl Med,* 12**,** 304.

Zou, W. (2005). Immunosuppressive networks in the tumour environment and their therapeutic relevance. *Nat Rev Cancer,* 5**,** 263-74.

CURRICULUM VITAE

Name Surname **: Gönül Seyhan**

Place and Date of Birth **: İstanbul; 01.01.1992**

E-Mail **: gonullseyhan@gmail.com**

EDUCATION

B.Sc. : 2014, Istanbul University, Faculty of Science, Molecular Biology and Genetics Department

PUBLICATIONS, PRESENTATIONS AND PATENTS ON THE THESIS:

Poster presentation:

- Seyhan, G., Turna, A., **Sayi Yazgan A.,** (2017): Akciğer Kanseri ve Mezotelyomalı Hastalarda İmmün Hücre Tiplerinin Karakterizasyonu. 24th National Immunology Congress, 27-30 April 2017, İstanbul/TURKEY.